SOI: 1.1/TAS
DOI: 10.15863/TAS
Scopus ASJC: 1000

ISSN 2308-4944 (print)
ISSN 2409-0085 (online)

№ 10 (162) 2026

Teoretičeskaâ i prikladnaâ nauka

Theoretical & Applied Science

Philadelphia, USA

Teoretičeskaâ i prikladnaâ nauka

Theoretical & Applied Science

10 (162)

2026

International Scientific Journal
Theoretical & Applied Science

Founder: **International Academy of Theoretical & Applied Sciences**

Published since 2013 year. Issued Monthly.

International scientific journal «Theoretical & Applied Science», registered in France, and indexed more than 45 international scientific bases.

Editorial office: **https://T-Science.org** Phone: **+777727-606-81**

E-mail: **T-Science@mail.ru**

Hirsch index:

Editor-in Chief: **Alexandr Shevtsov** **h Index RISC = 8 (87)**

Tech.& Editorial Secretary Vasilieva A.

Editorial Board:

1	Prof.	Vladimir Kestelman	USA	h Index Scopus = 3 (47)
2	Prof.	Arne Jönsson	Sweden	h Index Scopus = 10 (33)
3	Prof.	Sagat Zhunisbekov	KZ	-
4	Assistant of Prof.	Boselin Prabhu	India	-
5	Lecturer	Denis Chemezov	Russia	h Index RISC = 15 (204)
6	Associate Prof.	Elnur Hasanov	Azerbaijan	h Index Scopus = 10 (19)
7	Associate Prof.	Christo Ananth	India	h Index Scopus = - (1)
8	Prof.	Shafa Aliyev	Azerbaijan	h Index Scopus = - (1)
9	Associate Prof.	Ramesh Kumar	India	h Index Scopus = - (2)
10	Associate Prof.	S. Sathish	India	h Index Scopus = 2 (13)
11	Researcher	Rohit Kumar Verma	India	-
12	Prof.	Kerem Shixaliyev	Azerbaijan	-
13	Associate Prof.	Ananeva Elena Pavlovna	Russia	h Index RISC = 1 (19)
14	Associate Prof.	Muhammad Hussein Noure Elahi	Iran	-
15	Assistant of Prof.	Tamar Shiukashvili	Georgia	-
16	Prof.	Said Abdullaevich Salekhov	Russia	-
17	Prof.	Vladimir Timofeevich Prokhorov	Russia	-
18	Researcher	Bobir Ortikmirzayevich Tursunov	Uzbekistan	-
19	Associate Prof.	Victor Aleksandrovich Melent'ev	Russia	-
20	Prof.	Manuchar Shishinashvili	Georgia	-
21	Prof.	Konstantin Kurpayanidi	Uzbekistan	h Index RISC = 8 (67)
22	Prof.	Shoumarov G'ayrat Bahramovich	Uzbekistan	-
23	Associate Prof.	Saidvali Yusupov	Uzbekistan	-
24	PhD	Tengiz Magradze	Georgia	-
25		Dilnoza Azlarova	Uzbekistan	-
26	Associate Prof.	Sanjar Goyipnazarov	Uzbekistan	-
27	Prof.	Shakhlo Ergasheva	Uzbekistan	-
28	Prof.	Nigora Safarova	Uzbekistan	-
29	Associate Prof.	Kurbonov Tohir Hamdamovich	Uzbekistan	-
30	Prof.	Pakhrutdinov Shukritdin Il'yasovich	Uzbekistan	-

International Scientific Journal
Theoretical & Applied Science

Editorial Board:

				Hirsch index:
31	PhD	Mamazhonov Akramzhon Turgunovich	Uzbekistan	-
32	PhD	Ravindra Bhardwaj	USA	h Index Scopus = 2 (5)
33	Assistant lecturer	Mehrinigor Akhmedova	Uzbekistan	-
34	Associate Prof.	Fayziyeva Makhbuba Rakhimjanovna	Uzbekistan	-
35	PhD	Jamshid Jalilov	Uzbekistan	-
36		Guzalbegim Rakhimova	Uzbekistan	-
37	Prof.	Gulchehra Gaffarova	Uzbekistan	-
38	Prof.	Manana Garibashvili	Georgia	
39	D.Sc.	Alijon Karimovich Khusanov	Uzbekistan	
40	PhD	Azizkhon Rakhmonov	Uzbekistan	
41	Prof.	Sarvinoz Kadirova	Uzbekistan	
42	Prof., D.Sc.	Shermukhamedov Abbas Tairovich	Uzbekistan	
43	PhD	Bekjanova Ainura	Uzbekistan	
44		Anzhelika Bayakina	Russia	h Index RISC = 3 (18)
45	PhD	Abdurasul Martazayev	Uzbekistan	
46	PhD	Ia Shiukashvili	Georgia	
47	Associate Prof.	Lali Elanidze	Georgia	h Index Scopus = 0 (1)
48		Maka Kochauri	Georgia	
49	D.T.Sc.	Annaguly Rejepovich Deryaev	Turkmenistan	h Index RISC = 5 (71) h Index Scopus = 2 (13)
50	Dr.	Mohsen Zamani	Iran	
51	Prof.	Lali Khuntsaria	Georgia	h Index RISC = 0 (2)
52		Irina Pavlukhina	Russia	

International Scientific Journal
Theoretical & Applied Science

ISJ Theoretical & Applied Science, 10 (162), 71.
Philadelphia, USA

The percentile in the SCIENCE INDEX ranking = 59
Процентиль в рейтинге SCIENCE INDEX = 59

Impact Factor ICV = 6.630

Impact Factor ISI = 0.829
based on International Citation Report (ICR)

The percentage of rejected articles: 80% Accepted 20% Rejected

© Collective of Authors
© «Theoretical & Applied Science»

Impact Factor:

ISRA (India)	= **6.317**	**SIS** (USA)	= **0.912**	**ICV** (Poland)	= **6.630**
ISI (Dubai, UAE)	= **1.582**	**РИНЦ** (Russia)	= **0.191**	**PIF** (India)	= **1.940**
GIF (Australia)	= **0.564**	**ESJI** (KZ)	= **8.100**	**IBI** (India)	= **4.260**
JIF	= **1.500**	**SJIF** (Morocco)	= **6.004**	**OAJI** (USA)	= **0.350**

SOI: 1.1/TAS DOI: 10.15863/TAS

International Scientific Journal

Theoretical & Applied Science

p-ISSN: 2308-4944 (print) **e-ISSN:** 2409-0085 (online)

Year: 2026 **Issue:** 10 **Volume:** 162

Received: 05.10.2026
Accepted/Published: 30.10.2026

https://T-Science.org

Issue **Article**

M.J. Ibrahimova
Ministry of Science and Education of the Republic of Azerbaijan
İstitute of Petrochemical Processes named after academician Y.G.Mamedalıev
Baku, Azerbaijan

F.M. Abdullayeva
Ministry of Science and Education of the Republic of Azerbaijan
İstitute of Petrochemical Processes named after academician Y.G.Mamedalıev
Azerbaijan State Oil and Industry University
Baku, Azerbaijan

Z.N. Pashayeva
Ministry of Science and Education of the Republic of Azerbaijan
İstitute of Petrochemical Processes named after academician Y.G.Mamedalıev
Azerbaijan State Oil and Industry University
Baku, Azerbaijan

T.A. Ibrahimova
Ministry of Science and Education of the Republic of Azerbaijan
İstitute of Petrochemical Processes named after academician Y.G.Mamedalıev
Baku, Azerbaijan

E.N. Alizade
Ministry of Science and Education of the Republic of Azerbaijan
Azerbaijan State Oil and Industry University
Baku, Azerbaijan

B.F. Baghirova
Ministry of Science and Education of the Republic of Azerbaijan
İstitute of Petrochemical Processes named after academician Y.G.Mamedalıev
Baku, Azerbaijan

R.A. Ismayilova
Ministry of Science and Education of the Republic of Azerbaijan
İstitute of Petrochemical Processes named after academician Y.G.Mamedalıev
Baku, Azerbaijan

Kh.G. Gurbanova
Ministry of Science and Education of the Republic of Azerbaijan
İstitute of Petrochemical Processes named after academician Y.G.Mamedalıev
Baku, Azerbaijan

N.H. Suleymanova
Ministry of Science and Education of the Republic of Azerbaijan
İstitute of Petrochemical Processes named after academician Y.G.Mamedalıev
Baku, Azerbaijan

L.A. Jafarli
Ministry of Science and Education of the Republic of Azerbaijan
İstitute of Petrochemical Processes named after academician Y.G.Mamedalıev
Baku, Azerbaijan

SOME PHYSICAL AND THERMAL PROPERTIES OF IONIC LIQUIDS

Abstract: *The diverse application areas of ionic liquids based on their unique characteristics-and the expansion of these fields necessitate a detailed analysis of ionic liquids. In turn, this will facilitate the expansion of research into formulations based on various combinations of anions and cations enabling the synthesis of new ionic liquids with improved properties and lead to increased production volumes.*

Precise information regarding the thermal and physical properties of ionic liquids is essential for evaluating their suitability for various applications. Currently, significant attention is focused on issues such as why certain ionic liquids exhibit higher electrical conductivity than others and how this relates to ion diffusion rates—as well as the structural characteristics that determine the wide range of viscosities observed in ionic liquids.

Key words: *ionic liquid, viscosity, vapor pressure, nanostructures, thermal properties.*

Language: *English*

Citation: Ibrahimova, M.J., et al. (2026). Some physical and thermal properties of ionic liquids. *ISJ Theoretical & Applied Science, 10 (162),* 1-9.

Soi: https://s-o-i.org/1.1/TAS-10-162-1 ***Doi***: https://dx.doi.org/10.15863/TAS.2026.10.162.1

Scopus ASCC: *3100.*

Introduction

Ionic liquids (ILs) have emerged as a prominent class of materials that have received substantial scientific attention over the past several decades, owing to their distinctive physicochemical characteristics and broad application potential. Continuous advances in ionic-liquid chemistry have resulted in the development of diverse structural families and successive generations of ILs with specifically tailored properties. This rapid expansion has stimulated extensive research into the fundamental physicochemical behavior of ILs, the rational design and synthesis of novel ionic-liquid systems, their processing and chemical-engineering aspects, as well as their implementation in laboratory, pilot-scale, and industrial applications.

Early research on ILs was predominantly associated with the principles of green chemistry, where these materials were investigated as alternative solvents to conventional volatile organic compounds. Their negligible or low volatility, high thermal stability, and tunable chemical structure have subsequently facilitated their integration into a much broader range of technological disciplines. At present, ILs are being extensively investigated in areas including catalysis, organic and polymer synthesis, electrochemistry, analytical chemistry, energy conversion and storage, nanotechnology, and biotechnology.

Within the field of polymer science, ionic liquids have attracted particular interest because of their multifunctional roles in polymer-related processes. They have been employed as alternative reaction media for polymerization, specialized solvents for the dissolution and processing of biopolymers such as cellulose, and as co-catalysts or initiating species in polymerization reactions. In addition, their incorporation into polymer formulations has enabled the development of functional additives and advanced polymeric materials with tunable properties.

A particularly significant development has involved the covalent incorporation of ionic-liquid-derived functionalities into polymeric architectures. This approach has enabled the emergence of a distinct class of charged polymeric materials generally referred to as polymeric ionic liquids (PILs), or poly(ionic liquid)s. These materials combine the structural characteristics of polymers with the physicochemical features associated with ionic liquids, thereby providing considerable opportunities for the design of functional polyelectrolytes with controllable properties.

The introduction of ionic-liquid-derived cationic and anionic moieties, including imidazolium, pyrrolidinium, and pyridinium cations, as well as tetrafluoroborate, hexafluorophosphate, and triflate anions, has significantly expanded the structural diversity of functional polymeric systems. Taking these factors into account, the present article reviews the viscosity, vapor pressure, transport properties, thermal decomposition, and other characteristics of ionic liquids to shed light on these questions.

Viscosity of ionic liquids

Viscosity is considered a key characteristic of ionic liquid systems, as the ionic liquid medium strongly influences the dissolution process and the diffusion of dispersed particles. Factors such as the nature, size, and symmetry of the cations and anions, as well as hydrogen bonding, typically play a decisive role in determining the viscosity of ionic liquids. Achieving low viscosity is one of the most significant

objectives in research within the field of ionic liquids. Specifically, low viscosity facilitates use in the liquid state whether for various scientific research purposes or for commercial processes while also enhancing the performance of electrochemical devices by enabling high ion transport.

The viscosity of ionic liquids is significantly higher at least tenfold than that of other solvents, such as water (approaching the consistency of oil or even honey). This is due to strong intermolecular interactions within the ionic liquid, such as van der Waals forces, hydrogen bonding, and Coulombic forces. Although mixing ionic liquids (ILs) with molecular solvents is considered the most effective method for reducing viscosity, this leads to increased vapor pressure, a higher tendency for flammability, and reduced electrochemical stability. As with other properties of ionic liquids, the experimental measurement of viscosity requires pure, dry ionic liquid and an inert atmosphere. The choice of viscometer for this purpose is made by taking into account the Newtonian or non-Newtonian behavior of the ILs [1,2]. When ionic liquids exhibit Newtonian behavior, their viscosity can be accurately measured using falling-sphere, capillary, or other types of viscometers. A rotational viscometer is used to evaluate the non-Newtonian viscosity of the ionic liquid.

The currently employed magnetic resonance method is considered a research technique that enables the acquisition of extensive information regarding the actual behavior of ionic liquids, both with and without the presence of suspended nanoparticles [3]. This method can be linked to the actual behavior of ionic liquids as well as to the ordering effects within their liquid structure [4,5].

Vapor pressure of ionic liquids

Although vapor pressure is considered a physically significant property regarding the application of ionic liquids (ILs), it has not been extensively studied. For instance, the dependence of this parameter on the nature of the ionic liquid and the precise meaning of "negligible" vapor pressure remain unclear. Contrary to earlier understanding in this field, Earle and his colleagues demonstrated that certain aprotic ionic liquids actually possess significant vapor pressure, as they can be distilled [6]. A combination of a Knudsen effusion apparatus and a quartz crystal microbalance can be cited as a method for measuring vapor pressure as a function of temperature [7,8]. It should be noted that the vapor pressure of aprotic ionic liquids differs significantly from that of protic ionic liquids. Specifically, in protic ionic liquids, this process occurs through the evaporation of the constituent acid and base as neutral molecules into the gas phase [9].

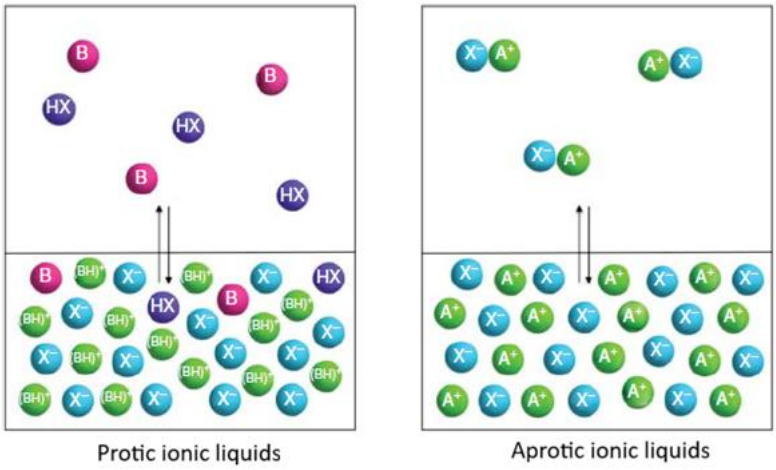

Pic.1. Description of the difference between protic ionic liquids and aprotic ionic liquids, which exist in the gas phase as tightly bound ion pairs.

It is currently understood that aprotic ionic liquids exist in the gas phase as strongly associated ion pairs. This has been confirmed by both experimental and theoretical studies [10, 11]. Data regarding the enthalpy of vaporization of ionic liquids also provide insight into the strength of the interactions between ions in the liquid phase.

Although aprotic ionic liquids are often characterized as compounds with negligible vapor pressure, it has been noted that certain ionic liquids, such as [Cnmim][NTf2] (where n = 2, 4, 6, 8, 10, 12, and 16), can be distilled. This indicates that, at a certain temperature, there is sufficient energy to overcome the strong inter-ionic interactions within the liquid phase of the ionic liquid (IL), thereby enabling vaporization. Furthermore, upon cooling, these ions can condense to reform the ionic liquid phase without undergoing decomposition. Following this discovery, significant interest has arisen in identifying ILs capable of vaporizing without decomposition and in

investigating the nature of ILs in the gas phase [9, 12]. The tendency of ionic liquids to vaporize under the influence of temperature is of considerable practical importance. The ΔH_vap parameter is also significant for the thermodynamic modeling of ionic liquids, as it allows for the characterization of the strength of interactions between ions in the liquid phase.

Ionic liquid binary mixtures can also undergo vaporization; in this process, the more volatile neutral ion pair is distilled first. As previously discussed, the specific combination of cations and anions is not critical when two ionic liquids are mixed, since they form a mixture of the same composition in the liquid phase ([Cat1][A1] + [Cat2][A2] ≡ [Cat1][A2] + [Cat2][A1]). Furthermore, in the ideal state of an ionic liquid (IL) mixture, the mixture's vapor pressure depends solely on the two components and their molar ratios. Initial studies have demonstrated ideal behavior in mixtures of two aprotic ionic liquids [13]. Analogous theory applies to the composition of the gas phase as well; if [Cat1][A1] is the more volatile ion pair, it is the first component to form, regardless of which two ionic liquids were used to prepare the mixture. At the same time, for the distillation of the four possible ILs to be feasible, their vapor pressures must differ significantly. While the distillation of aprotic ionic liquids (ILs) requires high temperatures and high vacuum, other ILs can be distilled more easily. These include protic ionic liquids (PILs) and carbamate-based ILs. As previously noted, protic ionic liquids are obtained through the transfer of a proton from an acid to a base. The distillation of PILs is governed by the volatility of the neutral acid and base species; consequently, the vaporization processes differ significantly from those of aprotic ionic liquids, which involve the formation of ion pairs (Fig.2) [9].

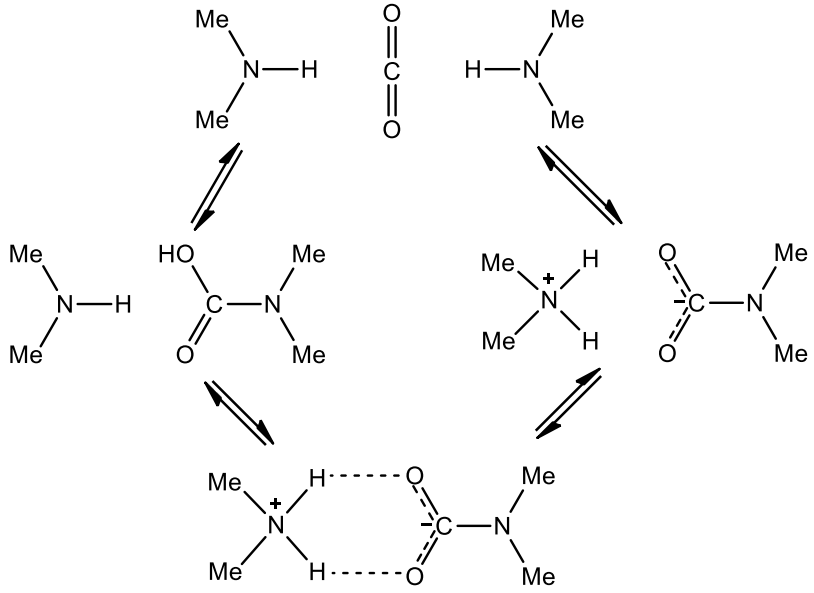

Scheme 1. Dynamic equilibrium of N,N-dimethylammonium N′,N′-dimethylcarbamate [16].

Carbamate-based ionic liquids (ILs) are synthesized by combining carbon dioxide and a secondary amine in a 1:2 molar ratio. For instance, N,N-dimethylammonium N′,N′-dimethylcarbamate (DIMCARB, Scheme 3.1) and N,N-diethylammonium N′,N′-diethylcarbamate (DIETCARB) exist as liquids at room temperature [14]. However, at moderate temperatures (up to 60°C), these ILs can dissociate in the gas phase into their starting materials—namely, the amine and carbon dioxide. Conversely, recombination of the constituent amine and CO_2 leads to the reformation of the IL. Thus, when used as reaction media for dissolving and processing valuable materials such as biomass and lignite, these ILs can be easily removed from the product via distillation under very mild conditions [14, 15].

Nanostructures in ionic liquids

Another complex characteristic of ionic liquids is the formation of nanoscale structures within the liquid phase. Although this feature is not necessarily considered a primary advantage, it can significantly influence the properties of ionic liquids and the reactions in which they participate. This is an emerging field of research that encompasses X-ray and neutron diffraction techniques used to detect nanoscale structures [17]. The structure of the IM is more complex at the surface and at phase boundaries (liquid-liquid or liquid-gas interfaces), which in turn significantly influences its behavior in many areas of application.

Thermal properties of ionic liquids

Ionic liquids possess a number of thermal properties that are significant for their applications. Among these properties, thermal stability is the most important and frequently cited. Precise information regarding the decomposition temperature of ionic liquids is crucial for evaluating their suitability for high-temperature applications. Such applications include lubrication, thermal energy storage, and use as heat-transfer fluids. Ionic liquids may also be subjected to temperature and other stresses when used as synthetic media to enhance the dissolution of biomaterials. Such a wide range of applications stems from the fact that the IM can be utilized under diverse conditions—such as in air or inert atmospheres, with or without gas flow, in contact with surfaces capable of catalyzing decomposition (e.g., aluminum), across volumes ranging from microliters to liters, and at high temperatures [18]. All these parameters can alter the thermal decomposition temperature or the rate of decomposition. Therefore, these factors must be taken into account when determining the most appropriate test conditions for evaluating thermal stability. The thermal stability of the IM, the quantitative measure of its decomposition rate, and the analysis of decomposition products are investigated using thermogravimetric analysis (TGA) coupled with mass spectrometry or via pyrolysis-mass spectrometry [19]. The most widely used method for evaluating the thermal stability of the IM is thermogravimetric analysis (TGA) conducted under conditions of linear temperature change (10°C per minute). This is a convenient and time-efficient method for the preliminary assessment of the thermal stability of various IMs. In some cases, this analysis also reveals a multi-stage decomposition process. In this analysis, the mass loss of the sample is recorded over time, making it possible to determine, for instance, the time required for a 1% mass loss. This enables the comparison of different insulating materials and allows one to track how the decomposition time changes with rising temperatures—specifically, the rate of the decomposition process at high temperatures. One significant outcome of such an analysis is the determination of the maximum operating temperature for the insulating material. In addition, it must be borne in mind that some ionic liquids (ILs) may vaporize at high temperatures, resulting in measurable mass loss (particularly when measured using TGA gas flow). Furthermore, when evaluating the impact of a specific structural change, the nature of the ions in the IL must also be considered a crucial factor. For instance, if the anion employed promotes decomposition at a relatively low temperature, then minor structural modifications to the cation may be disregarded. Based on the research conducted, certain general observations can be made:

– increasing the length of the alkyl chain in the cation slightly reduces the stability of the ionic liquid; this occurs because, as expected, compounds with longer alkyl chains form more stable carbocations or carbon radicals;

– the effect of branching in the alkyl chain depends on the anion used, as the decomposition mechanism may vary based on the anion (e.g., SN1 or SN2);

– the incorporation of oxygen-containing fragments into the cation typically results in reduced stability. – For instance, ionic liquids (ILs) bearing oxazolidinium or morpholinium cations are characterized by relatively lower stability compared to those with side chains containing alkoxy groups or with pyrrolidinium and piperidinium cations (which possess analogous ring structures but lack an oxygen heteroatom) [20-22];

– Dicationic ionic liquids (ILs) possess higher thermal stability compared to monocationic ILs. This applies to both nitrogen-based and phosphonium-based dicationic ILs [23, 24]. The stability of the cations varies in the following order: phosphonium > pyrrolidinium > imidazolium > tetraalkylammonium > sulfonium.

Replacing the acidic proton at the 2-position of the imidazolium ring via methylation enhances thermal stability. In contrast, the use of long alkyl chains at this position has little to no effect [18]. Anions with low nucleophilicity positively influence stability; this is because they exhibit a reduced tendency to attack the cation, allowing the overall stability to be ranked in the order: $[NTf2]^-$ > $[BF4]^-$ ≈ $[PF6]^-$ > halides. For example, the stability of [C_2mim]-based ionic liquids varies according to the following anion series [25]:

$[CF3SO3]^-$ > $[CH3SO3]^-$ > $[CH3CO2]^-$ > $[CF3CO2]^-$

The $[FSI]^-$ anion is less thermally stable than the $[NTf2]^-$ anion, owing to the susceptibility of the FSO_2 group to decomposition [21].

The thermal decomposition mechanism of ionic liquids is quite complex. The nature of the cation and anion plays a particularly significant role here. It is presumed that factors such as the substrate, the medium, and impurities further complicate the decomposition mechanism. Just as mathematical modeling is employed to predict the decomposition pathways requiring the lowest energy—allowing for comparison with experimentally determined products—the use of hyphenated techniques such as TGA-MS (thermogravimetric analysis-mass spectrometry) or Py-GC (pyrolysis-gas chromatography) is crucial for identifying both decomposition temperatures and decomposition products [26-29]. Furthermore, it should be noted that energetic materials (EMs) can decompose via endothermic or exothermic processes; this provides additional insight into the decomposition mechanism [18,29]. As an example, the possible decomposition

mechanisms for the widely used [C_2mim][NTf2] can be shown:

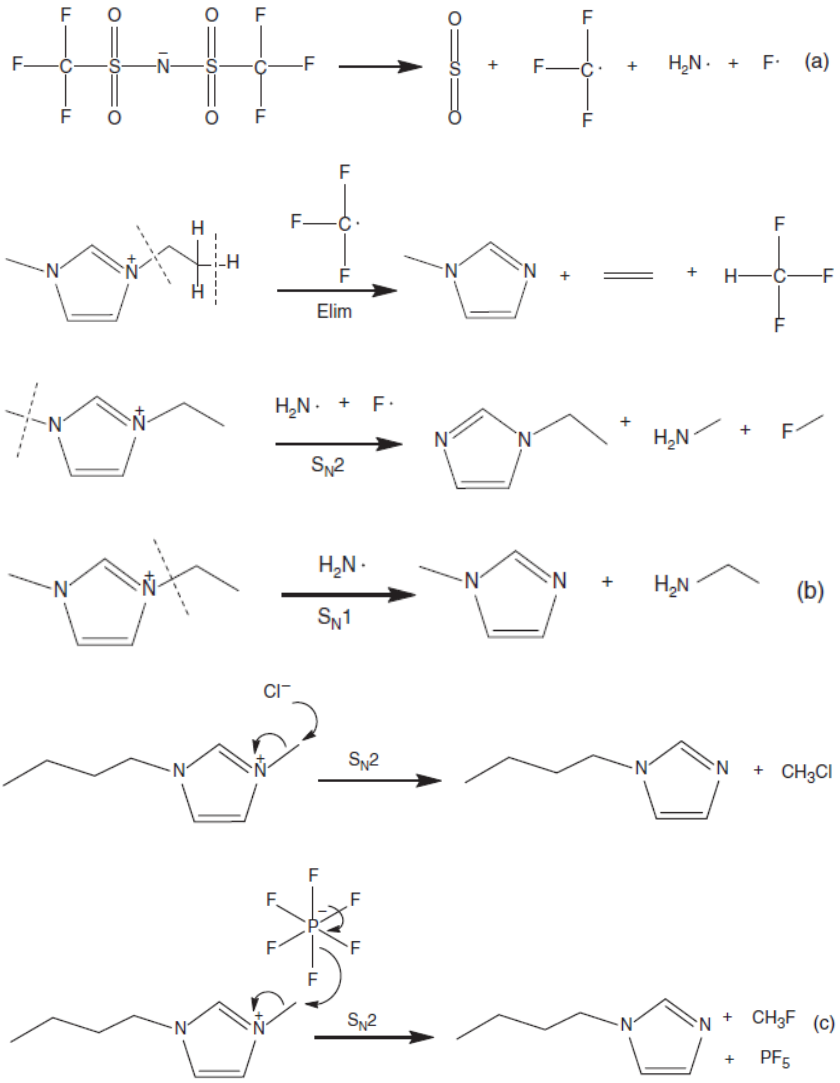

Scheme 2. Decomposition mechanism (a) in the presence of [C_4mim][PF_6], taking into account the possible mechanisms of subsequent attack by the NTf2 anion on the [C_2mim] cation in [C_2mim][NTf_2] (b) and the possible decomposition pathways of [C_4mim][Cl] (c).

Mass spectrometric analysis should demonstrate that, when the sampled material undergoes fragmentation or chemical transformation, distinct products are formed via various mechanisms. Elimination reactions are a commonly observed mode of fragmentation for ionic liquids, and this has been proposed as the dominant mechanism for [C2mim][NTf2] [29,30]. The nucleophilic attack of the anion on the cation can proceed via either a unimolecular (SN1) or a bimolecular (SN2) mechanism (Scheme 3.2, b). Of these two mechanisms, SN2 fragmentation is more favorable than SN1 fragmentation for [C_2mim][NTf2]. The theoretical differentiation of these mechanisms across various ionic liquids stems from the fact that the rate of the SN2 reaction depends not only on the strength of the nucleophile (e.g., variations observed with different halogens) but also on the nature of the substrate undergoing attack (e.g., steric hindrance associated with different cations). It should be noted that for [C_2mim][NTf2], since the anion does not act as the nucleophile in the substitution reaction, the anion must first dissociate—a phenomenon that has been experimentally observed [29]. Since the SN2 reaction is considered to have the lowest energy barrier, it has been accepted as the preferred

mechanism for the decomposition of [C_4mim][Cl], [C4mim][PF_6], and [C4mim][BF4] compounds (Scheme 3.2, c) [29]. It should be noted that this process occurs in the absence of water, as the $[PF_6]^-$ and $[BF_4]^-$ anions readily undergo hydrolysis in the presence of water to form HF. Experimental and computational studies also indicate that the decomposition of [C2mim][OAc] proceeds primarily via an SN2 mechanism (involving the attack of the acetate group on the methyl substituent of the imidazolium ring) [28]. These ionic liquids are being extensively studied for biomass processing, and research into their thermal decomposition indicates that they should not be used at temperatures exceeding 120°C.

CONCLUSION

Ionic liquids have emerged as versatile functional materials whose physicochemical properties can be systematically tailored through the appropriate selection and combination of cations and anions. Their distinctive characteristics, including low volatility, tunable viscosity, high ionic conductivity, and comparatively high thermal stability, have contributed to their expanding use in diverse scientific and technological applications [31-43].

The analysis presented in this review demonstrates that the physical and thermal properties of ionic liquids are strongly dependent on their molecular structure, the nature of the constituent ions, intermolecular interactions, and experimental conditions. Viscosity is particularly important because it directly affects mass transport, ion mobility, diffusion, and the performance of ionic-liquid-based electrochemical and catalytic systems. The ability to control viscosity through structural modification or appropriate formulation is therefore essential for optimizing the practical performance of ILs.

Although ionic liquids are commonly regarded as materials with negligible vapor pressure, studies have demonstrated that their vaporization behavior is more complex. Depending on their chemical structure, ionic liquids may undergo vaporization through the formation of strongly associated ion pairs or through the release of neutral molecular species. This distinction is particularly relevant for aprotic, protic, and carbamate-based ionic liquids and provides important information for their purification, processing, and potential recovery by distillation.

The presence of nanoscale structural organization represents another important characteristic of ionic liquids. Such structural heterogeneity can influence their transport, interfacial, and solvation behavior and may therefore play a significant role in determining their performance in technologically relevant systems. In parallel, thermal stability remains a critical parameter for evaluating the suitability of ILs for high-temperature applications. Thermal decomposition is governed by both the cation and anion structures and may proceed through different reaction pathways, including elimination and nucleophilic substitution mechanisms.

Thermogravimetric and mass-spectrometric techniques, together with complementary experimental and computational approaches, provide valuable tools for identifying decomposition temperatures, reaction pathways, and degradation products. The available evidence indicates that thermal stability can be enhanced or diminished by specific structural modifications, including changes in alkyl-chain length, ion symmetry, heteroatom incorporation, charge density, and anion nucleophilicity. Therefore, thermal stability should not be considered an intrinsic property of an ionic-liquid family alone but rather as a structure-dependent characteristic that must be evaluated under defined experimental conditions.

Overall, a comprehensive understanding of the relationships between ionic structure, physical properties, transport behavior, and thermal decomposition is essential for the rational design of next-generation ionic liquids. Such knowledge can facilitate the development of ILs with optimized properties for applications in energy storage, electrochemistry, catalysis, separation technologies, polymer science, biomass processing, and thermal management. Future research should focus on establishing more reliable structure–property relationships, improving the long-term stability and environmental compatibility of ionic liquids, and developing task-specific ILs capable of meeting the increasingly demanding requirements of advanced technological applications.

References:

1. Holbrey, J.D., Rogers, R.D., Mantz, R.A., et al. (2007). *Ionic Liquids in Synthesis*. Wiley-VCH Verlag GmbH & Co. KGaA. 2007. P.57-174.
2. Abbasov, V.M., Talıbov, A.H., & Əfəndiyeva, L.M. (2014). İon mayeləri sintezdə. *I cild.Bakı ş. Kövsər nəşriyyat.* 2014. 376 p., pp.130-135.
3. Novak, J., & Britton, M.M. (2013). Magnetic resonance imaging of the rheology of ionic

liquid colloidal suspensions. *Soft Matter*, 2013,Vol.9, -№ 9. -pp. 2730-2737.
4. Smith, J.A., Webber, G.B., Warr, G.G., & Atkin, R. (2013). Rheology of protic ionic liquids and their mixtures. *J. Phys. Chem.* B. -2013,Vol.117, № 44, pp.13930-13935.
5. Hu, Z., & Margulis, C.J. (2007). Room-temperature ionic liquids: slow dynamics, viscosity, and the red edge effect. *Acc. Chem. Res*, 2007,Vol.40,№11, pp.1097-1105.
6. Earle, M.J., Esperanca, J., Gilea, M.A., et al. (2006). The distillation and volatility of ionic liquids. *Nature*, 2006, p.439, p.831.
7. Santos, L.M.N.B.F., Lima, L.M.S.S., Lima, C.F.R.A.C., et al. (2011). New Knudsen effusion apparatus with simultaneous gravimetric and quartz crystal microbalance mass loss detection. J. *Chem. Thermodyn*,2011. -Vol.43. -№6, pp.834-843.
8. Rocha, M.A.A., Ribeiro, F.M.S., Schroder, B., et al. (2014). Volatility study of [ClClim][NTf2] and [C2C3im][NTf2] ionic liquids. *J. Chem. Thermodyn*,2014,Vol.68, pp.317-321.
9. Earle, M.J., Esperanca, J.M.S.S., Gilea, M.A., et al. (2006). The distillation and volatility of ionic liquids. *Nature*, 2006, Vol. 439,№7078, pp.831-834.
10. Neto, B.A.D., Meurer, E.C., Galaverna, R., et al. (2012). Vapors from ionic liquids: reconciling simulations with mass spectrometric data. *J. Phys. Chem. Lett*, 2012,Vol.3,№23, pp.3435-3441.
11. Leal, J.P., Esperanca, J.M.S.S., Minas da Piedade, M.E., et al. (2007). The nature of ionic liquids in the gas phase. *J. Phys.Chem*, 2007,Vol.111,№28, pp.6176-6182.
12. Rebelo, L.P.N., Canongia Lopes, J.N., Esperanca, J.M.S.S., & Filipe, E. (2005). On the critical temperature, normal boiling point, and vapor pressure of ionicliquids. *J. Phys. Chem.* B,2005,Vol.109,№13, pp.6040-6043.
13. Taylor, A.W., Lovelock, K.R.J., Deyko, A., et al. (2010). High vacuum distillationof ionic liquids and separation of ionic liquid mixtures. *Phys. Chem. Chem. Phys*,2010,Vol.12,№8, pp.1772-1783.
14. Kreher, U.P., Rosamilia, A.E., & Raston, C.L. (2004). Self-associated, "distillable"ionic media. *Molecules*,2004,Vol. 9,№6. pp.387-393.
15. Verheyen Qi, Y., Tikkoo, T.V., et al. (2015). High solubility of Victorian brown coal in 'distillable' ionic liquid DIMCARB. *Fuel*,2015,Vol.158, pp. 23-34.
16. Anderson, J.L., Ding, R., Ellern, A., & Armstrong, D.W. (2005). Structure and properties of high stability geminal dicationic ionic liquids. *J. Am. Chem. Soc*,2005. -Vol. 127,№2, pp.593-604.
17. Hayes, R., Warr, G.G., & Atkin, R. (2015). Structure and nanostructure in ionic liquids. *Chem. Rev*,2015, Vol.115,№13, pp.6357-6426.
18. Ngo, H.L., Le Compte, Hargens, K.L., & McEwen, A.B. (2000). Thermal properties of imidazolium ionic liquids. *Thermochim. Acta*,2000,Vol.357-358, pp.97-102.
19. Baranyai, K.J., Deacon, G.B., MacFarlane, D.R., et al. (2004). Thermal degradation of ionic liquids at elevated temperatures. *Aust. J. Chem*.-2004,Vol.57,№2. -pp.145-147.
20. Monteiro, M.J., Camilo, F.F., Ribeiro, M.C.C., & Torresi, R.M. (2010). Ether-bond-containing ionic liquids and the relevance of the ether bondposition to transport properties. *J. Phys. Chem.* B,2010,Vol.114,№ 39,pp.12488-12494.
21. Han, H.-B., Liu, K., Feng, S.W., et al. (2010). Ionic liquid electrolytes based on multi-methoxyethyl substituted ammoniums and perfluorinated sulfonimides: preparation, characterization, and properties. *Electrochim. Acta*, 2010. -Vol. 55,№ 23, pp.7134-7144.
22. Zhou, Z.-B., Matsumoto, H., & Tatsumi, K. (2006). Cyclic quaternary ammoniumionic liquids with perfluoroalkyltrifluoroborates: synthesis, characterization, and properties. *Chem. Eur*. J,2006. -Vol.12,№8,pp.2196-2212.
23. Breitbach, Z.S., & Armstrong, D.W. (2008). Characterization of phosphonium ionic liquids through a linear solvation energy relationship and their use as GLC stationary phases. *Anal. Bioanal. Chem*,2008,Vol.390,№ 6. -pp.1605-1617.
24. Anderson, J.L., Ding, R., Ellern, A., & Armstrong, D.W. (2005). Structure and properties of high stability geminal dicationic ionic liquids. *J. Am. Chem. Soc*, 2005,Vol.127,№2,pp.593-604.
25. Watanabe, M., & Tokuda, H. (2014). Ionicity in ionic liquids: origin of chara teristicproperties of ionic liquids in Ionic Liquids Further Uncoiled. *John Wiley & Sons, Inc*. 2014. pp.217-234.
26. Maton, C., De Vos, N., & Stevens, C.V. (2013). Ionic liquid thermal stabilities: decomposition mechanisms and analysis tools. *Chem. Soc. Rev*,2013,Vol.42,№13, pp.5963-5977.
27. Seeberger, A., Andresen, A.-K., & Jess, A. (2009). Prediction of long-term stability of ionic liquids at elevated temperatures by means of non-isothermal thermogravimetrical analysis. *Phys. Chem. Chem. Phys*, 2009, Vol.11, №41, pp.9375-9381.
28. Clough, M.T., Geyer, K., Hunt, P.A., et al. (2013). Thermal decomposition of carboxylate ionic liquids: trends and mechanisms. *Phys. Chem. Chem. Phys*, 2013,Vol.15.-№ 47, pp.20480-20495.
29. Kroon, M.C., Buijs, W., Peters, C.J., & Witkamp, G.-J. (2007). Quantum chemical aided

prediction of the thermal decomposition mechanisms and temperatures of ionic liquids. *Thermochim. Acta*,2007,Vol.465,№ 1-2, pp. 40-47.

30. Chen, Y., Cao, Y., Shi, Y., et al. (2012). Quantitative research on the vaporizationand decomposition of [EMIM][Tf2N] by thermogravimetric analysis-mass spectrometry. *Ind. Eng. Chem. Res*,2012,Vol.51,№21, pp.7418-7427.
31. Abdullayeva, F.M. (2025). Task specific ionic liquid. *Processes of Petrochemistry and Oil Refining*, Special issue, 2025, 313-324.
32. Ibragimova, M.D., Amirov, F.A., Bairamova, S.T., Ibragimova, T.A., Abdullaeva, F.M., & Pashaeva, Z.N. (2024). Modification of phenol-formaldehyde resin with alkyl aromatic hydrocarbons, *Polymer Science*, Series D, 2024, 17(3), pp.646-651, https://doi.org/10.1134/S1995421224701107
33. Pashayeva, Z.N., İbragimova, M.J., & Abdullayeva, F.M. (2024). Possibilities for using ionic liquids in the polymerization process, *Journal of Physics: Conference Series*, 2024, 2834(1), p.012185, https://doi.org/10.1088/1742-6596/2834/1/012185
34. Ibrahimova, M.J., Abdullaeva, F.M., Ibrahimova, T.A., & Pashayeva, Z.N. (2025). Phenol-formaldehyde based composites containing coal as a filler, *Polymer Science*, Series D, 2025, 18(4), pp.685-691, https://doi.org/10.1134/S1995421225700741
35. Ibrahimova, M.C., Abdullayeva, F.M., Pashaeva, Z.N., & Huseyinov, E.Z. (2025). Synthesis of a thermally stable ionic liquid monomer based on quaternization reaction, *Polymer Science*, Series D, 2025, 18(4), pp.692-697, https://doi.org/10.1134/S1995421225700753
36. Ibrahimova, M.J., Abdullayeva, F.M., Pashayeva, Z.N., Ibrahimova, T.A., Amirli, F.A., Huseynov, H.J., Bayramova, S.T., & Nabiyeva, A.Kh. (2026). Alkyl-aromatic-modified phenolic binders for high-performance wood waste biofuel briquettes, *SOCAR Proceedings*, 2026, Special Issue (1), pp.128-133, https://doi.org/10.5510/OGP2026SI101186
37. Abdullaeva, F.M., Maharramov, A.M., Huseyinov, E., Pashayeva, Z.N., & Safarova, A.S. (2026). Medicinal and therapeutic applications of pyrimidine derivatives, *New Materials, Compounds and Applications*, 2026, 10(1), pp.138-150, https://doi.org/10.62476/nmca.101138
38. Ibragimova, M.D., Abdullaeva, F.M., Ibragimova, T. A., & Pashaeva, Z. N. (2024). Synthesis and investigation of composites based on phenol-formaldehyde resin. *Processes of Petrochemistry and oil Refining*, Special Issue (N 1), 2024, pp.165-174.
39. Ibragimova, M.C., Amirov, F.A., Bayramova, S.T., Ibragimova, T.A., & Abdullaeva, F.M. (2022). *Composite compositions based on modified phenol-formaldehyde resin*, 2022, T-6, N-2, pp.139-144.
40. Ibragimova, M.D., Azizov, A.G., Pashayeva, Z.N., Abdullayeva, F.M., Yusifzade, F. Yu., & Dadasheva, S.D. (2015). Use of ionic liquids as solvent and as catalyst in the processes of synthesis polymers. *Khimiya v interesakh ustoychivoqo razvitiya*, T 23, N-3, pp.225-234.
41. Pashayeva, Z. N., Ibrahimova, M. J., Nasirov, F. A., et al. (2025). Living radical polymerization of methyl methacrylate in ionic liquids. *Processes of Petrochemistry and Oil Refining*, Special Issue, 242-248.
42. Ibragimova, M.G., Abdullayeva, F.M., & Pashayeva, Z.N. (2017). Carbon Dioxide Sorption by an Ionic Liquid Monomer that Is 2-Methacryloxyethyl Diethylammonium Chloride and copolymers based on It. *Chemistry for sustainable development*, 2017, Vol.25, pp.175-179.
43. Ibrahimova, M. J., Mammadova, T. A., Amirli, F. A., et al. (2024). Method for obtaining fuel briquettes. *AZ Patent* № I 2024, 0119.

Impact Factor:					
	ISRA (India) = 6.317	SIS (USA) = 0.912	ICV (Poland) = 6.630
	ISI (Dubai, UAE) = 1.582	РИНЦ (Russia) = 0.191	PIF (India) = 1.940
	GIF (Australia) = 0.564	ESJI (KZ) = 8.100	IBI (India) = 4.260
	JIF = 1.500	SJIF (Morocco) = 6.004	OAJI (USA) = 0.350

SOI: 1.1/TAS DOI: 10.15863/TAS

International Scientific Journal

Theoretical & Applied Science

p-ISSN: 2308-4944 (print) **e-ISSN:** 2409-0085 (online)

Year: 2026 **Issue:** 10 **Volume:** 162

Received: 13.10.2026
Accepted/Published: 30.10.2026 https://T-Science.org

Issue Article

Maftuna Ixtiyor qizi Ochilova
Karshi State Technical University
180100 Karshi, Uzbekistan
nurik_1980@mail.ru

INFLUENCE OF FOLIAR FERTILIZERS ON THE FORMATION OF FRUITING BRANCHES IN COTTON

Abstract: *The article presents the results of studying the effect of foliar fertilizers Uzbiogumin, PK-Maks, and Kaliy-450, used individually and in combination, on the formation of fruiting branches in cotton varieties "Bukhara-8" and "Marvarid". It was established that the most stable increase in the number of fruiting branches was provided by the combined application of PK-Maks 3.0 l/ha + Kaliy-450 2.5 l/ha + Uzbiogumin 0.5 l/ha.*

Key words: *cotton, fruiting branches, foliar feeding, Uzbiogumin, PK-Maks, Kaliy-450, variety, growth and development.*

Language: *English*

Citation: Ochilova, M.I. (2026). Influence of foliar fertilizers on the formation of fruiting branches in cotton. *ISJ Theoretical & Applied Science, 10 (162),* 10-14.

Soi: https://s-o-i.org/1.1/TAS-10-162-2 ***Doi***: crossref https://dx.doi.org/10.15863/TAS.2026.10.162.2

Scopus ASCC: *1100.*

Introduction

Currently, under the soil and climatic conditions of the Republic of Uzbekistan, research is being conducted on the cultivation of cotton using foliar fertilization, various biostimulants and physiologically active substances alongside conventional mineral fertilization practices. These preparations are of considerable importance because they can stimulate physiological and biochemical processes in plants, promote root system development, improve the formation of vegetative and reproductive organs, and enhance plant tolerance to adverse environmental conditions (Sh.Abdualimov, F.Abdullaev, 2010, Sh.Abdualimov et al., 2010).

The use of physiologically active substances and plant growth regulators is an important approach to improving seed germination and germination vigor, promoting plant growth and development throughout the growing season, and enhancing tolerance to drought, salinity, diseases, and insect pests (Davronov Q., Tuxtashev F., 2022).

Furthermore, physiologically active plant growth regulators can influence various physiological processes within plants, potentially improving photosynthetic efficiency, nutrient metabolism, and the formation of reproductive organs. The foliar application of these preparations in the form of working solutions may contribute to the development of higher yields and improved crop quality. (Sh.Abdualimov et al., 2010).

Upland cotton (*G.hirsutum* L.) is one of the most important fiber crops, playing a vital role in supplying raw materials to the global textile industry. This cotton species is characterized by its high yield potential, adaptability to diverse soil and climatic conditions, and the wide range of applications of its fiber. However, in recent years, global climate change, increasing weather variability, and adverse environmental factors have negatively affected cotton production, leading to impaired formation of yield components and a decline in fiber quality (Ahmed et al., 2024; Chorshanbiev et al., 2025).

At the same time, the development and improvement of Pima cotton (*G.barbadense* L.) varieties that are resistant to adverse environmental conditions are of considerable importance for expanding opportunities for the production of high-quality cotton fiber. This cotton species is distinguished by its superior fiber properties, including fiber length, fineness, strength, and uniformity. These characteristics make Pima cotton fiber a valuable raw material for manufacturing high-

quality yarns and premium textile products. Furthermore, investigating the valuable agronomic traits and biological characteristics of *G.barbadense* L. varieties, evaluating their responses under diverse soil and climatic conditions, and identifying genotypes with enhanced tolerance to stress factors are of considerable practical importance. Such studies can contribute to increasing the production of high-quality cotton fiber, improving the efficiency of cotton cultivation, and ensuring the sustainability of cotton production under changing climatic conditions (Amanov et al., 2020; Chorshanbiev et al., 2021; Avliyoqulov and Durdiev, 2021).

The formation of fruiting branches is one of the most important morphobiological indicators characterizing the transition of cotton to generative development. The formation of buds, flowers, and bolls, and consequently the realization of the potential productivity of plants, largely depends on the quantity and rate of formation of fruiting branches. In intensive agriculture, regulating cotton nutrition during critical growth phases is of particular importance, when the root system is not always able to fully meet the demand of above-ground organs for available nutrients.

Foliar feeding allows for the prompt correction of the mineral and physiological state of plants. Their effectiveness is determined by the composition of the preparation, application rate, crop development phase, weather conditions, and varietal characteristics. Therefore, when evaluating biostimulants and complex fertilizer preparations, it is important to consider not only the final yield, but also changes in individual elements of plant architectonics, including fruiting branches.

The purpose of the study was to determine the effect of Uzbiogumin, PK-Maks, and Kaliy-450, applied separately and in combination, on the dynamics of fruiting branch formation in cotton varieties "Bukhara-8" and "Marvarid" under field experiment conditions in 2023.

Materials and Research Methods

Field observations were carried out in 2023 on crops of two cotton varieties: "Bukhara-8" and "Marvarid". The experimental design included control variants without foliar feeding, variants with Uzbiogumin at rates of 0.3 and 0.5 l/ha, combinations of PK-Maks and Kaliy-450 at two application rate levels, and three-component combinations of these preparations. The evaluation was carried out at the same calendar dates for both varieties.

The number of fruiting branches was determined per single plant on July 1, August 1, and September 1. The analysis took into account the absolute value of the indicator, the increase relative to the corresponding varietal control, the relative change in percentage, and the dynamics between recording dates. Comparing the variants made it possible to evaluate both the effect of individual preparations and the possible effect of their combined application.



Plant height - 90-120 cm, not inclined to lie down.
Growing period – 120-125 days
The first fruit branches appear in 5-7 nodes.
Boll weight – 9.0-11.0 g
1000-seed weight – 125-130 g
Fiber belongs to type - IV
Fiber output – 35.0-36.0 %
Fiber length – 33-34 mm
Micronaire-4.3-4.5
Developed by A.M. Battalov and others. The variety is mid-ripening, and was included in the State Register in 2007.

Figure 1. Medium fiber cotton cultivar Bukhara-8



Plant height – 90-100 cm,
a branching type 0, growing period – 117-120 days, the number of branches in the main stem – 22, between of branches – 4.0 sm, cotton weight in one boll – 3.5-4.0 g, weight of 1000 seeds – 115-120 g, fiber output – 35-36 %, fiber index – 6.6 g, fiber length – 38 mm, productivity per plant -56,0 g and higher, micronеr-3,8-4,0, strength -48.8.
Developed by N.E. Chorshanbev and others. The cultivar is fast-ripening, and was included in the State Register in 2018.

Figure 2. Fine fiber cotton cultivar Marvarid.

Research Results and Discussion

By the first recording date, foliar feeding had already caused a noticeable differentiation of variants. In the "Bukhara-8" variety, 7.2 fruiting branches per plant were formed in the control. The application of Uzbiogumin at 0.3 l/ha increased this indicator to 7.5, and at 0.5 l/ha to 7.7 pcs/plant, which exceeded the control by 4.2% and 6.9%, respectively. With the combination of PK-Maks 3.0 l/ha and Kaliy-450 2.5 l/ha, the indicator was 7.6 pcs/plant, and an increase in the rates of these preparations to 6.0 and 5.0 l/ha was accompanied by an increase to 7.9 pcs/plant.

The most pronounced effect at the beginning of July was obtained with three-component application. In the variant with PK-Maks 3.0 l/ha + Kaliy-450 2.5 l/ha + Uzbiogumin 0.3 l/ha, 8.1 fruiting branches were formed, while with an increase in the Uzbiogumin rate to 0.5 l/ha, it was 8.4 pcs/plant. The latter value exceeded the control by 1.2 pcs/plant, or 16.7%. At higher rates of PK-Maks and Kaliy-450, the indicators were 8.2–8.3 pcs/plant. Consequently, the maximum rate of the complex did not automatically ensure a further increase in the number of fruiting branches.

Table 1. Influence of foliar fertilizers on the formation of cotton fruiting branches, 2023

No	Variety	Preparation and single rate	July 1, pcs/plant	August 1, pcs/plant	September 1, pcs/plant
1	Bukhara-8	Control	7.2	12.6	14.3
2	Bukhara-8	Uzbiogumin 0.3 l/ha	7.5	13.1	14.9
3	Bukhara-8	Uzbiogumin 0.5 l/ha	7.7	13.5	15.4
4	Bukhara-8	PK-Maks 3.0 + Kaliy-450 2.5 l/ha	7.6	13.4	15.2
5	Bukhara-8	PK-Maks 6.0 + Kaliy-450 5.0 l/ha	7.9	13.8	15.7
6	Bukhara-8	PK-Maks 3.0 + Kaliy-450 2.5 + Uzbiogumin 0.3 l/ha	8.1	14.3	16.3
7	Bukhara-8	PK-Maks 3.0 + Kaliy-450 2.5 + Uzbiogumin 0.5 l/ha	8.4	14.9	17.0
8	Bukhara-8	PK-Maks 6.0 + Kaliy-450 5.0 + Uzbiogumin 0.3 l/ha	8.2	14.6	16.6
9	Bukhara-8	PK-Maks 6.0 + Kaliy-450 5.0 + Uzbiogumin 0.5 l/ha	8.3	14.7	16.8
10	Marvarid	Control	6.9	12.4	14.2
11	Marvarid	Uzbiogumin 0.3 l/ha	7.2	12.9	14.8
12	Marvarid	Uzbiogumin 0.5 l/ha	7.4	13.3	15.3
13	Marvarid	PK-Maks 3.0 + Kaliy-450 2.5 l/ha	7.3	13.2	15.1
14	Marvarid	PK-Maks 6.0 + Kaliy-450 5.0 l/ha	7.6	13.6	15.6
15	Marvarid	PK-Maks 3.0 + Kaliy-450 2.5 + Uzbiogumin 0.3 l/ha	7.8	14.1	16.2
16	Marvarid	PK-Maks 3.0 + Kaliy-450 2.5 + Uzbiogumin 0.5 l/ha	8.1	14.7	16.9
17	Marvarid	PK-Maks 6.0 + Kaliy-450 5.0 + Uzbiogumin 0.3 l/ha	7.9	14.4	16.5

18	Marvarid	PK-Maks 6.0 + Kaliy-450 5.0 + Uzbiogumin 0.5 l/ha	8.0	14.5	16.7

For the "Marvarid" variety, the pattern was similar. In the control, there were 6.9 fruiting branches per plant. Against the background of Uzbiogumin 0.3 and 0.5 l/ha, the indicator reached 7.2 and 7.4 pcs/plant, respectively. Among the two-component combinations, the higher rate of PK-Maks + Kaliy-450 provided 7.6 pcs/plant. The highest result—8.1 pcs/plant—was noted in the variant with PK-Maks 3.0 l/ha + Kaliy-450 2.5 l/ha + Uzbiogumin 0.5 l/ha, which exceeded the control by 17.4%.

By August 1, the number of fruiting branches increased significantly in all variants. In the "Bukhara-8" variety, the control indicator was 12.6 pcs/plant, and with the application of Uzbiogumin it was 13.1–13.5 pcs/plant. In the variant with PK-Maks 3.0 + Kaliy-450 2.5 + Uzbiogumin 0.5 l/ha, 14.9 pcs/plant were formed, which was 2.3 pcs/plant, or 18.3%, higher than the control. In variants with increased rates of PK-Maks and Kaliy-450 and the addition of Uzbiogumin, 14.6–14.7 pcs/plant were obtained, which is slightly less than in the optimal combination.

For the "Marvarid" variety on August 1, the control was 12.4 pcs/plant. In the three-component variants, 14.1–14.7 pcs/plant were formed, with the highest value again obtained with the combination of PK-Maks 3.0 l/ha + Kaliy-450 2.5 l/ha + Uzbiogumin 0.5 l/ha. The excess over the control was 2.3 pcs/plant, or 18.5%. Thus, the advantage of the optimal combination of preparations persisted during the period of active formation of the generative part of the plant.

The recording results of September 1 confirmed the stability of the identified trend. In "Bukhara-8", 14.3 fruiting branches per plant were formed in the control. Uzbiogumin at a rate of 0.3 l/ha provided 14.9, and at 0.5 l/ha—15.4 pcs/plant. In the variant with PK-Maks 3.0 + Kaliy-450 2.5 + Uzbiogumin 0.5 l/ha, the indicator reached 17.0 pcs/plant, i.e., it was higher than the control by 2.7 pcs/plant, or 18.9%. In variants with increased rates of the three components, the values were 16.6 and 16.8 pcs/plant.

For "Marvarid" in the control variant by September 1, 14.2 fruiting branches were noted. Against the background of Uzbiogumin, the indicator increased to 14.8–15.3 pcs/plant, and in two-component variants—to 15.1–15.6 pcs/plant. The maximum of 16.9 pcs/plant was registered with PK-Maks 3.0 + Kaliy-450 2.5 + Uzbiogumin 0.5 l/ha. The excess of the control was 2.7 pcs/plant, or 19.0%. Increasing the rates of PK-Maks and Kaliy-450 in the presence of Uzbiogumin did not give an additional advantage: 16.5–16.7 pcs/plant were formed in the corresponding variants.

An analysis of the dynamics shows that the main increase in the number of fruiting branches occurred in the period from July 1 to August 1. In the control of "Bukhara-8", the growth was 5.4 pcs/plant, and in the best variant—6.5 pcs/plant. For "Marvarid", the corresponding values were 5.5 and 6.6 pcs/plant. From August 1 to September 1, the growth was smaller, but the optimal three-component variants retained their advantage: 2.1 pcs/plant for "Bukhara-8" and 2.2 pcs/plant for "Marvarid". This indicates a more intensive and prolonged formation of generative organs with a balanced combination of preparations.

When comparing varieties, the absolute values for "Bukhara-8" in most similar variants were 0.1–0.3 pcs/plant higher than for "Marvarid". At the same time, the relative reaction to complex feeding was comparable. By September 1, the advantage of the best variant over the control was 18.9% for "Bukhara-8" and 19.0% for "Marvarid". Consequently, differences in the initial morphological vigor of the varieties did not change the general nature of the response to foliar nutrition.

In general, all variants with the use of preparations exceeded the corresponding varietal controls. At the same time, an increase in the dose of each component separately was usually accompanied by an increase in the indicator, however, in the three-component system, the maximum rates were not the most effective. The most stable effect at all recording dates was provided by the combination of PK-Maks 3.0 l/ha + Kaliy-450 2.5 l/ha + Uzbiogumin 0.5 l/ha. Probably, such a combination created a more favorable ratio of nutrients and biologically active substances during the period of initiation and growth of fruiting branches.

Conclusion

Observations carried out in 2023 showed that the use of foliar fertilizers Uzbiogumin, PK-Maks, and Kaliy-450 positively affected the formation of fruiting branches in both studied cotton varieties. At all recording dates, the number of fruiting branches in the treated variants exceeded the control. The most pronounced advantage was noted with the combined application of PK-Maks 3.0 l/ha + Kaliy-450 2.5 l/ha + Uzbiogumin 0.5 l/ha: in the "Bukhara-8" variety on September 1, 17.0 pcs/plant were formed versus 14.3 in the control, and in the "Marvarid" variety—16.9 versus 14.2 pcs/plant. The relative increase was 18.9% and 19.0%, respectively.

Comparison of rates showed that a further increase in the doses of PK-Maks and Kaliy-450 in three-component variants did not provide an additional increase in the number of fruiting branches. This allows us to consider the combination of PK-Maks 3.0 l/ha + Kaliy-450 2.5 l/ha + Uzbiogumin 0.5 l/ha as the most promising among the studied variants from the standpoint of forming the generative structure of plants. The obtained results should be

taken into account in further comprehensive analysis of bud and boll formation, yield, and economic efficiency of cotton foliar feeding.

References:

1. Abdualimov, Sh., & Abdullaev, F. (2010). *Gumimax - an effective stimulant* //Resource and water saving technologies for obtaining high crop yields in farming systems: Proceedings of the International Scientific and Practical Conference. - Tashkent: Uzbek Research Institute of Cotton Growing, pp. 233-236.
2. Abdualimov, Sh., Davronov, Q., Soriyev, Karimov, Sh., & Abdullayev, F. (2010). Effect of the Gumimax Preparation on Cotton // AGRO ILM: Scientific Supplement to the Journal of Agriculture of Uzbekistan. Tashkent, №2 (14). pp.17-18.
3. Abdurakhimov, N.N., & Normamatova, M.N. (2016). *The effect of stimulants on the rate of increase in the number of crop elements and the opening of cotton bolls.* //Materials of the V International Scientific and Practical Conference of Young Scientists dedicated to the 25th anniversary of the Caspian Research Institute of Arid Agriculture. Solenoje Zaimishche, May 11-13, pp. 243-246.
4. Ahmed, A.I., Khan, A.I., Negm, M.A.M., Iqbal, R., Azhar, M.T., Khan, S.H., & Rana, I.A. (2024). Enhancing cotton resilience to challenging climates through genetic modifications. *J. Cotton Res*. 7: 10.
5. Amanov, B., Abdiev, F., Shavkiev, J., Mamedova, F., & Muminov, Kh. (2020). Valuable economic indicators among hybrids of Peruvian cotton genotypes. *Plant Cell Biotechnol. Mol. Biol.* 21(67-68), pp.35-46.
6. Anishin, P.A. (2006). *Technology of using plant growth regulators in agriculture.* MNTU "Agrobiotech". Kiev, pp. 1-12.
7. Avliyoqulov, M.A., & Durdiev, N.H. (2021). Agrotechnics of fine fiber cotton varieties. Popular Sci. Magazine of Cotton and Cereals, Tashkent, p. 77-84.
8. Chorshanbiev, N.E., Burieva, S.Z., & Khazratkulov, E.Sh. (2021). Analysis of an experiment carried out on the lines and varieties of fine fiber cotton. *Universal J. Agric. Res*. 9(1): 6-12.
9. Chorshanbiev, N.E., Pardaev, E.A., Nabiev, S.M., Azimov, A.A., Shavkiev, J.SH., Quziboev, A.O., Egamberdiev, R.R., Diyorov, G.K., Ergashev, O.R., & Makhmudov, T.KH (2025). Combining ability and inheritance studies in diallel crosses of the Pima cotton (*Gossypium barbadense* L.). *SABRAO J. Breed. Genet*. 57(3): 900-910.
10. Dospekhov, B.A. (1985). *Field Experiment Methodology*. Moscow: Agropromizdat, 351 p.
11. Davronov, Q., & Tuxtashev, F. (2022). Effect of foliar feeding on leaf number, weight, and surface area during different growth stages of cotton //*Academic Research in Modern Science*. 2022. №1(19). pp. 316-319.

Impact Factor:					
	ISRA (India) = **6.317**	**SIS** (USA) = **0.912**	**ICV** (Poland) = **6.630**
	ISI (Dubai, UAE) = **1.582**	**РИНЦ** (Russia) = **0.191**	**PIF** (India) = **1.940**
	GIF (Australia) = **0.564**	**ESJI** (KZ) = **8.100**	**IBI** (India) = **4.260**
	JIF = **1.500**	**SJIF** (Morocco) = **6.004**	**OAJI** (USA) = **0.350**

SOI: 1.1/TAS DOI: 10.15863/TAS

International Scientific Journal

Theoretical & Applied Science

p-ISSN: 2308-4944 (print) **e-ISSN:** 2409-0085 (online)

Year: 2026 **Issue:** 10 **Volume:** 162

Received: 12.10.2026
Accepted/Published: 30.10.2026 https://T-Science.org

Issue **Article**

Azizbek Turganbayevich Saparniyazov
Karakalpak Research Institute of Humanities
Karakalpak Branch of the Academy of Sciences of the Republic of Uzbekistan
PhD in Historical Sciences, DSc Doctoral Candidate
Nukus, Uzbekistan

THE SOCIAL STRUCTURE AND SOCIAL DIFFERENTIATION OF KARAKALPAK SOCIETY IN THE EIGHTEENTH CENTURY

Abstract: *This article examines the social structure of Karakalpak society in the eighteenth century, focusing on its principal social categories and the mechanisms of social differentiation. Drawing on written accounts by European travellers, Russian researchers, and archival and documentary sources, the study explores the social status and roles of töre (aristocratic elites), khojas, sheikhs, biys (customary-law judges and community leaders), batyrs (warriors distinguished by military prowess), clan elders, bais (wealthy individuals), and dependent groups, including enslaved persons. Particular attention is paid to the interplay of lineage, religious authority, political influence, military achievements, and material wealth in determining social status. The article also examines the categories aq süyek ("white bone") and qara süyek ("black bone"), their significance within the social hierarchy, and the functioning of traditional governance institutions. The findings demonstrate that social differentiation in Karakalpak society was shaped by a combination of kinship and tribal affiliations, political relations, religious factors, and economic conditions. The study concludes that the social organisation of the Karakalpaks in the eighteenth century was multilayered and complex, with material wealth constituting only one of several criteria determining an individual's position in society.*

Key words: *Karakalpaks, eighteenth century, social structure, social differentiation, social hierarchy, aq süyek, qara süyek, töre, khojas, sheikhs, biys, batyrs, bais, clan elders, enslaved persons, European travellers, historical sources.*

Language: *English*

Citation: Saparniyazov, A.T. (2026). The social structure and social differentiation of Karakalpak society in the eighteenth century. *ISJ Theoretical & Applied Science, 10 (162),* 15-19.

Soi: https://s-o-i.org/1.1/TAS-10-162-3 ***Doi***: crossref https://dx.doi.org/10.15863/TAS.2026.10.162.3

Scopus ASCC: *3300.*

Introduction

As the German traveler, naturalist, and explorer Alfred Edmund Brehm observed when describing the natural environment of Central Asia: "However rich the Central Asian steppe may be, however strikingly vivid its colours become in spring, and however much fertile land it contains, permanent settlement and life in one and the same place are possible only in its exceptionally favourable areas" [1, p. 131].

The natural and geographical environment was one of the significant factors shaping the historical development of the population of Central Asia. In the eighteenth century, the social and economic life of the Karakalpaks developed within a natural environment directly associated with the availability of water resources, the condition of pastures, seasonal landscape changes, and other ecological circumstances. These conditions had a considerable influence on the direction of economic activities while also necessitating diverse forms of adaptation to a changing environment.

Over a long historical period, the Karakalpaks accumulated considerable experience in exploiting their natural surroundings for economic purposes and adapted to the specific conditions of their environment. The natural, climatic, and landscape characteristics of the Aral Sea region contributed to the development of a diversified economic system combining agriculture, livestock breeding, fishing, hunting, and other activities. This diversity of

economic practices helped reduce the population's dependence on seasonal fluctuations and ensured a relative degree of stability in economic life.

Natural and economic conditions affected not only the economic sphere but also the social organization of Karakalpak society. The combination of agriculture with various forms of pastoralism, together with the need for the collective use of water, pastureland, and other resources, contributed to the formation of stable social relationships. The social structure of the Karakalpaks consisted of interconnected kinship-based, territorial, economic, and status-based groups. These forms of organization facilitated the regulation of internal relations, the distribution of resources, the maintenance of social solidarity, and the reproduction of collective life.

Thus, the natural environment was not merely a factor shaping economic activity but also one of the conditions underlying the formation of corresponding forms of social organization. Nevertheless, the influence of the natural and geographical environment should not be regarded as the sole cause of social differentiation. The social structure of Karakalpak society was also shaped by political, economic, religious, and kinship-based and tribal relations.

In the eighteenth century, the increasing complexity of social and economic relations was accompanied by the development of social institutions and hierarchies reflecting differences in the functions, status, and social roles of various population groups. An individual's social position was not necessarily determined directly by material wealth. In the society under consideration, high status could be associated primarily with lineage, religious authority, political influence, membership in particular kinship-based groups, or the performance of socially significant functions.

The position of sheikhs and khojas is particularly illustrative in this respect. In eighteenth-century Karakalpak society, they were regarded as representatives of Dervishism [6, p. 29], were associated with the religious sphere, and enjoyed considerable social authority. However, the high social standing of religious figures did not necessarily imply substantial material wealth. Sources describing Dervish communities note the prevalence of ascetic lifestyles and material deprivation. The observations of Ármin Vámbéry, a Hungarian Orientalist, Turkologist, and traveler [2, p. 7], provide grounds for taking this characteristic into account when examining the relationship between material circumstances and social status. Khojas and sheikhs were not confined to religious functions; they frequently also acted as political figures [7, p. 54]. They participated in negotiations with the Russian administration and could serve as signatories to official documents. Sources dating from the 1730s and 1740s mention Murad-Sheikh, whom Dmitry Gladyshev, a traveler and researcher of Central Asia, described as the head of the Jabin clan [12, p. 20], as well as his son, Khalvet-Sheikh. Both enjoyed considerable respect among the Karakalpaks [10, pp. 325–346].

Khojas enjoyed high social esteem not only among the Karakalpaks but also in other Central Asian societies. In describing their position, Vámbéry emphasized that "in Central Asia, the hajji enjoys incomparably greater respect than in other Muslim countries and is fully recompensed for the hardships he has endured. Protected by the respect and support of society, he is more secure than anyone else from arbitrariness and tyranny; the title he has acquired serves as his patent of nobility, which he bears on his seal during his lifetime and which adorns his tomb after his death" [2, p. 19]. This testimony is important for understanding how religious prestige could function as an independent source of social status rather than being directly reducible to an individual's material circumstances.

Pyotr Ivanovich Rychkov, a Russian official, traveler, economist, historian, and regional scholar, described the religious life of the Karakalpaks in comparison with that of other peoples of the region. He observed that the Karakalpaks "differ neither in law nor in language from the Kirghiz and other peoples of that region, except that they have more learned and literate people in the Mohammedan faith; consequently, they know the Mohammedan law and observe it more strictly than the Kirghiz. Therefore, a considerable number of khojas are found among them, whom Muslims regard as descendants of the Prophet and his disciples" [10, p. 175]. This testimony indicates the prominent role played by khojas in the religious and social life of eighteenth-century Karakalpak society. At the same time, it demonstrates that religious literacy and knowledge of Islamic tradition were regarded as significant components of social status.

Representatives of the Chinggisid nobility occupied a distinctive position within the social hierarchy. According to the available evidence, there were relatively few Karakalpaks who claimed descent from Genghis Khan. They constituted several families and referred to themselves as "people of the bone of Chinggis" [4, pp. 98–99]. Their lineage provided an important basis for their elevated social and political status. Within the Turco-Muslim political tradition, descendants of Genghis Khan were generally regarded as a distinct elite category, a perception reflected in the norms governing political and legal conduct.

In this connection, particular attention should be paid to the contrast between the categories *aq süyek* ("white bone") and *qara süyek* ("black bone"), which became established in the social terminology of the Turkic societies of the region. In the material examined here, the category *aq süyek* was associated primarily with notions of lineage and the distinctive social status of the *töre* and khojas. Members of these categories enjoyed a number of special social and

legal privileges. In particular, they were exempt from the jurisdiction of the *biys'* courts and from corporal punishment for offences they committed. Outward expressions of deference toward them included addressing a sultan not by personal name but by the honorific title *taqsyr* ("sir" or "my lord"), the requirement to kneel before him, and compliance with other established forms and symbols expressing authority and social status [13, p. 190].

The category *aq süyek* constituted a closed, privileged social group comprising primarily the *töre* and khojas. The *töre* (sultans) represented one of the highest-status categories within semi-nomadic society and played a significant role in its political organization. Their membership in the *aq süyek* category was based above all on claims of Chinggisid descent and the rights associated with it, particularly the right to participate in the exercise and legitimation of political authority.

Sources relating to eighteenth-century Karakalpak history contain references to members of the *töre* category who occupied significant political positions, including positions associated with khanal authority in the Khanate of Khiva [14, pp. 73–74]. Nevertheless, the specific forms and mechanisms through which the *töre* exercised political representation within different Karakalpak groupings require further source-critical investigation and clarification.

The recorded testimonies of the English traveler and researcher Reynold Hoag (also rendered as Reynold Hough) contain the names of several Karakalpak khans, including Khoja Khan, Raskul Khan, Kaiyp Khan, and Sultan Murat Khan [5, pp. 209–210]. These accounts add to our understanding of the political elite of eighteenth-century Karakalpak society and require comparison with other documentary and narrative sources.

As for the category *qara süyek*, in our view, it developed as the social and hierarchical antithesis of *aq süyek*. The privileged category *aq süyek* was contrasted with the general population, referred to by the term *qarasha* ("the common people" or "the masses"). Thus, *qara süyek* denoted the broader population that did not belong to privileged social categories. These concepts should not, however, be interpreted as rigidly defined estates in the modern sense. Rather, they represented historically formed categories associated with social status, lineage, and public prestige.

The *biys* occupied a particularly important position among the high-status social groups. The Russian military officer and researcher of Kazakhstan and Central Asia Yakov Petrovich Gaverdovsky explained the term *biy* as referring to "eloquent, wealthy, and resourceful people" [3, p. 73]. According to Dmitry Gladyshev, a *biy* was one of the key figures in the kinship-based organization, functioning either as its head or as an influential representative. The range of responsibilities associated with this position was extensive. It included participation in economic and political decision-making, regulation of relations within the clan and with neighboring groups, allocation of pastures and other economic lands, organization of communal work, and the settlement of disputes and legal claims. The institution of the *biys* therefore combined administrative, judicial and mediatory, and economic-regulatory functions [7, p. 53].

Batyrs also commanded considerable political and military authority. Baron Georg Wolter Konrad Freiherr von Meyendorff, a natural scientist and topographer, characterized *batyrs* as courageous, just, and enterprising individuals who distinguished themselves above all in times of war [8, p. 41]. The title *batyr* was not inherited through lineage; rather, it was earned through individual martial prowess. The presence of *batyrs* among influential members of society therefore demonstrates the considerable importance of military and political authority in the social organization of eighteenth-century Karakalpak society.

Clan elders (*starshinas*) also occupied a prominent position within the political system of governance, exercising leadership and representing particular kinship-based or territorial groups. The Swedish and Russian traveler and naturalist Johan Peter Falck observed that "these chiefs, or princes, are the wealthiest, highly respected, and the oracles of the aimaks; therefore, the khan can exercise considerable influence over these territories through them, notwithstanding their limited authority" [11, p. 191]. Among the Karakalpaks, comparable functions could be associated with the title or designation *aqsaqal* (literally, "white-bearded elder"). The sources suggest that the authority of a clan elder depended on a combination of factors, including lineage, life experience, personal qualities, material circumstances, and public recognition.

Texts associated with Reynold Hoag also mention several elders and influential figures who allegedly exerted a certain degree of influence over Karakalpak political and social life: Urazak-Batyr, Alimbay-Batyr, Klaubet-Biy, and Temirbek-Bay [5, pp. 209–210]. These names illustrate the multilayered nature of social and political organization, in which different statuses – those of clan elders, *biys*, *batyrs*, and *bays* – could overlap and coexist within an individual's social position.

Slaves and other forms of unfree dependents constituted a distinct population category. According to the sources cited in this article, a substantial proportion of enslaved persons consisted of prisoners of war, including Russians, Kalmyks, Persians, and members of other groups captured during military conflicts and subsequently held by individual leaders. Enslaved persons could also be acquired through buying and selling [7, p. 56]. Documents dating from

1722 provide evidence of variations in their circumstances. In some cases, Russian captives were granted freedom by their owners, while others entered into marital relationships with Karakalpak women [9, p. 779]. These accounts indicate that the status of enslaved persons was not uniform and that an analysis of this population category must take account of the specific forms of dependency involved.

Thus, the social structure of eighteenth-century Karakalpak society was multilayered and encompassed population groups distinguished by lineage, religious standing, political authority, military achievements, economic circumstances, and degrees of social dependency. The most prominent high-status categories included the *töre* and khojas, while the *biys*, *batyrs*, and clan elders played significant roles in the social and political organization of society. Alongside these groups existed various categories of ordinary people and dependent individuals, including enslaved persons. Social status, however, was not determined exclusively by material wealth. Lineage, religious authority, personal achievements, and the performance of important social functions could secure an individual a high position irrespective of their level of material prosperity. Taken together, the evidence examined here makes it possible to characterize eighteenth-century Karakalpak society as a socially differentiated system in which kinship-based, political, religious, military, and economic relations were closely interconnected.

References:

1. Brem, A. (1896). *Stepnye kochevniki-skotovody* [Steppe Nomadic Pastoralists]. Literaturnye prilozheniia k zhurnalu “Niva”. St. Petersburg: Izdanie A. F. Marksa, 1896, pp. 131-158.
2. Vamberi, A. (1868). *Ocherki Srednei Azii* [Essays on Central Asia]. Moscow: Tipografiia A. I. Mamontova i K°, 1868. 363 p.
3. Gaverdovskii, Ya. (n.d.). Obozrenie kirgiz-kaisatskoi stepi [A Survey of the Kirghiz-Kaisak Steppe]. Manuscript Department of the St. Petersburg Branch of the Institute of Russian History. *Collection* 115, No. 495, fol. 73.
4. Grebenkina, A. (1872). Tadzhiki [The Tajiks]. In: Russkii Turkestan: sbornik, izdannyi po povodu Politekhnicheskoi vystavki *[Russian Turkestan: A Collection Published on the Occasion of the Polytechnic Exhibition]*. Issue 2: Articles on Ethnography, Technology, Agriculture, and Natural History. Moscow, 1872. 119 p.
5. (1961). *Kazakhsko-russkie otnosheniia v XVI-XVIII vekakh: sbornik dokumentov i materialov* [Kazakh-Russian Relations in the 16th-18th Centuries: A Collection of Documents and Materials]. Alma-Ata: Izdatelstvo Akademii nauk Kazakhskoi SSR, 1961. 744 p.
6. Kamalov, S. (1968). *Karakalpaki v XVIII-XIX vekakh* (k istorii vzaimootnoshenii s Rossiei i sredneaziatskimi khanstvami) [The Karakalpaks in the 18th-19th Centuries: A History of Their Relations with Russia and the Central Asian Khanates]. Tashkent: Fan, 1968. 328 p.
7. (1935). *Materialy po istorii karakalpakov: sbornik* [Materials on the History of the Karakalpaks: A Collection]. Trudy Instituta vostokovedeniia Akademii nauk SSSR, vol. 7. Moscow; Leningrad: Izdatelstvo Akademii nauk SSSR, 1935. 299 p.
8. Meendorf, E. (1975). *Puteshestvie iz Orenburga v Bukharu* [A Journey from Orenburg to Bukhara]. Foreword by N. Khalfin. Moscow: Vostochnaia literatura, 1975. 183 p.
9. (1830). *Polnoe sobranie zakonov Rossiiskoi imperii* [Complete Collection of Laws of the Russian Empire]. Vol. 6. St. Petersburg: Tipografiia Vtorogo otdeleniia Sobstvennoi Ego Imperatorskogo Velichestva kantseliarii, 1830. 815 p.
10. Rychkov, P. (1762). *Topografiia Orenburgskaia, to est’: obstoiatel’noe opisanie Orenburgskoi gubernii* [The Topography of Orenburg, or a Detailed Description of the Orenburg Province]. Part 1. St. Petersburg: Pri Imperatorskoi Akademii nauk, 1762. 331 p.
11. (n.d.). *St. Petersburg Branch of the Archive of the Russian Academy of Sciences.* Fond 3, Inventory 35, File 47, fols. 191 verso-192.
12. Khanykov, Ya. (1851). Poezdka iz Orska v Khivu i obratno, sovershennaia v 1740-1741 godakh poruchikom Gladyshevym i geodezistom Muravinym [A Journey from Orsk to Khiva and Back, Undertaken in 1740-1741 by Lieutenant Gladyshev and Surveyor Muravin]. *Geograficheskie izvestiia Imperatorskogo Russkogo geograficheskogo obshchestva*, issue 4, section 2. St. Petersburg: Tipografiia Ministerstva vnutrennikh del, 1851. 88 p.
13. (2008). *Tsentral’naia Aziia v sostave Rossiiskoi imperii* [Central Asia within the Russian

Empire]. Moscow: Novoe literaturnoe obozrenie, 2008. 464 p.

14. Yusupov, O. (1993). *Jänibek batyr, Maman batyr, Murad shayikh, Aziz baba, Qorazbek biy-atalyq, Xojamurat biy häm Töremurat biy-sufilar yamasa "Mayli shengel" ótmishinen derekler* [Documents from the Past of "Mayli Shengel"]. Nukus: Qaraqalpaqstan, 1993. 104 p.

SOI: 1.1/TAS DOI: 10.15863/TAS

International Scientific Journal

Theoretical & Applied Science

p-ISSN: 2308-4944 (print) **e-ISSN:** 2409-0085 (online)

Year: 2026 **Issue:** 10 **Volume:** 162

Received: 08.10.2026
Accepted/Published: 30.10.2026 **https://T-Science.org**

Issue Article

Manuchar Chikovani
Akaki Tsereteli State University Kutaisi
Faculty of Exact and Natural Sciences,
Associate Professor, Department of Chemistry,
Georgia.Nakhunao Village, Martvili District.
Mob: +995 595 77 96 53
manuchar.Ciqovani@gmail.com

Lana Gegetchkori
Akaki Tsereteli State University Kutaisi
Third-year Student ,Mob: +995 598 20 14 40
gegetchkori.lana@atsu.edu.ge

Madona Samkharadze
Akaki Tsereteli State University
Faculty of Exact and Natural
Sciences Associate Professor, Department of Chemistry
Mob: +995 595 99 26 94
madona.samkharadze@atsu.edu.ge

Izolda Didbaridze
Akaki Tsereteli State University
Faculty of Exact and Natural
Sciences Associate Professor, Department of Chemistry
Mob: +995 595 93 60 05
izolda.didbaridze@atsu.edu.ge

Natalia Chkhartishvili
Akaki Tsereteli State University
Faculty of Exact and Natural
Sciences, Associate Professor Department of Biology,
Mob: +995 595 77 67 45
nato.chkhartishvili@atsu.edu.ge

QUANTITATIVE DETERMINATION OF BIOLOGICALLY ACTIVE IONS IN THE SPRING WATERS OF THE LAGVILAVA NEIGHBORHOOD, INCHKHURI VILLAGE, MARTVILI MUNICIPALITY, SAMEGRELO-ZEMO SVANETI (GEORGIA).

Abstract: *The objective of this study was to examine the chemical composition of spring waters in the Lagvilava neighborhood of Inchkhuri village, located in the Martvili Municipality of Samegrelo-Zemo Svaneti, Georgia. To achieve this, the studied springs were evaluated for pH, total water hardness, concentrations of Mg^{2+}, Ca^{2+}, Cu^{2+}, HCO_3^-, Br^-, Cl^-, and SO_4^{2-} ions, total iron (Fe), total arsenic (As), permanganate oxidizability, dissolved oxygen (O_2), 5-day biochemical oxygen demand (BOD_5), and free carbon dioxide (CO_2).*

The novelty and relevance of this work lie in the fact that the quantitative analysis of these biologically active ions in the specified spring sources was conducted for the first time.

***Key words**: Water, component, factor, significance, renewal, natural resource, life, spring, determination.*

***Language**: English*

Citation: Chikovani, M., Gegetchkori, L., Samkharadze, M., Didbaridze, I., & Chkhartishvili, N. (2026). Quantitative Determination of Biologically Active Ions in the Spring Waters of the Lagvilava Neighborhood, Inchkhuri Village, Martvili Municipality, Samegrelo-Zemo Svaneti (Georgia).. *ISJ Theoretical & Applied Science, 10 (162)*, 20-25.

Soi: https://s-o-i.org/1.1/TAS-10-162-4 ***Doi***: https://dx.doi.org/10.15863/TAS.2026.10.162.4

***Scopus ASCC**: 1602.*

Introduction

Georgia is a country rich in natural water resources, a quality attributed to its complex topography, diverse geological structure, and varied climatic conditions. Numerous springs of various types are formed throughout the country as atmospheric precipitation infiltrates subsurface layers, filters through rocks, and subsequently emerges at the surface. Spring waters are often characterized by high purity, natural balance, and pleasant taste characteristics.

The chemical and physical properties of Georgian spring waters depend significantly on the geological environment in which they are formed. Water composition varies according to the mineral makeup of the surrounding rocks, the depth of underground movement, and the residence time within subsurface reservoirs. Consequently, springs across different regions vary in their mineralization levels, temperature, acidity, and concentration of dissolved substances.

Georgia's territory features fresh as well as mineral and thermal springs. Fresh springs are primarily utilized as drinking water, whereas mineral and thermal waters are extensively used for therapeutic and preventative medical purposes.

Spring waters frequently contain elements essential for the human body, including calcium, magnesium, sodium, potassium, and various trace elements. These substances actively participate in metabolism, neurological functions, bone tissue formation, and the maintenance of overall systemic homeostasis. For these reasons, the quality and chemical composition of spring waters hold exceptional importance from the perspective of both daily consumption and therapeutic practice.

Water is the foundation of life—living organisms cannot survive without it. It plays a fundamental role in global biogeochemical cycles, where the hydrological cycle ensures the continuous renewal of water resources. It creates habitats for numerous plant and animal species, and plants absorb essential nutrients dissolved within it. Water is equally critical for human activity, serving imperative roles in drinking supply, industry, agriculture, hygiene, and energy production. Covering a vast portion of Earth's surface, water is ubiquitous—present around us and within our organisms. Like carbon, water is an indispensable chemical compound for living systems, making its importance to life impossible to overestimate.

Water is unevenly distributed across the globe. Beyond Earth's surface, it is present underground and in the atmosphere as water vapor. Soil also retains water alongside other compounds. Possessing unique physical and chemical properties, water is vital for vegetation, fauna, and human existence, representing a paramount natural resource. Under natural conditions, salts, gases, and organic substances are always dissolved in water in varying concentrations. Were it not so crucial for survival, human activity might have depleted this extraordinary substance long ago. Water constitutes an essential component of the diet, participating in metabolic processes, digestion, the excretion of metabolic waste products via urine, and thermoregulation. The biological demand for water varies based on climate, physical workload, health status, dietary composition, and other environmental factors.

Elements essential for living organisms that play a major role in their vital functions are termed **biogenic elements**. Many of these elements are present in organisms in minute quantities and are classified as **trace elements** (microelements). Trace elements enhance enzymatic activity and facilitate the synthesis of sugars, starches, proteins, nucleic acids, and vitamins. As a core component of nature, water sustains life, maintains ecosystem stability, and preserves ecological balance.

Geographical Context: Martvili Municipality

Martvili Municipality is situated in the north-eastern part of Western Georgia, spanning the Odishi Plain (southern part) and the foothills (central part) and southern slopes (northern part) of the Egrisi Range. It borders Lentekhi to the north, Khoni and Tsageri to the east, Senaki and Abasha to the south, and Chkhorotsku to the west.

The southern region of Martvili is occupied by a lowland that rises from the south-west to the north-east, with elevations ranging between 60 and 170 meters above sea level. The highest point—the source of the Tskhenistsqali/Tekhuri river system—reaches an altitude of 3,003 meters. The massifs of Mount Askhi border the south-west, featuring abundant karst caves, waterfalls, mineral deposits, and construction-

grade limestone. Furthermore, the mountain regions of Lebarde, Chegola, and Dviri are rich in therapeutic mineral waters.

Martvili Municipality is an administrative unit within the Samegrelo-Zemo Svaneti region of Georgia. Established in 1930, it was named Gegetchkori District from September 3, 1936, until 1990. Between 1963 and 1966, the Abasha District was temporarily merged into it. The administrative center is the town of Martvili.

River valleys form distinctive landforms along their banks, creating small alluvial plains and plateaus where orchards are cultivated on alluvial soils. The mountain massifs house unique flora and fauna species. The climate is humid subtropical. The primary water arteries are the Abasha, Inchkhia, and Tekhouri rivers. The municipality covers an area of 880.6 km², of which 300 km² is dedicated to agricultural land. Its major mineral wealth includes construction limestone as well as mineral waters (Lebarde, Chegola, among others).



Pic. 1

Results and Discussion:

The spring waters from the Lagvilava neighborhood of Inchkhuri village were analyzed for pH, water hardness, concentrations of Mg^{2+}, Ca^{2+}, Cu^{2+}, HCO_3^-, Br^-, Cl^-, and SO_4^{2-} ions, total Fe, total As, permanganate oxidizability, dissolved O_2, BOD_5, and free CO_2 using chemical and photocolorimetric analytical methods. Highly sensitive analytical procedures were selected. All testing was carried out at the Iason Moseshvili Hydrochemistry Laboratory, Department of Chemistry, Akaki Tsereteli State University. The analytical results are summarized in Table 1.

Table 1. Results of the Quantitative Determination of Biologically Active Ions in Spring Waters of the Lagvilava Neighborhood, Inchkhuri Village, Martvili Municipality

N	Angular name of spring waters	pH	mg-eq./L	Mg/L												
			Water hardness	Mg^{2+}	Ca^{2+}	total Fe	Cu^{2+}	Cl^-	Br^-	HCO_3^-	Free CO_2	Dissolved oxygen	total As	BOD_5	SO_4^{2-}	Permanganate oxidation
1	Tobashi	7,4	3,00	2,44	56,00	0,146	0.004	9,23	0,141	2,98	0,32	2,02	0,008	24,26	0,0011	0,96
2	Sakire	7,7	2,48	1,66	47,20	0,066	-	11,22	0,160	4,34	0,26	2,14	0,007	22,98	0,0048	0,56
3	Enveri	7,7	3,32	9,76	50,40	-	0,001	9,94	0,153	3,78	0,27	2,89	0.008	23,94	0,0105	0,66
4	Makhuzia	7,8	3,64	22,45	36,00	0,008	-	7,67	0,122	5.62	0,50	1,90	0,009	24,64	0,0170	0,80
5	Iosebi	7,5	3,08	11,22	43,20	0,100	-	8,38	0,213	4,46	0,58	1,25	0,006	22,72	0,0059	1,66
6	Jimsheri	7,4	2,20	0,97	42,40	0,333	0,001	9,37	0,081	4,56	0,51	1.70	0,010	19,20	0,0063	0,72
7	Lagvilava	7,8	4,20	20,98	49,60	0,144	0,002	10,08	0,210	3,38	0,38	2,27	0,009	24,70	0,0024	1,92

- **pH Values:** Ranged between 7.4 and 7.8 across all analyzed samples.
- **Water Hardness:** Highest in the Makhuzia spring (3.64 mEq/L) and lowest in the Jimsheri spring (2.20 mEq/L).
- **Mg^{2+} Content:** Reached its maximum in the Makhuzia spring (22.45 mg/L) and minimum in the Jimsheri spring (0.97 mg/L).
- **Ca^{2+} Content:** Highest in Tobashi (56.00 mg/L) and lowest in Makhuzia (36.00mg/L).
- **Total Fe:** Total Fe is higher in Tobashi spring (0.146 mg/L) and lowest in Makhuzia spring (0.008 mg/L); in Enveri spring, total iron was below the analytical detection limit.
- **Cu^{2+} Ions:** Cu^{2+} ions were highest in Tobashi spring (0.004 mg/L) and lower in Enveri and Jimsheri springs; Cu^{2+} was not detected in Sakire, Makhuzia, and Iosebi springs (below analytical sensitivity).
- **Cl^- Ions:** Measured highest in Sakire (11.22mg/L) and lowest in Iosebi (8.38 mg/L).
- **Br^- Ions:** Peak concentration observed in Lagvilava (0.210 mg/L) and minimum in Iosebi (0.081 mg/L).
- **HCO_3^- Ions:** Reached maximum levels in Makhuzia (5.62 mg/L) and minimum in Tobashi (2.98 mg/L).
- **Free CO_2:** Highest concentration found in Iosebi (0.58 mg/L) and lowest in Sakire (0.26 mg/L).
- **Total As:** Measured highest in Jimsheri (0.010 mg/L) and lowest in Iosebi (0.006 mg/L).
- **Dissolved O_2:** Highest in Lagvilava (2.27 mg/L) and lowest in Iosebi (1.25 mg/L).
- **BOD_5:** Maximum in Lagvilava (24.70 mg/L) and minimum in Jimsheri (19.20 mg/L).
- **Permanganate Oxidizability:** Peak value recorded in Lagvilava (1.92 mg/L), with the minimum in Sakire (0.5 mg/L).
- **SO_4^{2-} Ions:** Highest in Makhuzia (0.0170 mg/L) and lowest in Tobashi (0.0011 mg/L).

Experimental Part. Methodology for the Determination of Chemical Elements in Water. The analyses were carried out at the Iason Moseshvili Hydrochemistry Laboratory, Department of Chemistry, Faculty of Exact and Natural Sciences, Akaki Tsereteli State University. The analyses were performed using methods validated and widely applied in hydrochemical practice [4, 5, 6, 7].

1. **pH Determination:** Measured potentiometrically using a calibrated pH meter. (Potentiometer PH 673 – M)
2. **Ca^{2+}, Mg^{2+}, and Total Hardness:** The concentrations of Ca^{2+} and Mg^{2+}, as well as the total water hardness, were determined by complexometric titration using 0.01 N Complexone III. For the simultaneous determination of Ca^{2+} and Mg^{2+}, Eriochrome Black T was used as the indicator in the presence of an ammonia buffer. Ca^{2+} was determined using Murexide as the indicator in the presence of 2 N NaOH.
3. **HCO_3^- Ions:** Quantified acidimetrically using 0.1- 0.01 N HCl titrant with methyl orange as an indicator.
4. **Cl^- Ions:** Analyzed by mercurimetric titration using 0.01 N $Hg(NO_3)_2$_ with diphenylcarbazone indicator.
5. **Total Arsenic As:** Determined iodometrically using 0.05 N iodine solution as titrant and starch indicator.
6. **Total Iron Fe:** Spectrophotometrically analyzed after preliminary oxidation in alkaline media using sulfosalicylic acid (UN-5100B UV/VIS SPECTROPHOTOMETER).
7. **Cu^{2+} Ions:** Cu^{2+} ions were determined by spectrophotometry in an alkaline medium (ammonia) using sodium N,N-diethyldithiocarbamate as the complexing reagent with a (UN-5100B UV/VIS SPECTROPHOTOMETER**).**
8. **SO_4^{2-} Ions:** Determined gravimetrically via precipitation as barium sulfate ($BaSO_4$).
9. **NH_4^+ Ions:** Analyzed alkalimetrically using 0.1N NaOH} with phenolphthalein. Hydrogen ions liberated from the reaction between ammonium ions and formaldehyde were titrated with alkali.
10. **Free CO_2:** Quantified by alkalimetric titration (0.1 - 0.01 N NaOH) with phenolphthalein indicator in the presence of Rochelle salt.
11. **Permanganate Oxidizability:** Determined permanganometrically using 0.01 N $KMnO_4$, in acidic media, titrated back with 0.01 N $H_2C_2O_4$ oxalic acid.
12. **Dissolved O_2 and BOD_5:** The dissolved oxygen (DO) content and five-day biochemical oxygen demand (BOD5) were determined using the iodometric method (titrant: 0.01 N sodium thiosulfate). In an alkaline medium, manganese(II) ions are oxidized by dissolved oxygen present in the water, converting into a tetravalent manganese compound. Upon acidification of the solution in the presence of excess potassium iodide, free iodine is liberated, which is subsequently titrated.
13. **Br^- Ions**: Br^- ions were determined using the iodometric method. Sodium hydrogen phosphate, sodium hypochlorite, and sodium formate were added to the water sample, and the resulting mixture was heated and subsequently cooled. Potassium iodide, sulfuric acid, and ammonium molybdate were then added. The solution was titrated with 0.01 N sodium thiosulfate using starch as an indicator. Bromide ions were oxidized to bromate BrO_3^- ions by sodium hypochlorite.

Conclusion:

The physical and chemical parameters of the examined spring waters in the Lagvilava neighborhood of Inchkhuri village (Martvili Municipality)—including pH, hardness, major cations Mg^{2+}, Ca^{2+}, anions HCO_3^-, Cl-, SO_4^{2-}, microelements Cu^{2+}, total Fe, total As, Br^-, dissolved O_2, and oxygen demand parameters—generally comply with the Technical Regulations for Drinking Water of Georgia, with minor exceptions. Notably, bromide ion concentrations slightly exceed the national threshold limit (0.2 mg/L) in the osebi (0.213 mg/L) and Lagvilava (0.210 mg/L) springs. Overall, the investigated spring waters are deemed suitable for domestic and drinking purposes.

References:

1. Chikovani, M., Sophromadze, D., Gamkrelidze, E., Jikia, M., & Chiqvinidze, K. (2026). Hydrochemical investigation of biologically active ions in the spring waters of Lower Tkibuli, Tkibuli. *International Scientific Journal Theoretical & Applied Science*, 2026,158(06), pp.359–364.
2. Chikovani, M., Tabeshadze, E., Kakhidze, N., Kupatashvili, N., & Julakidze, N. (2026). Results of the analysis of spring waters of the village Ukheshi of Ambrolauri Municipality. *International Scientific Journal Theoretical & Applied Science*, 2026,157(05), pp.468–472.
3. Bregvadze, U., Natidze, M., & Mamulashvili, Z. (1997). *Chemistry and Microbiology of Water*. Ganatleba Publishing In Georgian, 1997, pp. 4–36.
4. Supatashvili, G. (2003). *Hydrochemistry of Georgia*. Tbilisi State University Publishing, 2003,pp. 3–10. (In Georgian)

5. Chikovani, M., Megrelishvili, N., Kakhidze, N., Julakidze, N., & Kopaliani, Z. (2025). Study of biologically active ions in the waters of the springs in Lasuriashi and Makhashi villages, Tsageri Municipality, Georgia. *International Scientific Journal Theoretical & Applied Science*, 2025,146(06), pp.66–69.
6. Cikovani, M., Gabelashvili, M., Ghambashidze, A., Akimchevi, N., Kupatashvili, N., Lomsianidze, I., & Endeladze, N. (2025). Investigation of physiologically active ions and microbiological characteristics of gastric spring water in the small town of Tskhaltubo. *International Scientific Journal Theoretical & Applied Science*, 2025,146(06), pp.45–50.
7. Chikovani, M., Gamkrelidze, E., Megrelishvili, N., Kakhidze, N., Natchkebia, I., & Khurcidze, L. (2025). Determination of some vital ions in spring waters of the village of Akhuti in the Chkhorotsku Municipality (Georgia). *International Scientific Journal Theoretical & Applied Science*, 2025,145(05), pp.66–70.
8. Chikovani, M., Samkharadze, M., Rusia, M., Endeladze, N., & Papava, N. (2025). Determination of the hydrochemical composition of water from some Georgian springs (in the village of Khidari, Kharagauli Municipality) by different analysis methods. *Asian Journal of Research*, 2025,pp.1–6.
9. Chikovani, M., Gegetchkori, L., Samkharadze, M., Didbaridze, I., & Chkhartishvili, N. (2026). The Hydrochemical Composition and Quantitative Determination of Physiologically Active Ions in the Inchkhuri – Patara Inchkhuri Spring System, Martvili Municipality, Georgia. *International Journal*, 2026,9(5), pp.1–13.
10. Chikovani, M., Gabelashvili, M., Gambashidze, A., Jikia, M., & Kupatashvili, N. (2025). Hydrochemical and sanitary-microbiological investigation of the spring waters of Dimi and Nergeti in the Baghdati Municipality to determine drinking water suitability. *International Scientific Journal Theoretical & Applied Science*, 2025,144(04), pp.84–88.
11. Chikovani, M., Julakidze, N., Jikia, M., Lomsianidze, I., Didbaridze, I., & Mogeladze, A. (2024). Quantitative Study of Some Biologically Active Ions In The Fresh Waters of Sukhche Village (Khoni Municipality, imereti Region) And Their Significance The Vitalitu of living organisms. Proceedings of te Georgian National Academy of Sciences. Biomedikal series.2024, 50 (4-6), pp. 159-161.
12. Chikovani, M., Kupatashvili, N., Endeladze, N., Rukhaia, K., & Makhareishvili, M. (2024). Hydrochemical analysis of some springs of Salominao village of Vani Municipality. *Georgian Scientists*, 2024,6(2), pp.433–438.
13. Chikovani, M., Megrelishvili, N., Julakidze, N., & Furtskhvanidze, M. (2024). Examination of the chemical composition of water from the well of Rufoti village, Terjola Municipality. *International Scientific Journal Theoretical & Applied Science*, 2024,133(05), pp.40–44.
14. Supatashvili, G. (2010). *Quantitative Analysis*. Tbilisi University Press, pp. 20–81. (In Georgian)
15. Supatashvili, G. (2016). *Practicum of Quantitative Analysis*. Tbilisi University Press, pp. 56–90. (In Georgian)
16. Chikovani, M., Kupatashvili, N., & Jolokhava, M. (2023). Hydrochemical analysis of some fresh waters of Lejokhe, Letane and Mikava villages of Tsalenjikha Municipality. *International Scientific Journal Theoretical & Applied Science*, 11(127), 238–241.
17. Chikovani, M., Kakhidze, N., Balavadze, L., Giorgadze, N., & Pataridze, M. (2023). Examination of the chemical composition of spring waters in Aketi village of Lanchkhuti Municipality. *RS Global: World Science*, 3(81), 1–4.
18. Chikovani, M., Megrelishvili, N., & Kvastiani, A. (2022). Hydrochemical examination of Muashi and Lentekhi mineral water of Lentekhi district. *RS Global Journals: World Science*, 4(76), 1–3.
19. Chikovani, M., Gabelashvili, M., Kupatashvili, N., Gambashidze, A., & Zedashidze, G. (2022). Hydrochemical and sanitary microbiological examination of spring waters of Nakhunao community of Martvili Municipality. *International Scientific Journal Theoretical & Applied Science*, 08(112), 308–313.
20. Chikovani, M., Gabelashvili, M., Zarqua, M., & Megrelishvili, N. (2020). Hydrochemical and sanitary microbiological research of the Elena Hill spring waters in the Nakhunao community of Martvili Municipality. *World Science*, 1(6/58), 27–32.
21. Chikovani, M., Kupatashvili, N., & Kurasbediani, M. (2019). Hydrochemical analysis of some mineral waters. *European Sciences Review*, 1, 123–126.
22. Chikovani, M., & Gabelashvili, M. (2018). Hydro-chemical and hydro-biological research of the water from the Rioni. *Indian Journal of Applied Research*, 8(5), 127–130.
23. Kikalishvili, M., & Kurasbediani, M. (2016). Determination of the chemical composition of mineral water in Babili village, Lentekhi district. *Bulletin of the Georgian National Academy of Sciences (Chemical Series)*, 42(3), 416–418. (In Georgian)

Impact Factor:					
	ISRA (India) = 6.317	SIS (USA) = 0.912	ICV (Poland) = 6.630
	ISI (Dubai, UAE) = 1.582	РИНЦ (Russia) = 0.191	PIF (India) = 1.940
	GIF (Australia) = 0.564	ESJI (KZ) = 8.100	IBI (India) = 4.260
	JIF = 1.500	SJIF (Morocco) = 6.004	OAJI (USA) = 0.350

SOI: 1.1/TAS DOI: 10.15863/TAS

International Scientific Journal

Theoretical & Applied Science

p-ISSN: 2308-4944 (print) **e-ISSN:** 2409-0085 (online)

Year: 2026 **Issue:** 10 **Volume:** 162

Received: 21.10.2026
Accepted/Published: 30.10.2026

https://T-Science.org

Issue Article

Jakhongir Tojiboev
Namangan State University
Doctoral student

REFUGEES IN TURKESTAN DURING THE FIRST WORLD WAR: TERRITORIAL DISTRIBUTION AND ADMINISTRATIVE APPROACHES

Abstract: *This article examines the issue of refugees forcibly displaced to Turkestan from the western frontline regions of the Russian Empire during the First World War. Drawing on statistical data as of November 15, 1915, the study analyzes the settlement of refugees in the Transcaspian, Syrdarya, Fergana, and Samarkand regions. The article highlights the uneven territorial distribution of refugees and demonstrates that major administrative, transport, and economic centers became the principal areas of reception and accommodation. It also discusses the arrival and placement of refugees in the Emirate of Bukhara, particularly in Charjui and New Bukhara. The findings show that the refugee question in Turkestan was not an isolated or temporary phenomenon, but rather a large-scale and systematic manifestation of wartime migration. The study contributes to a broader understanding of the demographic, social, and administrative consequences of the First World War in Central Asia.*

Key words: *First World War, Turkestan region, refugees, forced migration, Transcaspian region, Syrdarya region, Fergana region, Samarkand region, Emirate of Bukhara, settlement policy.*

Language: *English*

Citation: Tojiboev, J. (2026). Refugees in Turkestan during the first world war: territorial distribution and administrative approaches. *ISJ Theoretical & Applied Science, 10 (162),* 26-30.

Soi: https://s-o-i.org/1.1/TAS-10-162-5 ***Doi***: crossref https://dx.doi.org/10.15863/TAS.2026.10.162.5

Scopus ASCC: *1202.*

Introduction

The First World War left a profound mark on history not only through military and political developments but also through large-scale demographic shifts, forced displacement, and social crises. During the war, military operations along the western borders of the Russian Empire compelled millions of civilians to leave their homes. As a result, people displaced from territories such as Poland, Lithuania, Belarus, Ukraine, and Latvia were directed to the empire's interior governorates, the Volga region, Siberia, the Far East, and Central Asia. This process became one of the largest episodes of forced migration in the history of the Russian Empire.

This migratory movement also directly affected Turkestan. Situated far from the front and regarded as a relatively stable interior territory, the Governor-Generalship of Turkestan became one of the empire's important regions for the temporary accommodation and supervision of refugees and for their potential employment as a labor force. Railway networks, major administrative centers, urban infrastructure, and the capacities of local authorities played particularly important roles in receiving refugees.

By 1915, the number of refugees in the Transcaspian, Syrdarya, Fergana, and Samarkand regions of Turkestan had increased substantially. Their distribution among regions and uyezds (districts) was uneven: certain localities, notably the administratively and logistically significant centers of Tashkent, Ashgabat, Merv, Skobelev, and Samarkand, became principal reception points. Conversely, the small numbers recorded in certain uyezds, or the incompleteness of their statistical records, also reveal problems in wartime recordkeeping. This suggests that refugee settlement was not implemented according to a strictly centralized plan but rather in accordance with local capacities, infrastructural resources, and administrative functions.

The study of refugees in Turkestan is important for a deeper understanding of the socioeconomic processes of the First World War. The influx of refugees directly affected local administration, food supplies, housing, sanitary and medical conditions, labor markets, and the activities of charitable organizations. Accordingly, this issue should be examined not merely as a demographic or statistical phenomenon but as a complex historical process that influenced the social, economic, and administrative life of wartime Turkestan.

This article aims to analyze the scale, territorial distribution, and settlement patterns of refugee movements into Turkestan during the First World War on the basis of historical and statistical evidence. Drawing on archival records dated November 15, 1915, region-level statistics, and existing scholarship, it examines refugee settlement in the Transcaspian, Syrdarya, Fergana, and Samarkand regions and the Emirate of Bukhara. Through historical-comparative analysis, statistical analysis, and a territorial approach, the article seeks to demonstrate that the refugee question in Turkestan was a large-scale, systemic social phenomenon.

LITERATURE REVIEW AND METHODS

The refugee crisis that emerged in the Russian Empire during the First World War has developed into a distinct field of historical scholarship. Researchers regard it not only as a consequence of a military-political crisis but also as a major socioeconomic and demographic displacement within the empire, an instance of forced migration, and a serious test for the state administration.

The studies of I. B. Belova are particularly important to this subject. Belova examines forced migrants in the Russian Empire during the First World War, including refugees and prisoners of war, from an empire-wide perspective, focusing on their numbers, composition, accommodation, and social circumstances [4]. Her approach makes it possible to understand the refugee question not simply as evacuation from frontline areas but as a complex historical phenomenon affecting socioeconomic life in the interior regions.

P. Gatrell's scholarship is distinguished by its placement of the Russian Empire's refugee crisis within international historiography. In A Whole Empire Walking: Refugees in Russia during World War I, he interprets wartime refugee movements as a demographic and humanitarian crisis encompassing the entire empire [6]. His article "War, Refugeedom, Revolution: Understanding Russia's Refugee Crisis, 1914–1918" likewise examines the refugee question in relation to war, revolution, and the weakening of state institutions [5]. This approach provides a theoretical basis for assessing the refugee influx into Turkestan as part of the Russian Empire's wider migratory processes.

The studies of A. M. Tikhonova and S. Kuznetsova likewise address refugees' difficult social circumstances, exploitation, employment, and dependence on assistance from state and public organizations [7; 11].

M. Stockdale analyzes patriotism, mobilization, and citizenship in Russian society during the First World War [10]. This perspective allows the refugee question to be considered not only as a humanitarian challenge but also as a process associated with the empire's political and social mobilization systems.

At the same time, most existing studies examine the refugee question in the Russian Empire as a whole or in selected central governorates. The movement of refugees to Turkestan, their distribution among regions and uyezds, the local administrative system, and the territorial characteristics of settlement have received insufficient focused attention. The contribution of this article therefore lies in its specific examination of refugee settlement in Turkestan using documents from the National Archives of Uzbekistan and statistical information dated November 15, 1915 [1; 2; 3; 4; 5; 6].

RESULTS AND DISCUSSION

The First World War (1914–1918) inflicted enormous losses on the Russian Empire, and the exceptionally large number of people forcibly displaced within the country was among its most serious consequences. Beginning in 1914, refugees from areas affected by military operations began arriving in various parts of the empire. Between 1914 and 1917, approximately five million people were compelled, under orders and pressure from military authorities, to leave their homes and places of birth and move to interior governorates in central Russia, the Volga region, Siberia, the Far East, and Central Asia. They came primarily from areas affected by fighting on the Western Front, including the territories of present-day Poland, Lithuania, Belarus, Ukraine, and Latvia [14]. Refugees also began moving into the regions of the Governor-Generalship of Turkestan, and by late 1915 their numbers had become substantial.

Table 1. Refugee population in the Transcaspian Region (as of November 15, 1915) [5]

No.	Uyezd (district)	Present-day name	Number of refugees
1	Ashgabat	Ashgabat	6033
2	Krasnovodsk	Turkmenbashi	1258
3	Merv	Mary	6687
4	Tejen	Tejen	520
5	Mangyshlak	Mangyshlak	—
	Total		14498

The table indicates that, by late 1915, refugee settlement in the Transcaspian Region was geographically extensive and unevenly distributed. Nearly 14,500 refugees were living across four uyezds, demonstrating that the region had become an important reception area during the war. This situation was directly related to its geographical location, proximity to railway and port infrastructure, and administrative capacity.

The largest numbers of refugees were accommodated in Merv and Ashgabat uyezds, suggesting that these districts had relatively greater capacity to receive displaced people. The presence of 756 refugees in the settlement of Yolotan in Merv uyezd and 500 in Kaakhka in Ashgabat uyezd shows that refugees were settled not only in major urban centers but also in smaller localities with suitable transport connections and living conditions.

In addition, 801 refugees found shelter in the town of Kizyl-Arvat in Krasnovodsk uyezd, indicating that this transport and industrial center played a significant role in receiving refugee movements. This evidence supports the importance of economic infrastructure and employment opportunities as factors in refugee settlement policy.

These figures suggest that settlement in the Transcaspian Region was organized not according to a uniform centralized plan but on the basis of each territory's practical capacity and functional significance. The wartime migration policy was therefore adaptable, although the burden of refugee reception remained uneven across districts.

Table 2. Refugee population in the Syrdarya Region (as of November 15, 1915) [5]

No.	Uyezd (district)	Present-day name	Number of refugees
1	Tashkent	Tashkent	16584
2	Chimkent	Shymkent	2883
3	Aulie-Ata	Taraz	2038
4	Perovsk	Kyzylorda	585
5	Kazalinsk	Kazaly	588
	Total		22678

The table reveals a clear tendency toward concentration in refugee settlement in the Syrdarya Region. The largest number of refugees was recorded in Tashkent uyezd, indicating that its administrative, economic, and infrastructural capacity exceeded that of the other districts. Approximately 14,000 refugees resided in the city of Tashkent alone, confirming the city's role as a principal wartime reception and distribution center.

Nearly 3,000 refugees were accommodated in the town of Chernyaev in Chimkent uyezd, making it the second-largest reception point in the Syrdarya Region. This may be explained by Chernyaev's proximity to transport routes, economic activity, and employment opportunities. At the same time, the marked numerical difference between Tashkent and Chernyaev points to an unequal distribution of the settlement burden.

These indicators demonstrate that refugee settlement in the Syrdarya Region was directed primarily toward major urban centers and that territories with stronger administrative institutions and infrastructure absorbed the main flow of displaced people.

Table 3. Refugee population in the Fergana Region (as of November 15, 1915) [6]

No.	Uyezd (district)	Present-day name	Number of refugees
1	Kokand	Kokand	2163
2	Skobelev	Fergana	9767
3	Namangan	Namangan	2900
4	Andijan	Andijan	4425
5	Osh	Osh	1440
	Total		20695

These data show that refugee settlement in the Fergana Region was characterized by territorial inequality and a tendency toward concentration. The largest share of refugees was accommodated in Skobelev uyezd, suggesting that its infrastructure, proximity to transport routes, and administrative capacity were superior to those of other districts. Almost half of the region's prisoners of war—approximately 10,000 individuals—were reportedly accommodated in this district, further underscoring Skobelev's role as a strategic and organizational center.

Andijan, Namangan, and Kokand uyezds followed in terms of refugee numbers, suggesting a policy of phased distribution. In particular, 807 and 258 refugees found shelter in Jalal-Abad and Bazar-Korgon, respectively, in Andijan uyezd. This indicates that refugees were accommodated not only in major urban centers but also, to a lesser extent, in smaller settlements, reflecting an effort to make wider use of local economic and social resources.

These circumstances indicate that refugee settlement policy in the Fergana Region took shape through a combination of geographical, demographic, and administrative factors, with some uyezds bearing a considerably greater burden than others.

Table 4. Refugee population in the Samarkand Region (as of November 15, 1915) [6]

No.	Uyezd (district)	Present-day name	Number of refugees
1	Samarkand	Samarkand	8400
2	Kattakurgan	Kattakurgan	2849
3	Jizzakh	Jizzakh	—
4	Khujand	Khujand	—
	Total		11249

By November 15, 1915, more than 11,000 refugees had been recorded in the Samarkand and Kattakurgan uyezds of the Samarkand Region, demonstrating the importance of these districts as reception centers. At the same time, the absence of figures for refugees residing in Jizzakh and Khujand uyezds may reflect territorial variations in statistical recordkeeping, gaps in documentation, or a lower administrative priority assigned to those districts. This allows the tentative conclusion that the wartime system of administrative accounting did not function fully or consistently.

Refugees were also brought to and accommodated within the Emirate of Bukhara. Official documents recorded 792 refugees in the emirate at that time [6]. Following the establishment of a designated residential facility for refugees, arrivals increased in Charjui, which belonged to the emirate. At the beginning of 1915, 560 adult refugees and 156 children were recorded there [1]. According to information from the imperial political agency in Bukhara, approximately 800 refugees were accommodated in New Bukhara (Kagan) and Charjui [2]. By late 1915, a further 200 refugees had arrived at each of the refugee camps in Charjui and New Bukhara. One-sixth of these arrivals were children [3; 4].

CONCLUSION

A comparative analysis of the tables above indicates that, as of November 15, 1915, the number of refugees in Turkestan approached 70,000. This figure demonstrates the considerable scale of wartime migration and confirms that Turkestan had become one of the Russian Empire's major regions for receiving and accommodating refugees.

The rapid growth in refugee numbers can be attributed, on the one hand, to the intensity of military operations and forced displacement in the frontline territories and, on the other, to Turkestan's

geographical position, transport networks, and relative stability as an interior region. The regional differences documented in the tables suggest that refugee settlement was carried out not through a single centralized system but according to the practical capacities of individual regions and uyezds.

The presence of nearly 70,000 refugees also placed a sharply increased burden on Turkestan's socioeconomic and sanitary systems. This situation presented state and public institutions with complex challenges concerning food supplies, housing, employment, and healthcare. Under these conditions, organizational, financial, and medical measures undertaken by government bodies and charitable organizations played an important role in managing the refugee influx.

Overall, the figures established through analysis of these tables support the conclusion that the refugee question in Turkestan during the First World War was not an episodic occurrence but a large-scale, systemic social phenomenon that significantly influenced the region's demographic, economic, and social development.

References:

1. (n.d.). National Archives of Uzbekistan (NAUz), fond I-1, opis 3, delo 1270, fol. 3.
2. (n.d.). National Archives of Uzbekistan (NAUz), fond I-1, opis 3, delo 1270, fol. 17.
3. (n.d.). National Archives of Uzbekistan (NAUz), fond I-1, opis 3, delo 1270, fol. 19.
4. (n.d.). National Archives of Uzbekistan (NAUz), fond I-1, opis 3, delo 1270, fol. 20.
5. (n.d.). National Archives of Uzbekistan (NAUz), fond I-1, opis 3, delo 1270, fol. 24.
6. (n.d.). National Archives of Uzbekistan (NAUz), fond I-1, opis 3, delo 1270, fol. 25.
7. Belova, I. B. (2014). *Forced Migrants: Refugees and Prisoners of War of the First World War in Russia, 1914-1925*. Moscow: AIRO-XXI, 2014, p. 15. [In Russian.].
8. Gatrell, P. (2017). *"War, Refugeedom, Revolution: Understanding Russia's Refugee Crisis, 1914-1918."* 2017, nos. 1-2 (58), pp. 123-146. Retrieved from https://doi.org/10.4000/monderusse.10073
9. Gatrell, P. (2005). *A Whole Empire Walking: Refugees in Russia during World War I.* Bloomington: Indiana University Press, 2005, p. 217.
10. Kuznetsova, S. (2025). "*Refugees Are the Most Inhumanely Exploited Group."* Retrieved November 10, 2025 from https://www.kommersant.ru/doc/5651263 [In Russian.].
11. Mikhalev, N. A., & Pyankov S. A. (2015). "Refugees of the First World War in the Russian Empire: Numbers, Settlement, and Composition." *Ural Historical Journal*, 2015, no. 4 (49), pp. 95-105. [In Russian.].
12. Solovyova, E. A. (2019). "The Fate of Refugees during the First World War (Based on Materials from Simbirsk Governorate)." *Vlast*, 2019, no. 5, pp. 216-222. [In Russian.].
13. Stockdale, M. (2016). *The Mobilizing the Russian Nation: Patriotism and Citizenship in the First World War*. Cambridge University Press, 2016, p. 110.
14. Tikhonova, A. M. (2013). *"Refugees of the First World War."* Retrieved from https://svrt.ru/lib/savel-2013/tihonova.pdf [In Russian.].

Impact Factor:					
	ISRA (India) = 6.317	SIS (USA) = 0.912	ICV (Poland) = 6.630
	ISI (Dubai, UAE) = 1.582	РИНЦ (Russia) = 0.191	PIF (India) = 1.940
	GIF (Australia) = 0.564	ESJI (KZ) = 8.100	IBI (India) = 4.260
	JIF = 1.500	SJIF (Morocco) = 6.004	OAJI (USA) = 0.350

SOI: 1.1/TAS DOI: 10.15863/TAS

International Scientific Journal

Theoretical & Applied Science

p-ISSN: 2308-4944 (print) **e-ISSN:** 2409-0085 (online)

Year: 2026 **Issue:** 10 **Volume:** 162

Received: 22.10.2026
Accepted/Published: 30.10.2026

https://T-Science.org

Issue Article

Dilshod Normurod ugli Quziev
Karshi State Technical University
180100 Karshi, Uzbekistan
Corresponding author
nurik_1980@mail.ru

EFFECT OF BENTONITE APPLICATION METHOD, TIMING AND RATE ON FIELD EMERGENCE, GROWTH, NODULATION AND YIELD STRUCTURE OF SOYBEAN

Abstract: *The effects of the method, timing and rate (100–750 kg ha^{-1}) of bentonite application against an $N_{90}P_{60}K_{90}$ background on field emergence, plant density, growth, nodulation and yield structure of soybean cv. 'Uzbek-6' were studied on light serozem soils of Kashkadarya region (2024–2026). Bentonite applied at sowing increased field emergence from 84.1 % to 84.8–87.2 % and final plant density by 1.5–6.8 %, whereas split application at budding and flowering increased seed mass per plant by 3.6–13.8 %. Plant density correlated closely with bentonite rate (r = 0.925–0.991) and field emergence (r = 0.924), and seed mass per plant with plant survival (r = 0.903).*

Key words: *soybean, bentonite, light serozem, field emergence, plant density, leaf area index, nodulation, yield structure, correlation, regression.*

Language: *English*

Citation: Quziev, D.N. (2026). Effect of bentonite application method, timing and rate on field emergence, growth, nodulation and yield structure of soybean. *ISJ Theoretical & Applied Science, 10 (162),* 31-37.

Soi: https://s-o-i.org/1.1/TAS-10-162-6 ***Doi***: https://dx.doi.org/10.15863/TAS.2026.10.162.6

Scopus ASCC: *1100.*

Introduction

Soybean (*Glycine max* (L.) Merr.) is a protein and oil-rich legume capable of biological nitrogen fixation. The light serozem soils of Kashkadarya region are low in humus and retain little water, so uniform emergence and an optimal plant stand are key yield factors there. Soybean emergence declines sharply with the number of days of insufficient seed-zone moisture (T.C.Helms *et al*., 1996) and with increasing soil crust strength (R.J.Hanks va Thorp F.C.; 1957).

Natural mineral amendments such as bentonite, zeolite and glauconite are increasingly used to improve soils (F.A.Mumpton, 1999). In semi-arid China, 6-30 t ha^{-1} of bentonite increased field water-holding capacity, millet emergence and photosynthesis (J.Mi, *et al*., 1996) and soil microbial biomass by 3-50 % (J.Mi, *et al*., 2021). In a long-term Polish experiment, bentonite increased organic carbon, total nitrogen (J.Czaban *et al*., 2013), cation exchange capacity and available P and K in sandy soil (J.Czaban and Siebielec G., 2013); similar effects were found in tropical sandy soil (J.Croker *et al*., 2004), and a bentonite-humic acid amendment remained effective for 4-5 years (L.Zhou *et al*., 2022, B.Ma *et al*., 2022).

Soybean productivity depends on nodule bacteria, whose activity is inhibited by soil mineral nitrogen, especially nitrate (J.G.Streeter, 1988, N.Yamashita, 2019). Locally, bentonite seed coating has been studied for winter wheat on light serozem soils (X.R.Tog'ayeva, 2026), but the effects of the method, timing and low rates (100–750 kg ha^{-1}) of bentonite application on soybean have not been sufficiently studied.

The aim of the study was to determine the effect of bentonite application method, timing and rate on field emergence, plant density, growth, nodulation and yield structure of soybean and to assess the correlation and regression relationships between these traits.

MATERIALS AND METHODS

Field experiments were conducted in 2024-2026 at the central experimental site of the Southern Research Institute of Agriculture (Karshi district, Kashkadarya region) on light serozem soils in a 1:1 (legume: cereal) short-rotation system. Variety of soybean "Uzbek-6", included in the State Register, was sown as a main crop at 60×5 cm (theoretical density 333.3 thousand plants ha^{-1}); seeds were treated with nitragin before sowing.

The experiment comprised 14 treatments (Table 1) in three replications arranged in a single tier. Plots were 4.8 m wide (furrow spacing 60 cm) and 50 m long (240 m^2), with a recorded area of 120 m^2; the total experimental area was 1.0 ha.

Mineral fertilizers (ammonium nitrate, 34 % N; superphosphate, 20 % P_2O_5; potassium salt, 40 % K_2O) were applied at $N_{90}P_{60}K_{90}$ kg ha^{-1} in all treatments except treatment 8: phosphorus and potassium entirely before ploughing, and nitrogen in two equal doses at the beginning of budding and at flowering (75-80 % of plants flowering).

Bentonite clay was applied at 100, 200, 300, 400, 500 and 750 kg ha^{-1} together with mineral fertilizers using a cultivator: at sowing (treatments 9-14), in equal parts at budding and flowering (treatments 3-7), or at sowing, budding and flowering at 250 kg ha^{-1} each (treatment 2). Treatment 1 ($N_{90}P_{60}K_{90}$) and treatment 8 (no mineral fertilizers; 750 kg ha^{-1} bentonite before autumn ploughing) served as controls.

Field emergence and final plant density were determined by plant counts, and survival as the ratio of final to emerged plants (B.A.Dospekhov, 1985). In 2024, plant height, leaf area (disc method; LAI calculated from leaf area per plant and plant density), nodule number and mass (A.A.Nichiporovich, 1963) and yield structure were determined. Correlation and regression analyses were performed on treatment means in Python 3 (SciPy); model significance was assessed by F- and t-tests ($p < 0.05$), and application methods were compared using a paired t-test.

RESULTS AND DISCUSSION

In the control ($N_{90}P_{60}K_{90}$), field emergence was 84.1 % and the number of emerged plants was 280.2 thousand ha^{-1} (Table 1). Bentonite applied at sowing increased field emergence from 84.8 % (100 kg ha^{-1}) to 87.2 % (750 kg ha^{-1}), and the number of emerged plants exceeded the control by 2.6-10.3 thousand ha^{-1}.

When bentonite was applied at budding and flowering (treatments 3-7), emergence (83.8-84.4 %) did not differ from the control, since bentonite was applied after emergence ($r = 0.293$; $p = 0.573$).

Table 1. Effect of bentonite application method, timing and rate on field emergence and plant density of soybean (mean of 2024–2026)

No.	Treatment (bentonite rate, kg ha^{-1})	Bentonite application timing, kg ha^{-1}			Field emergence, %	Emerged plants, thousand ha^{-1}	Final plant density, thousand ha^{-1}	Plant survival, %
		at sowing	budding	flowering				
1	Control ($N_{90}P_{60}K_{90}$)	–	–	–	84.1	280.2	245.9	87.8
2	$N_{90}P_{60}K_{90}$ + 750	250	250	250	85.6	285.3	257.1	90.1
3	$N_{90}P_{60}K_{90}$ + 100	–	50	50	84.2	280.8	248.3	88.4
4	$N_{90}P_{60}K_{90}$ + 200	–	100	100	83.8	279.2	248.9	89.1
5	$N_{90}P_{60}K_{90}$ + 300	–	150	150	83.9	279.7	251.0	89.7
6	$N_{90}P_{60}K_{90}$ + 400	–	200	200	84.4	281.3	252.4	89.7
7	$N_{90}P_{60}K_{90}$ + 500	–	250	250	84.2	280.5	253.5	90.4
8	Control (750 kg ha^{-1} before autumn ploughing)	–	–	–	84.9	283.1	249.3	88.1
9	$N_{90}P_{60}K_{90}$ + 750	750	–	–	87.2	290.5	262.6	90.4
10	$N_{90}P_{60}K_{90}$ + 100	100	–	–	84.8	282.8	249.7	88.3
11	$N_{90}P_{60}K_{90}$ + 200	200	–	–	85.5	284.8	253.4	89.0
12	$N_{90}P_{60}K_{90}$ + 300	300	–	–	86.3	287.8	258.0	89.7
13	$N_{90}P_{60}K_{90}$ + 400	400	–	–	87.0	290.1	260.8	89.9
14	$N_{90}P_{60}K_{90}$ + 500	500	–	–	86.9	289.5	260.3	89.9

Note: seeds were sown as a main crop at 60 × 5 cm (theoretical density 333.3 thousand plants ha^{-1}).

Plant density and survival

In the control, final plant density was 245.9 thousand ha^{-1} and plant survival 87.8 %. Bentonite applied at sowing increased final density to 249.7–262.6 thousand ha^{-1}, i.e. by 3.8–16.7 thousand ha^{-1} (1.5–6.8 %); the difference between 750 and 400 kg ha^{-1} was only 1.8 thousand ha^{-1} (0.7 %).

When bentonite was applied at budding and flowering, emergence did not change, but survival increased from 88.4 % (100 kg ha^{-1}) to 90.4 % (500 kg ha^{-1}), and final density exceeded the control by 2.4–7.6 thousand ha^{-1} (1.0–3.1 %). At equal rates (100–500 kg ha^{-1}), application at sowing provided 1.4–8.4 thousand ha^{-1} more plants than split application ($p = 0.010$), mainly due to better emergence ($p = 0.007$).

Table 2. Effect of bentonite application method, timing and rate on plant height, leaf area index and nodule number of soybean (2024)

No.	Treatment (bentonite rate, kg ha^{-1})	Plant height, cm				Leaf area index, m^2 m^{-2}					Nodules, no. plant^{-1}		
		B	F	PG	M	TL	B	F	PF	PR	B	F	PG
Control treatments													
1	Control ($N_{90}P_{60}K_{90}$)	34.3	61.3	87.8	94.1	0.23	1.15	3.04	3.85	2.08	13.9	26.7	20.2
8	Control (750 kg ha^{-1} before autumn ploughing)	30.3	55.1	78.9	84.6	0.23	0.98	2.66	3.24	1.53	20.2	35.9	28.2
Bentonite at sowing													
10	$N_{90}P_{60}K_{90}$ + 100	35.1	62.0	90.9	97.8	0.24	1.17	3.18	3.87	2.17	15.3	27.5	23.3
11	$N_{90}P_{60}K_{90}$ + 200	35.6	62.7	92.1	97.8	0.25	1.22	3.23	4.03	2.26	16.2	29.1	23.5
12	$N_{90}P_{60}K_{90}$ + 300	35.6	62.7	91.2	96.7	0.26	1.23	3.21	4.12	2.29	17.0	29.4	24.0
13	$N_{90}P_{60}K_{90}$ + 400	35.8	63.5	91.6	97.5	0.25	1.26	3.34	4.13	2.27	17.6	29.3	24.8
14	$N_{90}P_{60}K_{90}$ + 500	35.9	63.1	92.5	98.9	0.25	1.26	3.35	4.17	2.37	17.5	29.6	24.9
9	$N_{90}P_{60}K_{90}$ + 750	36.4	63.7	92.2	99.6	0.25	1.27	3.33	4.28	2.39	17.4	31.2	24.1
Bentonite at budding and flowering (50 : 50)													
3	$N_{90}P_{60}K_{90}$ + 100	33.8	61.4	89.8	96.9	0.25	1.13	3.10	4.10	2.21	14.1	26.8	22.3
4	$N_{90}P_{60}K_{90}$ + 200	33.9	61.7	91.7	97.5	0.24	1.16	3.20	4.17	2.28	14.3	27.7	24.1
5	$N_{90}P_{60}K_{90}$ + 300	34.3	62.4	92.6	100.3	0.24	1.14	3.18	4.27	2.40	13.4	28.0	23.6
6	$N_{90}P_{60}K_{90}$ + 400	33.9	61.4	93.3	99.4	0.24	1.16	3.19	4.31	2.42	14.2	27.5	24.4
7	$N_{90}P_{60}K_{90}$ + 500	34.2	61.4	93.8	101.3	0.24	1.14	3.16	4.36	2.46	14.3	28.5	24.4
Bentonite at sowing, budding and flowering (250 + 250 + 250 kg ha^{−1})													
2	$N_{90}P_{60}K_{90}$ + 750	35.8	64.8	94.2	101.5	0.25	1.20	3.39	4.41	2.45	16.6	31.6	27.0

Note: TL – trifoliate leaf, B – budding, F – flowering, PF – pod formation, PG – pod filling, PR – pod ripening, M – maturity; seeds were treated with nitragin; nodules were counted by the monolith method on five plants from replications 1 and 3.

Plant height and leaf area index

Bentonite applied at sowing accelerated growth from the early stages: plant height was 35.1–36.4 cm at budding (control 34.3 cm; +2.3–6.1 %) and 96.7–99.6 cm at maturity (control 94.1 cm; +2.8–5.8 %) (Table 2). Split application did not affect height up to flowering, but accelerated later growth: at maturity plants reached 96.9–101.3 cm (+3.0–7.7 %). The tallest plants were recorded in treatment 2 (101.5 cm) and the shortest in treatment 8 without mineral fertilizers (84.6 cm; 10.1 % below the control).

LAI peaked at pod formation (control 3.85 m^2 m^{-2}). Bentonite applied at sowing increased LAI at budding by 1.7–10.4 % and at flowering by 4.6–10.2 %. Split application did not change LAI in the early stages, but at pod formation it reached 4.10–4.36 m^2 m^{-2} (+6.5–13.2 %), significantly exceeding application at sowing ($p < 0.001$); leaf area per plant was also the largest in these treatments (1651–1720 cm^2). The highest LAI was found in treatment 2 (4.41) and the lowest in treatment 8 (3.24; 15.8 % below the control).

Nodulation

Nodulation peaked at flowering (Table 2). Bentonite applied at sowing enhanced nodulation already at budding: nodule number increased to 15.3–17.6 per plant (control 13.9; +10.1–26.6 %) and nodule fresh mass to 0.42–0.52 g per plant (+13.5–40.5 %). Split application increased nodule number only at pod filling (22.3–24.4 per plant; +10.4–20.8 %), whereas at budding ($p = 0.005$) and flowering ($p = 0.002$) application at sowing was superior. Most nodules were formed in treatment 8 without mineral fertilizers (+34.5–45.3 %), although its plants were the shortest, owing to the absence of nitrogen inhibition. Among $N_{90}P_{60}K_{90}$ treatments, the best nodulation was observed in treatment 2 (31.6 nodules and 1.25 g per plant at flowering).

Yield structure

Bentonite improved all yield components (Table 3). In the control, a plant had 2.1 branches, 38.0 pods and 87.4 seeds with a seed mass of 13.76 g, and the 1000-seed weight was 157.4 g. Application at sowing increased seed mass per plant to 14.01–15.29 g (+1.8–11.1 %), mainly at 400–750 kg ha^{-1}. Split application at budding and flowering was more effective: plants had 38.4–39.8 pods and 88.3–95.5 seeds, seed mass reached 14.25–15.66 g per plant (+3.6–13.8 %) and the 1000-seed weight 161.4–164.1 g. At equal rates, split application exceeded application at sowing in the number of branches ($p = 0.004$) and pods ($p = 0.001$) and in seed mass per plant ($p = 0.025$).

Among $N_{90}P_{60}K_{90}$ treatments, the highest seed mass per plant was obtained in treatments 7 (500 kg ha^{-1} split; 15.66 g) and 2 (15.62 g). Treatment 8 had the poorest yield structure (29.1 pods, 58.2 seeds and 8.24 g of seeds per plant; −40.1 %), indicating that abundant nodulation did not compensate for the absence of mineral fertilizers.

Correlation and regression analysis

With application at sowing, bentonite rate was closely related to field emergence ($r = 0.919$) and final plant density ($r = 0.925$) (Table 4). Quadratic models fitted better ($r^2 = 0.984$): the maximum plant density (262.6 thousand ha^{-1}) corresponds to about 680 kg ha^{-1}, while at 400 kg ha^{-1} density reaches 98.9 % of the maximum. Quadratic models for nodule number at budding ($r^2 = 0.992$) and seed mass per plant ($r^2 = 0.908$) reach their maxima at about 560 and 710 kg ha^{-1}, respectively.

With split application, bentonite rate was not related to emergence or early nodulation, but showed close linear relationships with final density ($r = 0.991$), LAI at pod formation ($r = 0.943$) and seed mass per plant ($r = 0.974$): each additional 100 kg ha^{-1} increased density by 1.5 thousand ha^{-1} and seed mass by 0.41 g per plant.

Table 3. Effect of bentonite application method, timing and rate on yield structure of soybean (2024)

No.	Treatment (bentonite rate, kg ha^{-1})	Height of first pod, cm	Per plant				1000-seed weight, g
			branches, no.	pods, no.	seeds, no.	seed mass, g	
Control treatments							
1	Control ($N_{90}P_{60}K_{90}$)	13.5	2.1	38.0	87.4	13.76	157.4
8	Control (750 kg ha^{-1} before autumn ploughing)	12.9	1.8	29.1	58.2	8.24	141.6
Bentonite at sowing							
10	$N_{90}P_{60}K_{90}$ + 100	13.7	2.2	38.2	87.9	14.01	159.5
11	$N_{90}P_{60}K_{90}$ + 200	14.1	2.2	38.3	88.1	14.24	161.7
12	$N_{90}P_{60}K_{90}$ + 300	14.3	2.3	38.8	89.2	14.50	162.5

13	$N_{90}P_{60}K_{90}$ + 400	14.3	2.2	39.2	94.1	15.29	162.5
14	$N_{90}P_{60}K_{90}$ + 500	14.4	2.3	39.4	94.6	15.25	161.3
9	$N_{90}P_{60}K_{90}$ + 750	14.1	2.3	39.0	93.6	15.22	162.6
Bentonite at budding and flowering (50 : 50)							
3	$N_{90}P_{60}K_{90}$ + 100	14.1	2.3	38.4	88.3	14.25	161.4
4	$N_{90}P_{60}K_{90}$ + 200	13.9	2.3	38.7	89.0	14.41	161.9
5	$N_{90}P_{60}K_{90}$ + 300	14.3	2.4	39.2	94.1	15.27	162.3
6	$N_{90}P_{60}K_{90}$ + 400	14.2	2.4	39.5	94.8	15.56	164.1
7	$N_{90}P_{60}K_{90}$ + 500	14.5	2.4	39.8	95.5	15.66	163.9
Bentonite at sowing, budding and flowering (250 + 250 + 250 kg ha^{−1})							
2	$N_{90}P_{60}K_{90}$ + 750	14.4	2.4	39.8	95.5	15.62	163.5

Note: the number of branches refers to first-order branches of the main stem.

Table 4. Regression equations of soybean traits on bentonite rate

Trait (y)	Method	Regression equation	r	R^2	p
Field emergence, %	At sowing	$y = 84.00 + 0.00976x - 7.32 \cdot 10^{-6}x^2$	0.919	0.984	< 0.001
	Split	not significant	0.293	0.086	0.573
Final plant density, thousand ha^{-1}	At sowing	$y = 245.53 + 0.0502x - 3.68 \cdot 10^{-5}x^2$	0.925	0.984	< 0.001
	Split	$y = 246.26 + 0.0150x$	0.991	0.983	< 0.001
Nodules at budding, no. $plant^{-1}$	At sowing	$y = 13.98 + 0.0136x - 1.21 \cdot 10^{-5}x^2$	0.840	0.992	< 0.001
	Split	not significant	0.217	0.047	0.679
LAI at pod formation, m^2 m^{-2}	At sowing	$y = 3.873 + 0.000594x$	0.958	0.918	0.001
	Split	$y = 3.942 + 0.000937x$	0.943	0.890	0.005
Seed mass per plant, g	At sowing	$y = 13.62 + 0.00473x - 3.31 \cdot 10^{-6}x^2$	0.899	0.908	0.009
	Split	$y = 13.80 + 0.00408x$	0.974	0.950	0.001

Note: x – bentonite rate, kg ha^{-1}; r – Pearson correlation coefficient; R^2 – coefficient of determination of the model; p – significance level of the model. At sowing n = 7 (0–750 kg ha^{-1}); split application (budding + flowering) n = 6 (0–500 kg ha^{-1}).

Table 5. Pairwise correlation coefficients between traits (n = 13)

Traits	1	2	3	4	5	6	7
1. Field emergence	1						
2. Final plant density	0.924**	1					
3. Plant survival	0.493	0.788**	1				
4. Nodule number (F)	0.756**	0.855**	0.735**	1			
5. Plant height (F)	0.745**	0.772**	0.550	0.923**	1		
6. LAI (F)	0.776**	0.863**	0.705**	0.886**	0.902**	1	
7. Seed mass per plant	0.274	0.594*	0.903**	0.546	0.428	0.603*	1

*Note: * – p < 0.05; ** – p < 0.01; F – flowering; treatment 8 was excluded because of its different fertilizer background.*

Across the 13 treatments with the same fertilizer background, final plant density was closely correlated with field emergence (r = 0.924), nodule number (r = 0.855), LAI (r = 0.863) and plant survival (r = 0.788) (Table 5); according to the coefficient of determination (d = 85.4 %), most of the variation in density is explained by emergence. Plant height and LAI at flowering were closely related to nodule number (r = 0.923 and 0.886); the LAI–density correlation is partly methodological. Seed mass per plant was closely related to plant survival (r = 0.903), LAI at pod formation (r = 0.905) and plant height at maturity (r = 0.849), but not to field emergence (r = 0.274).

Thus, bentonite at sowing mainly increases plant density through emergence, whereas later application improves individual plant productivity through survival and leaf area in the reproductive period. Unlike earlier studies, where bentonite was applied at several to tens of tonnes per hectare [5–9], 0.1–0.75 t ha^{-1} applied with mineral fertilizers was effective here.

CONCLUSIONS

1. On light serozem soils, bentonite applied at sowing at 100–750 kg ha^{-1} with $N_{90}P_{60}K_{90}$ increased soybean field emergence from 84.1 % to 84.8–87.2 %, final plant density by 1.5–6.8 %, nodule number at budding by 10.1–26.6 % and LAI at flowering by 4.6–10.2 %.

2. Split application at budding and flowering did not affect emergence or early growth, but increased plant survival up to 90.4 %, LAI at pod formation by 6.5–13.2 % and seed mass per plant by 3.6–13.8 %, exceeding application at sowing in yield structure.

3. Final plant density was closely related to bentonite rate (r = 0.925–0.991), field emergence (r = 0.924) and nodule number (r = 0.855), and seed mass per plant to plant survival (r = 0.903) and LAI at pod formation (r = 0.905).

4. Bentonite at 400 kg ha^{-1} applied at sowing provides 99.3 % of the plant density obtained at 750 kg ha^{-1} while reducing bentonite use by 46.7 %, whereas 400–500 kg ha^{-1} split between budding and flowering provides the best yield structure. The final choice of rate and timing should be based on grain yield and economic efficiency.

References:

1. Helms, T.C., Deckard, E., Goos, R.J., & Enz, J.W. (1996). Soybean seedling emergence influenced by days of soil water stress and soil temperature. *Agronomy Journal*, 1996, 88(4), pp.657-661.
2. Helms, T.C., Deckard, E.L., Goos, R.J., & Enz, J.W. (1996). Soil moisture, temperature, and drying influence on soybean emergence. *Agronomy Journal*, 1996, 88 (4), pp.662-667.
3. Hanks, R.J., & Thorp, F.C. (1957). Seedling emergence of wheat, grain sorghum, and soybeans as influenced by soil crust strength and moisture content. *Soil Science Society of America Journal,* 1957, 21 (4), pp.357-359.
4. Mumpton, F.A. (1999). La roca magica: uses of natural zeolites in agriculture and industry. *Proceedings of the National Academy of Sciences of the USA*, 1999, 96 (7), pp.3463-3470.
5. Mi, J., Gregorich, E.G., Xu, S., McLaughlin, N.B., & Liu, J. (2020). Effect of bentonite as a soil amendment on field water-holding capacity, and millet photosynthesis and grain quality. *Scientific Reports*, 2020, 10. DOI: 10.1038/s41598-020-75350-9.
6. Mi, J., Gregorich, E.G., Xu, S., McLaughlin, N.B., Ma, B., & Liu, J. (2021). Changes in soil biochemical properties following application of bentonite as a soil amendment. *European Journal of Soil Biology*, 2021, 10, pp.103-110.
7. Czaban, J., Siebielec, G., Czyż, E., & Niedźwiecki, J. (2013). Effects of bentonite addition on sandy soil chemistry in a long-term plot experiment (I); effect on organic carbon and total nitrogen. *Polish Journal of Environmental Studies*, 2013, 22(6), pp.1661-1667.
8. Czaban, J., & Siebielec, G. (2013). Effects of bentonite on sandy soil chemistry in a long-term plot experiment (II); effect on pH, CEC, and macro- and micronutrients. *Polish Journal of Environmental Studies*, 2013, 22(6), pp.1669-1676.
9. Croker, J., Poss, R., Hartmann, C., & Bhuthorndharaj, S. (2004). Effects of recycled bentonite addition on soil properties, plant growth and nutrient uptake in a tropical sandy soil. *Plant and Soil*, 2004, 267 (1-2), pp.155-163.
10. Zhou, L., Xu, S., Monreal, C.M., McLaughlin, N.B., Zhao, B., Liu, J., & Hao, G. (2022). Bentonite-humic acid improves soil organic carbon, microbial biomass, enzyme activities and grain quality in a sandy soil cropped to maize (Zea mays L.) in a semi-arid region. *Journal of Integrative Agriculture*, 2022, 21(1). pp.33-42.
11. Ma, B., Bao, Y., Ma, B., McLaughlin, N.B., Li, M., & Liu, J. (2022). Residual effect of bentonite-humic acid amendment on soil health and crop performance 4-5 years after initial application in a dryland ecosystem. *Agronomy*, 2022, 12(4), pp.853-865.
12. Streeter, J.G. (1988). Inhibition of legume nodule formation and N2 fixation by nitrate. *CRC Critical Reviews in Plant Sciences*, 1988, 7, pp.1-23.
13. Yamashita, N., Tanabata, S., Ohtake, N., Sueyoshi, K., Sato, T., Higuchi, K., Saito, A., & Ohyama, T. (2019). Effects of different chemical forms of nitrogen on the quick and reversible inhibition of soybean nodule growth and nitrogen fixation activity. *Frontiers in Plant Science*, 2019, 10, 131. DOI: 10.3389/fpls.2019.00131.
14. Tog‘ayeva, X.R. (2026). *Effect of irrigation regime and seed coating rate with bentonite clays on winter wheat yield (light serozem soils of Kashkadarya region).* PhD dissertation (Agricultural Sciences). Samarkand, 2026.

15. Dospekhov, B.A. (1985). *Field Experiment Methodology*. Moscow: Agropromizdat, 1985. 351 p.
16. Posypanov, G.S. (1991). *Methods for studying biological fixation of atmospheric nitrogen.* Moscow: Agropromizdat, 1991. 300 p.
17. Nichiporovich, A.A. (1963). *Photosynthesis and problems of plant productivity*. Moscow: Izd-vo AN SSSR, 1963. 158 p.

SOI: 1.1/TAS DOI: 10.15863/TAS

International Scientific Journal

Theoretical & Applied Science

p-ISSN: 2308-4944 (print) **e-ISSN:** 2409-0085 (online)

Year: 2026 **Issue:** 10 **Volume:** 162

Received: 18.10.2026
Accepted/Published: 30.10.2026

https://T-Science.org

Issue Article

S. U. Zhanatauov
META university
Academician of International Academy
of Theoretical and Applied Sciences (USA),
Candidate of physics and mathematical sciences, Professor
sapagtu@mail.ru

MATHEMATICAL SPLITTING OF THE MATHEMATICAL FORMULA FOR THE Y-REACTION

Abstract: *The article models and analyzes mathematical formulas for y-reactions (representing the informational and mathematical levels of describing an absorption reaction). The study addresses the decomposition of these mathematical formulas, as well as the categorization of the meanings derived from this decomposition into two distinct types (representing the cognitive level of describing an absorption reaction). An equation of the following form is established: (meaning(y_1) + … + meaning(y_{15})) = (Resource1 + Resource2 + Resource3 + Resource4 + Resource5). The sum of the mathematical formulas for five y-reactions is equal to the sum of the decomposed (split) mathematical formulas. Based on five previously developed multi-meaning equations—containing both known and unknown semantic (meaning-based) variables—new semantic equalities have been derived: the sum of two decomposed mathematical formulas and their respective meanings is equal to the complete formula and meaning of a given y-reaction. There are five such y-reactions (y_1, y_2, y_3, y_4, y_5) that possess complete mathematical formulas. The five meanings of the y-reactions (y_1, y_2, y_3, y_4, y_5) are broken down into components, as expressed in the following terms: meaning(y_1) = BOD1 + COD1; meaning(y_2) = COD2 + Resource2; meaning(y_3) = COD3 + Resource3; meaning(y_4) = BOD4 + Resource4; meaning(y_5) = SS5 + Resource5. The decomposed components on the right-hand side of these equations cannot be summed; this semantic decomposition does not allow for them to be recombined into a single, unified meaning.*

Key words: *Formula unit, decomposition of the mathematical formula of an absorbent, multi-meaning equations with semantic variables and numerical parameters, biochemical absorption reaction, absorbate, absorbent.*

Language: *Russian*

Citation: Zhanatauov, S. U. (2026). Mathematical splitting of the mathematical formula for the Y-reaction. *ISJ Theoretical & Applied Science, 10 (162),* 38-46.

Soi: https://s-o-i.org/1.1/TAS-10-162-7 ***Doi***: crossref https://dx.doi.org/10.15863/TAS.2026.10.162.7

Scopus ASCC: *2604.*

МАТЕМАТИЧЕСКОЕ РАСЩЕПЛЕНИЕ МАТЕМАТИЧЕСКОЙ ФОРМУЛЫ Y-РЕАКЦИИ

Аннотация: *В статье моделируются и анализируются математические формулы y-реакций (информационный и математический уровни описания реакции абсорбции). Решены задачи расщепления математических формул и расщепления смыслов полученных расщепленных математических формул на 2 типа (когнитивный уровень описания реакции абсорбции). Получено равенство вида (смысл(y_1)+…+смысл(y_{15})) =(Ресурс1+Ресурс2+Ресурс3+Ресурс4+Ресурс5). Сумма математических формул пяти y-реакций равна сумме расщепленных математических формул. Из ранее разработанных 5 многосмысловых уравнений с известными и не известными семантическими (смысловыми) переменными получены новые смысловые равенства: сумма двух расщепленных математических формул и их смыслов равна полной формуле и смыслу формулы y-реакции. Количество y-реакций y_1,y_2,y_3,y_4,y_5, имеющих полные математические формулы, равно пяти. Пять смыслов y-реакций y_1,y_2,y_3,y_4,y_5 расщеплены на части, фразы которых приведены выше: смысл(y_1)=БПК1+ХПК1; смысл(y_2)=ХПК2+ Ресурс2; смысл(y_3)=ХПК3+ Ресурс3;*

смысл(y_4)=БПК4+Ресурс4; смысл(y_5)=ВВ5+Ресурс5. Расщепленные смыслы из правых частей этих равенств нельзя суммировать, смысловое расщепление смыслов не допускает обратного объединения в один смысл; смысл(y_3)=ХПК3+ Ресурс3; смысл(y_4)=БПК4+Ресурс4; смысл(y_5)=ВВ5+Ресурс5.

Ключевые слова: *Формульная единица, расщепление математической формулы абсорбента, многосмысловые уравнения с семантическими переменными и числовыми параметрами, биохимическая реакция абсорбции, абсорбат, абсорбент.*

Введение

В математической химии не рассматривалась биохимическая реакция абсорбции. Математическая химия - раздел теоретической химии, область исследований, посвящённая новым применениям математики к химическим задачам [1]. Основная область интересов - это математическое моделирование гипотетически возможных физико-химических и химических явлений и процессов, а также их зависимость от свойств атомов и структуры молекул. Математическая химия допускает построение моделей без привлечения квантовой механики. Критерием истины в математической химии являются математическое доказательство, вычислительный эксперимент и сравнение результатов с экспериментальными данными [2]. Важнейшую роль в математической химии играет математическое моделирование с использованием компьютеров. В связи с этим математическую химию, в узком смысле, иногда называют компьютерной химией (Computer chemistry), которую не следует путать с вычислительной химией (Computational chemistry). В математической химии разрабатывают новые приложения математических методов в химии. Новизна обычно выражается одним из двух способов: развитие новой химической теории; развитие новых математических подходов, которые позволяют проникнуть в суть или решить проблемы химии. При этом используемые математические средства чрезвычайно разнообразны [3]. В отличие от чисто математических наук, в математической химии исследуются химические задачи и проблемы методами современной математики. Одной из самых известных моделей математической химии является молекулярный граф. Молекулярный граф — связный неориентированный граф, находящийся во взаимно-однозначном соответствии со структурной формулой химического соединения таким образом, что вершинам графа соответствуют атомы молекулы, а рёбрам графа — химические связи между этими атомами. Структура молекул может быть удобно изображена на языке теории графов, что не просто приводит к новой формализации, но имеет эвристическое значение.

Матричные представления молекулярных графов связываются с матричными методами квантовой химии. В силу квантового характера движения электронов и ядер решение задачи нахождения межмолекулярных взаимодействий сводится, строго говоря, к приближенному решению уравнения Шредингера для системы взаимодействующих молекул [4]. Квантово-механическое обоснование этой модели (молекулярный граф) дано сравнительно недавно в теории Р. Бейдера [5]. Составляющими элементами языка этой теории являются различные математические, в том числе топологические, характеристики электронной плотности, которая может быть доступна экспериментальному измерению. При этом химические реакции и структурные изменения в молекулах могут описываться на языке теории катастроф и бифуркаций. Другие знаменитые модели — это закон действующих масс, созданный математиком К. Гульдбергом и химиком-экспериментатором П. Ваге, граф механизма химических превращений и дифференциальные уравнения химической кинетики. Один из создателей «химической динамики» Вант-Гофф писал о себе: «Двойное стремление: к математике, с одной стороны, и к химии — с другой, проявилось во всех моих научных устремлениях» [3].

Расщепление абсорбатов (если говорить точнее - десорбция или регенерация абсорбента) - это физико-химический процесс выделения поглощенного вещества (абсорбата) из объема поглощающей жидкости (абсорбента). В химической технологии этот этап необходим для повторного использования растворителя и выделения целевого компонента в чистом виде.

Вместо химического процесса выделения поглощенного вещества (абсорбата) из объема поглощающей жидкости (абсорбента - воды) мы рассматриваем математические формулы пяти абсорбентов. Нами найдены фразы смыслов математических формул виртуальных абсорбентов, равных линейным комбинациям смыслов реальных абсорбентов. Рассмотрены и решены задачи расщепления математических формул у–реакций (когнитивная модель расщепила на 5 многосмысловых семантических уравнений пяти у–реакции одну биохимическую реакцию абсорбции) на формулы частей формулы у–реакций, получаемых математическим методом. Математическое расщепление математического абсорбата равно линейной комбинации смыслов частей абсорбата. Все рассматриваемые смыслы математических абсорбатов, подвергаемых математическому

расщеплению, являются семантическими переменными из одной системы многосмысловых уравнений с известными и неизвестными семантическими переменными.

Формирование таблицы «объект-свойства»

Из реальных данных, опубликованных в Отчете, выделим 5 показателей (содержание физико-химического вещества, мг/(м^3): ионы аммония (z_1), растворенный кислород (z_2), поглощения взвешенных веществ(z_3), биологически поглощенного кислорода (z_4, БПК), химически поглощенного кислорода (z_5, ХПК). В Отчете https://www.kazhydromet.kz/uploads/calendar/5/kvartal_1_file/rk-1-kvartal-2020-rus.pdf?cache=1587614814 были даны интервалы значений этих веществ, а не значения, привязанные к точкам забора проб воды. Например, содержание взвешенных веществ (z_3) в тексте отчета задано в виде интервала значений 8.8-12 мг/(м^3, удельный объем растворенного кислорода в озере Бурабай - 10.02-11.46 мг/м^3, БПК воды из озера Щучье - 0,46-0,99 мг/м^3, ХПК воды из озера Щучье - 24-29,1 мг/м^3, ионы аммония из вод 12 водоемов - 4.15-4.573 мг/м^3. В качестве значения, привязанного к точке забора пробы воды из реки\озера, было нами взято одно значение, близкое к максимальному значению. Таких «привязочных» значений подставлялись в Таблицу 2 многократно. После каждого изменения значения содержания физико-химического вещества для полученной матрицы данных X^0_{m5} вычислялась ее корреляционная матрица, матрица собственных векторов. Таких вычисленных матриц собственных векторов C_{55} проанализировано 17 штук: по 3 матрицы C_{55} на каждый показатель (на одну из 4-х столбцов матрицы данных X^0_{m5}). Первый столбец матрицы данных X^0_{m5} был заполнен 10 случайными числами, равномерно распределенных внутри интервала 4.15-4.573. Критерием остановки процесса ручного подбора «привязочных» значений служило эмпирическое правило: «1-ый собственный вектор $\mathbf{c_1}$ имеет 4 компоненты, значения которых принадлежат интервалу (0.4;0.5), а компонента №2: c_{21}– близка к 0», 2-ой собственный вектор $\mathbf{c_2}$ имеет 3 компоненты, значения которых принадлежат интервалу (0.44;0,7)». При этом мы соблюдали условие: все номера компонент 1,2,3,4,5 присутствуют в составах указанных выше 4-х и 3-х компонент. Одна из таких пар матриц (R_{55},C_{55}) приведена в Таблице 1.

Информационный уровень описания реакции абсорбции

Представление абсорбатов в реакции абсорбции водного раствора в виде системы многосмысловых уравнений с семантическими переменными является формульным инструментом и эмпирически осмысленным методом [6,7]. Это представление отличается от предыдущих методов [8?10] применяемым инструментом -обратной моделью главных компонент [9]. Роли и силы поглощения абсорбатов соответствуют уменьшению\увеличению масс ионов аммония, растворенного кислорода, ВВ, БХП, ХПК в толще воды. Полученные вычисленными методами извлеченные знания являются подтвержденными числовым материалом двух типов. Исходные и известные фразы смыслов пяти абсорбатов порождают многосмысловые уравнения (с известными не известными смысловыми переменными). Линейная комбинация смысловых переменных [11] соответствует аддитивному взаимодействию абсорбатов и аддитивному правилу объединения знаний об абсорбатах (с учетом знака и величины силы его участия в реакции). Это иное смысловое представление символических систем, которыми реальные люди пользуются в реальной практике для придания краткой лаконичной формы своим мыслям о реакции самоочищения воды рек и озер Восточного Казахстана. Исследование осуществлялось на материале о смысловых, числовых данных. Записи формульных единиц в смысловых нехимических уравнениях с смысловыми (семантическими) переменными (присущих реакции абсорбции) выявляют не только то, что реагируют между собой отдельные абсорбаты, но и их математически расщепленные - неразделенные химическими формулами части абсорбатов. Каждая математическая формула – реакции (математический абсорбат) имеет свое новое описание на информационном и когнитивном уровнях описания реакции абсорбции самоочищения воды рек и озер Восточного Казахстана. В новом описании содержатся не отраженные в химических формулах понятия, термины из междисциплинарных областей. В количественных вычислениях когнитивного моделирования [8-21] мы перешли от (z,r)-значений к (y,c)-значениям измерения парных связей. Переход от значений (z,r)–изменчивостей измеряющих силы связи между z-переменными (z_1,…,z_5) к вычисляемым значениям (y,z)–изменчивостей, измеряющих силы связи между одной вычисляемой переменной (из множества y_1,…,y_5) и набором z-переменных. Если известна Z, то матрица $R=(1/m)Z^TZ$ (z,r)-значений изменчивостей к

влияет на матрицы Y=ZC (z,y)-значений изменчивостей. Матрица $C=(1/m)Z^TY\ \Lambda^{-1}$ (z,y)-корреляций является преобразователем любой матрицы изменчивостей в матрицу других изменчивостей. Она может моделироваться в паре матриц (R,C), (Λ,C) , она может моделироваться независимо, обладающей свойством ортонормированности $C^TC=CC^T=I=diag(1,\ldots,1)$. Матрица $C=(1/m)Z^TY\ \Lambda^{-1}$, обладая выделенными элементами, может порождать (моделировать) матрицы изменчивостей Y, Z: $C=(1/m)Z^TY\ \Lambda^{-1}$.

Мы рассматриваем случаи разбиения матриц по столбцам, руководствуясь химическими доводами, смыслами z-, y– изменчивостей. Формула строки матрицы Y=ZC (формула y-реакции) разделяется на несколько формульных единиц, имеющих свои подсмыслы вычисляемой химической y-реакции, относящихся к одному из смыслов подтипов БПК/ХПК.

Модельные числовые значения z-переменных для математических формул расщепленных частей математической формулы y-реакции

Для информационного описания реакции абсорбции требуется модельные числовые значения z- и y-переменных. Они используются придания случайности величинам заметных «весов» в математических формулах всех частей математических формул абсорбатов. Модельные числовые значения образуют две случайные матрицы (многомерных выборок) Z_{m5}, Y_{m5}, связанных друг с другом - $Z_{m5}=Y_{m5}C^T_{55}$ посредством матрицы «весов» C_{55}. Матрица $\mathbf{C_{55}}$ **(**таблица 2**)** соответствует как паре матриц (R_{55},Λ_{55}) таких, что: $R_{55}C_{55}=C_{55}\Lambda_{55}$, так и паре матриц $(C_{55}\Lambda_{55})$, где C_{55} смоделирована, исходя из матрицы Λ_{55} [14]. Используемая матрица C_{55} не вычислена при решении прямой спектральной задачи**:** $R_{55}=>(C_{55}\Lambda_{55})$, где $R_{55}=R^T_{55}$ – вычисленная выборочная матрица (z,z)-корреляций $R_{55}=(1/m)Z^T_{m5}Z_{m5}$. Матрица C_{55} – модельная, смоделирована при решении обратной спектральной задачи**:** $\Lambda_{55}=>(C_{55},R_{55})$, где R_{55} не применяется в нашей модели. Мы не доверяем нестабильной корреляционной матрице R_{55} (не применяем формулу стабильности $(\alpha R_{55})C_{55}=C_{55}(\alpha\Lambda_{55},\ \alpha>0)$ матрицы C_{55}), а используем стабильную матрицу C_{55}, соответствующей своей диагональной матрице $\Lambda_{55}=diag(1.0666,1.0091,0.9967,0.9695,\ 0.9581)$. Они соответствуют 20-ому интервалу времени, когда силы поглощений абсорбатов ослабевают, дисперсии y-переменных мало отличаются друг от друга. Состояние информационных характеристик соответствует концу y-реакции. Диагональные элементы матрицы Λ_{55} являются дисперсиями пяти y–изменчивостей: $\Lambda_{55}=(1/m)Y^T_{m5}Y_{m5}$, матрицы случайных значений y– и z-изменчивостей $Y_{m5}=U_{m5}\Lambda^{1/2}_{55}$, $Z_{m5}=Y_{m5}C^T_{55}$ моделируются нами из любой случайной матрицы V^0_{m5} случайных чисел, равномерно распределенных внутри интервала (-1;+1). Этим достигается случайность значений y– и z-изменчивостей. Случайная матрица U_{m5} получена случайным преобразованием преобразованной матрицы V^0_{m5}, зависящим от самой матрицы V^0_{m5}. Поэтому элементы матрицы U_{m5} теряют равно мерный закон распределения, а сама матрица U_{m5} обладает ценным свойством: $(1/m)U^T_{m5}U_{m5}=I_{55}$. Вычислительная схема $\mathbf{(U_{m5},\Lambda_{55})=>Y}_{m5}$ пред шествует схеме вычисления многомерной выборки $Z_{m5}=Y_{m5}C^T_{55}$.

Значения y-изменчивостей из матрицы вычисляются по алгебраическим формулам. Назовем их математическими формулами y–реакций.

$y_1=z_1*0,5868+z_2*0,1536+z_3*0,1538+z_4*(-0,4609)+z_5*0,6293$;

$y_2=0,0793+z_2*(-0,8827)+z_3*(-0,1386)+z_4*(-0,2542)+z_5*0,3615$;

$y_3=0,5506+z_2*0,2589+z_3*(-0,3283)+z4*(-0,3545)+z_5*(-0,6296)$;

$y_4=0,4689+z_2*0,3439+z_3*(-0,4096)+z_4*0,6972+z_5*0,0896$;

$y_5=z_1*0,3555+z_2*(-0,1091)+z3*0,8256+z_4*0,3335+z_5*(-0,2625)$.

Критерии выделения части из математической формулы y-реакции и отбора «весов» для математически расщепления формулы y-реакции

Из пяти разнородных формульных единиц математической формулы y-реакции требуется выделить часть, которая соответствовала бы одному из трех типов поглощения. Три типа поглощения – это поглощение водой взвешенных веществ (смысл(z_3)), биологическое поглощение кислорода(смысл(z_4)), химическое поглощение кислорода(смысл(z_5)). Трем типам поглощения соответствует тройка математических z-переменных (z_3,z_4,z_5). Рассмотрим все формульные единицы в математических формулах пяти y - реакций. Обнаружена закономерность: существуют абсорбаты с z-изменчивостями с совпадающими знаками, где изменчивость одного абсорбата имеет возрастающую динамику z-изменчивости с знаком плюс (из-за увеличения поглощаемой его массы), а изменчивость другого абсорбата – уменьшающуюся динамику z-изменчивости с знаком минус (из-за уменьшения поглощаемой его массы). Такая связь имеет место быть для пары абсорбатов в математической формуле y-реакции $y_{i2}=(z_{i1})*0,0793+(z_{i2}(-0,8827)+z_{i3}(-0,1386)+z_{i4}*(-0,2542)+z_{i5}*(0,3615)$, где выделяются формульные единиы $z_{i3}(-0,1386)$, $z_{i4}*(-0,2542)+$

z_{i5}*(0,3615) с заметными «весами» z_{i3}(-0,1386)+ z_{i4}*(-0,2542)+z_{i5}(0,3615) при z-переменных z_3,z_4,z_5, соответствующие поглашающимся абсрбатам с смыслами смысл(z_{i3})=ВВ, смысл(z_{i4}) = БПК, смысл(z_{i5})=ХПК. Здесь знак минус в формульной единице z_{i4}*(-0,2542) противоположен знаку плюс в формульной единице z_{i5}(0,3615). Здесь знак плюс уместен из-за увеличения поглощаемой массы химически поглощенного кислорода и знак минус – из-за уменьшающегося поглощения биологически поглощающегося кислорода. Из одного ресурса химическое поглощение возрастает, а биологическое поглощение уменьшается. Такая ситуация естественна для реакции абсорбции. Из формулы стабильности матрицы C_{55} вида (αR_{55}) C_{55}=C_{55}($\alpha\Lambda_{55}$) следует существование этих критериев.

Приведем пример ошибочности выделения набора формульных единиц, отличающегося от этой тройки. Рассмотрим математические z-переменные (z_3,z_4,z_5). В математической формуле y-реакции y_4 влияющими на формулу y-переменной y_4 выделим 2 формульные единицы z_{i1}*0.4689 и «z_{i4}*0.6972», имеющие положительные «веса» 0.4689, 0.6972, умноженные на знакопеременные изменчивости z_{i1}, z_{i4}, i=1,…,12. При положительных весах c_{11}=0.4689, c_{44}=0.6972 значения z-изменчивостей с смыслом(z_{i1}) и со смыслом (z_{i4}) имеют одинаковые знаки. Это противоречит химическому факту, когда ионы аммония влияют как катализатор на абсорбат «взвешенные вещества». Поэтому нельзя расщеплять формулу y -реакции y_4 на такую сумму формульных единиц. Расщепленная сумма формульных единиц должна содержать только формульные единицы, относящиеся к поглощенным абсорбатам. Этим абсорбатам соответствуют математические переменные z_3,z_4,z_5 с семантическими смысловыми переменными смысл(z_3)=«**ВВ**», (z_4)=«БПК», смысл(z_5)=«ХПК»). Остальные 2 смысла соответствуют ресурсу «растворенный кислород» и катализатору «ионы аммония», сопутствующих своим реакциям поглощения. Во всех расщеплениях пяти математических формул y-реакций будем руководствоваться этим правилом «трех формульных единиц» выделения части формульных единиц из математической формулы y-реакции.

Другой целью для нашего анализа является поиск значений компонент {c_{ik}=$corr(z_i,y_k)$}, значения которых принадлежат к правой части интервала (0,3-0,5) – обозначает «умеренная корреляция» и к левой части интервала (0,5-0,7), обозначающего «заметная корреляция». В результате указанных выше циклических вычислений удалось получить 3 собственные векторы (Таблица 2), компоненты («веса») которых попали в объединение интервалов (0.3;0.5)∪(0.5; 0,7). Эти значения «весов» при учете значений своих z-изменчивостей (z_{i3}*c_{3j},z_{i4}*c_{4j},z_{i5}*c_{5j}) по абсолютной величине превышают порог 0.4 - заметного «веса» из формульной единицы каждого поглощенного абсорбата (из трех абсорбатов с смыслами смысл(z_3), смысл(z_4), смысл(z_5)). По шкале Чэддока значения, превышающие пороговое значение 0.4, относится к нашему интервалу (0.3;0.5)∪(0.5;0,7) заметных корреляций. В параграфе «Модельные числовые значения z-переменных для математических формул расщепленных частей математической формулы абсорбата» приведены значения «весов», отобранных по данному критерию. Мы не учитывали «веса», относящиеся интервалам (0.1;0.3)=«слабая». Стабильный (в достигнутом выше понимании) «вес» входит в произведение величины c_{ik}=$corr(z_i,y_k)$ и случайной величины изменчивости z_{kj}, образуя стабильное слагаемое вида (+c_{ik}*z_{kj}+**)** в математической формуле расщепленной части математической формулы абсорбата**.**

Математическое расщепление математической формулы поглощенной в воде y-реакции

Измеренным показателям ресурсных веществ (растворенный в воде кислород, ионы аммония) и поглощенных видов кислорода и взвешенных веществ соответствуют 5 вычисленных в когнитивной модели математических формул. Проведем математическое расщепление каждой математической формулы на части, соответствующие типу поглощения абсорбата из имеющихся трех типов – поглощение взвешенных веществ, биологическое поглощение кислорода (БПК), химическое поглощение кислорода (ХПК). Название смысла полученной расщепленной части математической формулы назначим равным смыслу доминирующей формульной единицы из расщепляемой части математической формулы, соответствующему доминирующему абсорбату. **м**атричные смысловые равенства видов смысл(Y_{m5})=смысл(Z_{m5})*C_{55} =смысл(**z_1**)*C_{55}+…+смысл(**z_5**)*C_{55}=(смысл(z_1),…, смысл(z_5)) - текстовая вектор-строка. Произведение смысл(**z_1**)*C_{55} равно вектору, его 1-ая компонента равна произведению смысла(z_1)*c_{11}, 2-ая компонента равна произведению смысла(z_1)*c_{21}, а пятая компонента равна произведению смысла(z_1)*c_{51}. Аналогично вычисляются слагаемые смысл(**z_2**)*C_{55}, смысл(**z_3**)*C_{55}, смысл(**z_4**)*C_{55}. Произведение смысл(**z_5**)*C_{55} равно вектору, его 1-ая компонента равна произведению смысла(z_5)*c_{15}, 2-ая компонента равна - произведению смысла(z_5)*c_{25}, а пятая на компонента равна произведению

смысла(z_5)*c_{55}. Фразы слагаемых текстов видов смысл($\mathbf{z_1}$)*C_{55}+…+смысл($\mathbf{z_5}$)*C_{55} соответствуют принципу аддитивного мышления человека. Ниже мы убедимся: каждое смысловое уравнение из системы многосмысловых уравнений соответствует принципу аддитивного мышления человека. Они соответствуют числовым алгебраическим равенствам $Y_{m5}=Z_{m5}*C_{55}$. Получается текстовая «таблица фраз (новых знаний) смыслов» вида [смысл($Y_{m5}=Z_{m5}*C_{55}$)].

В названии смысла каждой расщепленной формулы обозначим цифру номера j y-переменной, математической формуле которой принадлежит расщепленная формула. Например, смысл((z_{i3}*(-0.3283)+z_{i4}*(-0.3545)+z_{i5}*(-0.6296))= ХПК3 обозначает аббревиатуру смысла расщепленной математической формулы вида (z_{i3}*(-0.3283)+z_{i4}*(-0.3545)+z_{i5}*(-0.6296), соответствующую химически поглощенной части кислорода в y-реакции y_3 (в y-абсорбате y_3).

Из математической формулы y-переменной $y_1=z_1*0{,}5868+z_2*0{,}1536+z_3*0{,}1538+z_4*(-0{,}4609)+z_5*0{,}6293$ выделим формульные единицы $z_{i3}(0{,}1538)$, $z_{i4}(-0{,}4609)$, $z_{i5}(0{,}6293)$ с заметными «весами» $z_{i3}(0{,}1538)$, $z_{i4}(-0{,}4609)$, $z_{i5}(0{,}6293)$ z-переменных, соответствующих поглощающимся абсорбатам со смыслами смысл(z_{i3})=ВВ, смысл(z_{i4})=БПК, смысл(z_{i5})=ХПК. Доля силы поглощения химически поглощаемого кислорода доминирует, следователь но имеем математическую формулу математического расщепления математической формулы, соответствующей части химически поглощенного кислорода (ХПК-абсорбата). Смысл этой части математической формулы назовем ХПК1= смысл(z_5*0,6293), обозначая химически поглощенную часть кислорода в y-реакции y_1 (в y-абсорбате y_1 из множества математических y-абсорбатов. Второй доминирующей долей силы поглощения ($c^2_{41}=(-0{,}4609^2)$), входящей в эту же формульную единицу, является расщепленная формула биологи чески поглощаемого кислорода, следовательно имеем вторую математическую формулу математического расщепления математической формулы, соответствующей части биологически поглощенного кислорода (БПК-абсорбата). Смысл этой расщепленной части математической формулы назовем БПК1=смысл(z_4*(-0,4609)), обозначая биологически поглощенную часть кислорода в y-реакции y_1 (в y-абсорбате y_1 из множества математических y-абсорбатов. уменьшающимся (с силой $c^2_{41}=(-0{,}4609)^2$) биологическим поглощением кислорода из-за препятствования поступлению из атмосферы растворенного кислорода, объем которого мало заметно уменьшается (с силой $c^2_{25}=(-0{,}1091^2)$) из-за большого объема в воде (с силой $c^2_{35}=0{,}8256^2$) медленно поглощаемых взвешенных веществ. Другая расщепленная часть математической формулы y-реакции y_1 имеет вид $z_1*0{,}5868+z_2*0{,}1536$. Смысл этой расщепленной части математической формулы назовем Ресурс1=смысл(z_1*0,5868+z_2*0,1536), обозначая силы проявлений ионов аммония и растворенного кислорода в y-реакции y_1. Смысл Ресурс1 расщепленной математической формулы ресурсов относится к смыслам БПК1 ХПК1 двух активных реакций с математическими формулами, полученными выше.

Из математической формулы y-переменной $y_{i2}=(z_{i1})*0{,}0793+(z_{i2}(-0{,}8827)+z_{i3}(-0{,}1386)+z_{i4}*(-0{,}2542)+z_{i5}*(0{,}3615)$ выделим формульные единицы $z_{i3}(-0{,}1386)$, $z_{i4}*(-0{,}2542)$ $+z_{i5}*(0{,}3615)$ с заметными «весами» $z_{i3}(-0{,}1386)+z_{i4}*(-0{,}2542)+z_{i5}(0{,}3615)$ при z-переменных z_3,z_4,z_5, соответствующие поглашающимся абсрбатам с смыслами смысл(z_{i3})=, смысл(z_{i4})=БПК, смысл(z_{i5})=ХПК. Доля силы поглощения химически поглощаемого кислорода доминирует, следовательно имеем математическую формулу химического поглощения кислорода, соответствующей части абсорбата ХПК. Смысл этой части математической формулы назовем ХПК2=смысл($z_{i3}(-0{,}1386)+z_{i4}*(-0{,}2542)+z_{i5}(0{,}3615)$, обозначая химически поглощенную часть кислорода в y-реакции y_2 (в y-абсорбате y_2 из множества пяти математических y-абсорбатов. Другая расщепленная часть математической формулы y-реакции y_2 имеет вид $z_{i1}*0{,}0793+z_{i2}(-0{,}8827)$. Смысл этой расщепленной части математической формулы назовем Ресурс2=смысл($z_{i1}*0{,}0793+z_{i2}(-0{,}8827)$), обозначая силы проявлений ионов аммония и растворенного кислорода в y-реакции y_2. Смысл Ресурс2 расщепленной математической формулы ресурсов для -реакции y_2 относится только к смыслу ХПК2 одной активной реакции с математической формулой, полученной выше.

Из математической формулы y-переменной $y_{i3}=z_{i1}*0.5506+z_{i2})*0.2589+z_{i3}*(-0.3283)+z_{i4}*(-0.3545)+z_{i5}*(-0.6296))$ выделили формульные единицы с заметными «весами» $z_{i3}*(-0.3283)+z_{i4}*(-0.3545)+z_{i5}*(-0.6296))$ z-переменных z_3,z_4,z_5, соответствующих поглощающимся абсорбатам со смыслами смысл(z_{i3})=ВВ, смысл(z_{i4})=БПК, смысл(z_{i5})=ХПК. Доля силы поглощения химически поглощаемого кислорода доминирует, следовательно, имеем математическую формулу химического поглощения кислорода, соответствующей части абсорбата ХПК. Смысл этой математической формулы назовем ХПК3= смысл(z_{i3}*(-0.3283)+z_{i4}*(-0.3545)+z_{i5}*(-0.6296)), обозначая химически поглощенную часть кислорода в y-реакции y_3 (в y-абсорбате y_3 из множества пяти математических y-абсорбатов. Другая расщепленная часть математической формулы y-реакции y_3 имеет вид

z_{i1}*0.5506+z_{i2}*0.2589. Смысл этой расщепленной части математической формулы назовем Ресурс3= смысл(z_{i1}*0.5506+z_{i2}*0.2589), обозначая силы проявлений ионов аммония и растворенного кислорода в у-реакции y_3. Смысл Ресурс3 расщепленной математической формулы ресурсов для у-реакции y_3 относится только к смыслу ХПК3 одной активной реакции с математической формулой, полученной выше.

Из математической формулы у-переменной y_4=(z_{i1})*0.4689+(z_{i2})*0.3439+(z_{i3})*(-0.4096)+(z_{i4})* 0.6972+(z_{i5})*0.0896 выделили формульные единицы (z_{i3})*(-0.4096)+(z_{i4})*0.6972+(z_{i5})*0.0896 с заметными «весами» (z_{i3})*(-0.4096)+(z_{i4})*0.6972+ (z_{i5})*0.0896 z-переменных z_3,z_4,z_5, соответствующих поглощающимся абсорбатам со смыслами смысл(z_{i3})=ВВ, смысл(z_{i4})=БПК, смысл(z_{i5})=ХПК. Доля силы поглощения биологически поглощаемого кислорода доминирует, следовательно имеем математическую формулу биологического поглощения кислорода, соответствующей части абсорбата БПК. Смысл этой математической формулы назовем БПК4=смысл((z_{i3})*(-0.4096) +(z_{i4})*0.6972+(z_{i5})*0.0896), обозначая биологически поглощенную часть кислорода в у-реакции y_4 (в у-абсорбате y_4 из множества пяти математических у-абсорбатов. Другая расщепленная часть математической формулы у-реакции y_4 имеет вид z_{i1}*0.4689+z_{i2}*0.3439. Смысл этой расщепленной части математической формулы назовем Ресурс4=смысл(z_{i1})*0.4689+ z_{i2}*0.3439), обозначая силы проявлений ионов аммония и растворенного кислорода в у-реакции y_4. Смысл Ресурс4 расщепленной математической формулы ресурсов для у-реакции y_4 относится только к смыслу БПК4 одной активной реакции с математической формулой, полученной выше.

Из математической формулы у-переменной y_5=(z_{i1})*0,3555+(z_{i2})*(-0,1091+(z_{i3})*0,8256+ (z_{i4})*0,3335+(z_{i5})*(-0,2625) выделим формульные единицы (z_{i3})*0,8256+z_{i4}*0,3335+z_{i5}*(-0,2625) с заметными «весами» (z_{i3})*0,8256+(z_{i4})*0,3335+ (z_{i5})*(-0,2625) при z-переменных z_3,z_4,z_5, соответствующих а)сильному поглощению (с силой c^2_{35}=0,8256^2) взвешенных веществ (абсорбата со смыслом смысл(z_{i3})=ВВ); б)мало заметным (с силой c^2_{45}=0,3335^2) биологическим поглощением кислорода; в)уменьшающимся (с силой c^2_{55}=(-0,2625)^2) химическим поглощением кислорода из-за препятствования поступлению из атмосферы растворенного кислорода, объем которого мало заметно уменьшается (с силой c^2_{25}=(-0,1091^2) из-за большого объема в воде (с силой c^2_{35}=0,8256^2) медленно поглощаемых взвешенных веществ. Смысл этой расщепленной математической формулы назовем смысл(ВВ5)=смысл((z_{i3})*(-0.4096)+(z_{i4})*0.6972+ (z_{i5})*0.0896), обозначая поглощенные взвешенные вещества в у-реакции y_5. Другая расщепленная часть математической формулы у-реакции y_5 имеет вид z_{i1}*0,3555+z_{i2}*(-0,1091). Смысл этой расщепленной части математической формулы назовем Ресурс5= смысл(z_{i1}*0,3555+z_{i2}*(-0,1091)), обозначая силы проявлений ионов аммония и растворенного кислорода в у-реакции y_5. Смысл Ресурс5 расщепленной математической формулы ресурсов для у-реакции y_5 относится только к смыслу ВВ5 одной активной реакции с математической формулой, полученной выше. Только наличие большого объема медленно поглощаемых взвешенных веществ немного замедляет приток в воду из атмосферы над поверхностью воды рек и озер Восточного Казахстана растворенного кислорода. Этим фактом объясняется знак минус при «весе» c_{55}=(-0,1091.

В других математических формулах у-реакций «веса» имеют знак плюс (y_4=+z_{i2}*0.3439+; y_{i3}=+z_{i2}*0.2589; y_1=+z_2*0,1536), что свидетельствует о беспрепятственном притоке растворенного кислорода в воду из атмосферы над поверхностью воды рек и озер Восточного Казахстана.

Получено равенство смысл(y_1)+…+ смысл(y_{15})=(Ресурс1+Ресурс2+ Ресурс3+Ресурс4+ Ресурс5).

Сумма математически формул пяти - реакций равна сумме расщепленных формул.

Таблица 1. Числовые данные 12 водоемов по пяти показателям (содержание физико-химических веществ, мг/(м3): ионы аммония (z_1), растворенный кислород (z_2), поглощения взвешенных веществ(z_3), биологически поглощенного кислорода (z_4, БПК), химически поглощенного кислорода (z_5, ХПК).

Название реки\озера	Ионы аммония	Растворенный кислород	Взвеш. вещ-ва	БПК	ХПК
река Сарыбулак	4,1500	7,6300	0,00	5,8900	0
река Есиль	4,3615	10,2000	0,00	2,6100	0

река Нура	4,3615	10,2000	0,00	3,1400	0
канал Нура-Есиль	4,3615	10,2000	0,00	0,5900	53
озеро Копа	4,3615	0,00	0,00	0,00	44
озеро Бурабай	4,3615	11,4167	0,0000	0,0000	0
озеро Улькен Шабакты	4,3615	11,416	8,8000	1,1600	51
озеро Щучье	4,3615	11,1034	8,8000	0,9900	29
озеро Киши Шабакты	4,3615	11,0323	8,8000	1,0800	95
озеро Сулуколь	4,3615	10,5200	8,8000	1,9900	83
озеро Карасье	4,573	9,2600	8,2000	1,2500	51
озеро Жукей	4,3615	7,8300	8,2000	1,8100	89

Таблица 2. Матрица $C_{55}=\{c_{ij}=corr(z_i,y_j)\}$ (z,y)-корреляций при $\Lambda^{(20)}_{55}=diag(1.0666,1.0091,0.9967, 0.9695,0\ .9581)$

1	2	3	4	5
0,5868	**0,0793**	**0,5506**	**0,4689**	**0,3555**
0,1536	**-0,8827**	**0,2589**	**0,3439**	**-0,1091**
0,1538	**-0,1386**	**-0,3283**	**-0,4096**	**0,8256**
-0,4609	**-0,2542**	**-0,3545**	**0,6972**	**0,3335**
0,6293	**0,3615**	**-0,6296**	**0,0896**	**-0,2625**

Заключение

В статье не рассматриваются физико-химические процессы (химический уровень описания реакции абсорбции) выделения поглощенного вещества (абсорбата) из объема поглощающей жидкости (абсорбента). В статье моделируются и анализируются математические формулы у-реакции (информационный и математический уровни описания реакции абсорбции). Рассмотрены задачи расщепления математических формул и расщепления смыслов полученных расщепленных математических формул на 2 типа (когнитивный уровень описания реакции абсорбции). Получено равенство вида (смысл(y_1)+…+смысл(y_{15}))=(Ресурс1+Ресурс2+ Ресурс3+Ресурс4+Ресурс5). Сумма математических формул пяти у-реакций равна сумме расщепленных математических формул.

Из ранее разработанных 5 многосмысловых уравнений с известными и не известными семантическими (смысловыми) переменными получены новые смысловые равенства: сумма двух расщепленных математических формул и их смыслов равна полной формуле и смыслу формулы у-реакции. Количество у-реакций y_1,y_2,y_3,y_4,y_5, имеющих полные математические формулы, равно пяти. Пять смыслов у-реакций y_1,y_2,y_3,y_4,y_5 расщеплены на части, фразы которых приведены выше: смысл(y_1)=БПК1+ХПК1; смысл(y_2)=ХПК2+Ресурс2; смысл(y_{13})=ХПК3+ Ресурс3; смысл(y_4)=БПК4+Ресурс4; смысл(y_5)=ВВ5+Ресурс5.

Расщепленные смыслы из правых частей этих равенств нельзя суммировать, смысловое расщепление смыслов не допускает обратного объединения в один смысл. Расщепленные пары математических формул можно соединить знаком плюс и получится полная математическая формула.

Разработка физико-химических процессов (на новом уровне описания) для расщепленных пар математических формул является задачей будущего.

Пока нужны другие доказательства реальности 6 когнитивных смыслов шести расщепленных математических формул виртуальных у-реакций. Тогда смыслы БПК1, ХПК1, ХПК2, ХПК3, БПК4, ВВ5, удовлетворяющие критерию доминирования силы поглощения, получат новые описания, возможно, в терминах неизвестных технологий.

Мы привели очередную ситуацию моделирования и извлечения когнитивных знаний [4-8] из многомерных данных типа «объект-свойства». Извлеченные значимые знания в начальный момент из данных типа «объект-свойства» делает возможным извлечение знаний и в конечный момент завершения процесса самоочищения воды.

References:

1. Rouvray D. H., (1987). Editorial Foreword (nedostupnaja ssylka), *Journal of Mathematical Chemistry*, Volume 1, Number 1, March, 1987.
2. (1999). Lindemann «Matematicheskie modeli v himii» Per. s nem.: *Himija*, 1999.
3. Gorban`, A.N., & Jablonskij, G. S. (1987). Matematik — himik: vzaimodejstvie i konflikty Arhivnaja kopija ot 6 maja 2011 na Wayback Machine, *Himija i zhizn`*, 1987, № 12, 23-27.
4. Ocheredko, Jy. A. (n.d.). Modelirovanie processov vzaimodejstvija dioksinov so strukturnymi jelementami kletochnoj membrany.
5. Bejder, R. (2001). *Atomy v molekulah. Kvantovaja teorija*. — Moscow: Mir, 2001. — 532 p. — ISBN 5-03-003363-7.
6. Zhanatauov, S.U. (2023). Mathematically calculated reality, supplementing biochemistry of self-purification of the water of rivers and lakes. *ISJ «Theoretical&Applied Science».* 2023, №1, vol.116, 609-623. www.t-science.org
7. Zhanatauov, S.U. (2022). Multiple-sense equations with known and unknown semantic variables, corresponding to multiple equations with numerical parameters and variables. *ISJ «Theoretical & Applied Science»*. 2022, №12, vol.116, pp.1079-1089. www.t-science.org
8. Zhanatauov, S.U. (2021). Cognitive omputing: models. calculations, applica tions, results. *ISJ «Theoretical&AppliedScience»*, №5, vol. 97, pp.594-510. www.t-science.org
9. Zhanatauov, S.U. (2013). *Obratnaja model` glavnyh komponent.* Almaty, Kazstatinform, 2013, 201 p.
10. Zhanatauov, S.U. (2025). *Kognitivnye modeli iskusstvennogointellekta*: monografija. 2025, Almaty: EDP Hub Idipi hab; Moskva:Aj PmAj, Moskva: Aj Pi Ar Media -424p. Tekst-jelektronnyj. ISBN 978-5-4497-5158-4 UDK 004.8 BBK 16.Zh27.
11. Zhanatauov, S.U. (2022). Multiple-sense equations with known and unknown semantic variables, corresponding to multiple equations with numerical parameters and variables. *ISJ «Theoretcal&Applied Science»*. №12, vol.116, 1079-1089. www.t-science.org
12. Zhanatauov, S.U. (2020).Transformation of a system of equations into a system of sums of cognitive meaning of variability of individual consciousnessin-dicators. *ISJ «Theoretical & Applied Science»*. №11, vol. 91, 531-546. www.t-science.org
13. Zhanatauov, S. U. (2021). Modeling the variability of variables in the multidimensional equation of the cognitive meanings of the variables. *ISJ «Theoretical&Applied Science»*. №1, vol.93, 316-328. www.t-science.org
14. Chalmers, C.P. (1975). Generation of correlation matrices with a given eigen-structure. *-J. Stat. Comp. Simul.*, 975, vol.4, pp.133-139.
15. Zhanatauov, S.U. (2019). *Obratnaja spektral`naja zadacha.* Tezisy dokladov Mezhdunarodnoj konferencijai «Matematika v prilozhenijah» v chest` 90-letija Sergeja Konstantinovicha Godunova 4-10 avgusta 2019, Novosibirsk, Rossija, p.132.
16. Zhanatauov, S.U. (2018). Inverse spectral problem with indicated values of components of the eigenvectors. *ISJ Theoretical &Applied Science*. 2018, vol.67, №11, 358-370. www.t-science.org
17. Zhanatauov, S.U. (2017). Theorem on the Λ-samples. *International scientific journal «Theoretical &Applied Science».* № 9, vol. 53, 177-192. www.T-Science.org
18. Zhanatauov, S.U. (2019). A matrix of values the coefficients of combinational proportionality. *Int. Scientific Journal Theoretical&Applied Science*.2019, vol. 71, №3, 401-419. www.t-science.org
19. Zhanatauov, S.U. (2018). Inverse spectral problem. *ISJ Theoretical &Applied Science*. vol.68, №12, 101-112. www.t-science.org
20. Zhanatauov, S.U. (1988). Funkcional`noe napolnenie PPP “Spektr”. -10. Novosibirsk, 1988, pp.3-11.
21. Zhanatauov, S.U. (1979). Organization of a set of programs for operation with binary arrays. *Programmirovanie* №1,1979g., pp.41-42.

Impact Factor:					
	ISRA (India) = 6.317	SIS (USA) = 0.912	ICV (Poland) = 6.630
	ISI (Dubai, UAE) = 1.582	РИНЦ (Russia) = 0.191	PIF (India) = 1.940
	GIF (Australia) = 0.564	ESJI (KZ) = 8.100	IBI (India) = 4.260
	JIF = 1.500	SJIF (Morocco) = 6.004	OAJI (USA) = 0.350

SOI: 1.1/TAS DOI: 10.15863/TAS

International Scientific Journal

Theoretical & Applied Science

p-ISSN: 2308-4944 (print) **e-ISSN:** 2409-0085 (online)

Year: 2026 **Issue:** 10 **Volume:** 162

Received: 23.10.2026
Accepted/Published: 30.10.2026

https://T-Science.org

Issue Article

Alisher Jurakulovich Siddikov
Tashkent State University of Economics
Uzbekistan, DSc. Professor
ORCID: https://orcid.org/0009-0007-2890-043X
siddikovalisher1@gmail.com

Gulchehraxon Ne'matova
Institute for Advanced Training of Personnel and Statistical Research
PhD Student,
Tashkent, Uzbekistan
ORCID: https://orcid.org/0009-0002-6951-7852
gulchehrahonnematova@gmail.com

REGIONAL MISALLOCATION OF LABOUR AND HUMAN CAPITAL IN UZBEKISTAN

Abstract: *Official statistics in the Republic of Uzbekistan indicate the volume of human capital present in each region, yet they fail to reveal where this human capital is most productive. This article applies the "factor-distortion" framework developed by Lu, Peng, and Fang (2024) to Uzbekistan's 14 regions, utilizing SIAT panel data from 2017-2024 to analyze the distribution of formal-sector employees and those with higher education relative to regional output. The analysis incorporates a wage-differential index adjusted for region-specific labour elasticity, decomposes regional disparities using the Dagum Gini coefficient, and tests for σ- and β-convergence employing wild cluster bootstrap inference.*

The findings indicate that human capital is over-allocated relative to output in the Southern regions, the Fergana Valley, and the Lower Amudarya region, while it is under-allocated in Tashkent City and the Navoi region. Notably, the observed disparities are significantly smaller when considering formal employment alone, compared to total employment a broader category that encompasses informal workers and labour migrants. The observed disparity in current prices (the SD of the log index rose from 0,32 to 0,49) is primarily a relative price effect: at constant prices, the dispersion for total employment increased to only 0,35 and showed no significant trend for formal or highly educated workers. There is no strong β-convergence, and the magnitude of inter-zonal differences is not statistically significant when compared to random grouping. Reallocating total employment would increase output by 3-16% at the upper bound, while the impact on formal employment would be approximately 1% or less. In the Kashkadarya region, the labour share grew faster than the share of real output. These results caution against interpreting regional productivity gaps as labour market distortions without accounting for prices, informality, and migration.

Key words: *misallocation; human capital; regional labour productivity; Dagum Gini coefficient; convergence; informal employment.*

Language: *English*

Citation: Siddikov, A.J., & Ne'matova, G. (2026). Regional misallocation of labour and human capital in uzbekistan. *ISJ Theoretical & Applied Science, 10 (162),* 47-55.

Soi: https://s-o-i.org/1.1/TAS-10-162-8 ***Doi***: crossref https://dx.doi.org/10.15863/TAS.2026.10.162.8

Scopus ASCC: *1804.*

Introduction

The regions of Uzbekistan exhibit significant disparities in output per worker more so than in almost any other economic indicator. In 2024, the Gross Regional Product (GRP) per employed person in the Navoi region was approximately 3,2 times the national average, and 2,3 times the national average in Tashkent City; conversely, in the Surkhandarya,

Fergana, and Namangan regions, this figure stood at only 0,59-0,66 of the national average. Such disparities raise a critical question for growth and regional policy: are labour and human capital located where they are most productive? If marginal products differ widely across regions, reallocating workers or shifting jobs and capital toward workers could increase national output without requiring additional inputs (Restuccia & Rogerson, 2008; Hsieh & Klenow, 2009).

While official statistics indicate the quantity of labour and human capital present in each region, they do not reveal how these resources are distributed relative to production potential that is, they do not provide measures of productivity. This article specifically measures this indicator. While the approach of Lu, Peng, and Fang (2024) measures the misallocation of human capital in Chinese cities using relative factor-price-distortion coefficients, the present article examines this issue by decomposing regional disparities utilizing the Dagum (1997) Gini coefficient and testing for both σ-convergence and β-convergence. The application is not straightforward: Uzbekistan consists of only 14 first-level administrative units; its employment statistics include labour migrants working abroad; and the output of the Navoi mining region, measured in current prices, is highly sensitive to global metal prices. Each of these characteristics alters the interpretation of the index, and the article addresses them explicitly.

The article explores the following questions: how are total employment, formal employment, and the highly educated workforce distributed in relation to regional output? Do regional disparities primarily exist between or within economic zones? Has the distribution converged between 2017 and 2024? And how significant are the potential gains from reallocation of resources? In the authors' view, the contribution consists of presenting the first regional misallocation indices for Uzbekistan constructed based on official statistics and distinguishing between general, formal, and highly educated labour and demonstrating that the conclusion regarding divergence depends on the price basis used for output; it further shows that, for these same regions, resource allocation and the efficiency of human capital utilization previously assessed using Data Envelopment Analysis (DEA) are distinct phenomena.

Literature review. Misallocation. If disparities in the marginal productivity of factors of production arise across various economic units due to barriers or policy interventions, the total volume of output will fall below the level achievable under an efficient allocation (Restuccia & Rogerson, 2008). According to estimates by Hsieh and Klenow (2009), equalizing marginal productivity across manufacturing firms could increase total factor productivity (TFP) by 30-50 percent in China and by 40-60 percent in India. This approach was subsequently extended to sectors and regions: Aoki (2012) linked sector-specific factor price disparities to total factor productivity (TFP); Chen and Hu (2011) proposed relative distortion coefficients, which have been widely used in studies of Chinese regions; Brandt, Tombe, and Zhu (2013) quantified distortions across Chinese provinces; and Hsieh and Moretti (2019) demonstrated how housing-related constraints in highly productive U.S. cities have dampened overall economic growth. Regarding human capital, Vollrath (2014) found that equalizing returns across various sectors in developing countries leads to a relatively modest increase in total output. Meanwhile, Lu et al. (2024) observed a decline in the misallocation of human capital across Chinese cities; disparities between urban agglomerations serve as a primary factor, with the process exhibiting characteristics of both σ-convergence and β-convergence.

Measurement caveats. Differences in average productivity reflect differences in marginal productivity only if production elasticities are identical across all units; capital intensity and resource rents violate this condition (Restuccia & Rogerson, 2017). Disparities in nominal wages and productivity also incorporate factors such as the cost of living and amenities (Roback, 1982), as well as the distribution of the skilled workforce (Combes, Duranton, & Gobillon, 2008; Young, 2013). In developing economies, part of the productivity gap between rural and urban areas is explained by the informal sector and selection processes (Gollin, Lagakos, & Waugh, 2014). β-convergence regressions are prone to "regression-to-the-mean" bias (Friedman, 1992; Quah, 1993), while "fixed-effects" estimates often used with short panel data tend to be biased toward convergence (Nickell, 1981).

Research gap. The authors have not encountered any research in Uzbekistan that examines the regional distribution of labour resources and human capital in relation to production output. In general, when applying the relative distortion index, the extent to which factors such as production prices, informal employment, and labour migration influence the measured level of distortion is rarely analyzed.

Data and methodology. Data and unit of analysis. All data were obtained from the Statistical Information System (SIAT) of the Statistics Agency under the President of the Republic of Uzbekistan and were downloaded in October 2026. The units of analysis are the first-level administrative divisions: the Republic of Karakalpakstan, 12 regions (viloyats), and the city of Tashkent (n = 14). The study period covers the years 2017-2024 (T = 8); this represents the longest period for which data are available at the regional level across all indicators. The year 2025 was excluded from the analysis because the Gross Regional Product (GRP) figures for that year are preliminary, and data regarding higher education

have not yet been published. The list of indicators is presented in Table 1.

Table 1. Indicators used (SIAT, 14 regions, 2017-2024) [13]

Symbol	Indicator and definition	Unit	Role in the analysis
Y	Gross regional product (GRP), current prices	bn soum	Output share s_i (Eqs. 1-4)
Yr	GRP in constant 2017 prices, chained from official regional volume growth rates	bn soum, 2017 prices	Constant-price robustness check
E	Employed population: formal and informal employment and labour migrants working abroad	thousand persons	Total labour; $\hat{\gamma}_E$
F	Average number of employees in legal entities (formal employment)	persons	Formal labour; $\hat{\gamma}_F$
H	Employees with higher education in legal entities	persons	Human capital; $\hat{\gamma}_H$
w	Average nominal monthly wage	soum	Wage bill $W = 12 \cdot w \cdot F$; $\hat{\gamma}_W$
-	Share of the informal economy in GRP	%	Interpretation of results

Two definitions are particularly important here. According to the methodology of the Statistics Agency, the "employed population" includes migrants working abroad; meanwhile, the categories of "employees" and "employees with higher education" encompass only hired workers employed by legal entities and registered via an official employment record book. Since a portion of the Gross Domestic Product (GDP) is not allocated by region, the shares of production volume are calculated relative to the sum of the Gross Regional Products (GRP).

Relative distribution index. In accordance with Chen and Hu (2011) and Lu et al. (2024), the relative distortion coefficient for factor L in region i and year t is as follows:

$$\hat{\gamma}_{L,it} = \frac{\frac{L_{it}}{L_t}}{s_{it}\frac{\beta_{L,i}}{\beta_L}}, \qquad s_{it} = \frac{Y_{it}}{Y_t},$$

$$\beta_L = \sum_i s_{it}\,\beta_{L,i}, \qquad (1)$$

Here s_{it} represents the region's share of output, and $\beta_{L,i}$ is the output elasticity of the factor. A value of $\hat{\gamma} > 1$ indicates that the region's share of the factor exceeds its output share (i.e., the factor is over-allocated to the region), while $\hat{\gamma} < 1$ indicates under-allocation. Lu et al. (2024) estimate region-specific elasticities using a production function that incorporates capital stocks; however, since data on regional capital stocks are unavailable for the 14 units over the eight-year period, two alternative approaches are employed here.

Productivity-gap index (common elasticity). If $\beta_{L,i} = \beta_L$ for all regions, Eq. (1) reduces to

$$\hat{\gamma}_{L,it} = \frac{L_{it}/L_t}{Y_{it}/Y_t} = \frac{Y_t/L_t}{Y_{it}/L_{it}}, \qquad (2)$$

which is the reciprocal of relative average labour productivity. This indicator is calculated for total employment ($\hat{\gamma}_E$), formal sector employment ($\hat{\gamma}_F$) and employees with higher education ($\hat{\gamma}_H$).

Wage-gap index (region-specific elasticity). Under conditions of competition in the markets for factors of production, the output elasticity of labour is equal to labour's share in income: $\beta_{F,i} = W_i/Y_i$, where W_i is the formal wage bill (average monthly wage × 12 × formal employees). Substituting into Eq. (1) gives

$$\hat{\gamma}_{W,it} = \frac{F_{it}/F_t}{W_{it}/W_t} = \frac{\bar{w}_t}{w_{it}}, \qquad (3)$$

the ratio of the national average wage to the regional wage. This approach allows for regional variations in elasticity indicators; however, it covers only formal employment and is influenced by regional living costs and skill levels.

Output volume is measured in current prices (as published) and in constant 2017 prices. The figures for constant prices were calculated by chaining official regional growth rates. This is because changes in relative prices specifically, fluctuations in metal prices, as seen in the Navoi region can alter the shares of output, even if the actual volume of production remains unchanged.

Aggregate measures and counterfactual. Dispersion is measured by the standard deviation (SD) of ln $\hat{\gamma}$ across regions. To gauge the cost of misallocation, let regional output be $Y_i = A_i L_i^{\beta}$, where A_i absorbs capital, land and technology, which are held fixed in place. Output is maximised when marginal products are equal, i.e., $L_i^* = L \cdot A_i^{1/(1-\beta)} / \Sigma_j A_j^{1/(1-\beta)}$, and the potential gain is

$$Gain = \frac{\sum_i A_i\,(L_i^*)^{\beta}}{\sum_i Y_i} - 1, \qquad (4)$$

Because β is not identified, results are reported for β = 0,3-0,6. The gain is an upper bound that ignores migration costs, congestion, skill differences and the mobility of capital.

Dagum Gini decomposition. Regional differences in $\hat{\gamma}$ are decomposed with the Dagum (1997) Gini coefficient into within-zone (G_w), net between-zone (G_{nb}) and transvariation (G_t) components, $G = G_w + G_{nb} + G_t$. Regions are grouped into six economic zones commonly used in Uzbek economic geography: Tashkent (Tashkent City, Tashkent region), Fergana Valley (Andijan, Namangan, Fergana), Mirzachul (Syrdarya, Jizzakh), Zarafshan (Samarkand, Bukhara, Navoi), Southern (Kashkadarya, Surkhandarya) and Lower Amudarya (Karakalpakstan, Khorezm). Because zones contain two or three regions, a large between-zone share can arise mechanically, so the observed share is compared with 4 999 random assignments of regions to zones of equal size (permutation test).

Convergence tests. σ-convergence is tested by a linear trend in the SD of ln $\hat{\gamma}$; β-convergence is tested by

$$\Delta \ln \hat{\gamma}_{it} = \alpha + b \ln \hat{\gamma}_{i,t-1} + \mu_i + \eta_t + \varepsilon_{it}, \qquad (5)$$

where b < 0 indicates convergence. Three variants are estimated: pooled OLS (absolute convergence), two-way fixed effects, and a long-difference cross-section of the 2017-2024 change on the 2017 level. With 14 clusters, pooled p-values are taken from a wild cluster bootstrap with Webb weights and 1 999 replications (Cameron, Gelbach, & Miller, 2008; Webb, 2023). The fixed-effects estimate carries a Nickell (1981) bias of about -(1+b)/(T-1), large for T = 7, and is not used as evidence of convergence.

Robustness. Results are re-estimated without Navoi and Tashkent City, with Tashkent City and Tashkent region merged (their boundary changed: Tashkent City's population grew by 4,8% in 2021 and 6,2% in 2022 against 1,7-3,3% in other years), and for 2019-2024.

Research results.

Regional pattern of allocation. Table 2 and Figure 1 show the indices. Measured against current-price output, total employment was over-allocated in 11 of the 14 regions in 2024 and strongly under-allocated in Navoi ($\hat{\gamma}_E$ = 0,31) and Tashkent City (0,44), with Tashkent region also below 1 (0,77). The highest values were in Surkhandarya (1,69), Fergana (1,56), Karakalpakstan (1,53), Namangan (1,51) and Kashkadarya (1,44). These are the regions where output per employed person is lowest.

Table 2. Relative allocation indices by region, 2017 and 2024 [13]

Region	Zone	$\hat{\gamma}_E$ 2017	$\hat{\gamma}_E$ 2024	$\hat{\gamma}_E$ 2024, const. prices	$\hat{\gamma}_F$ 2024	$\hat{\gamma}_H$ 2017	$\hat{\gamma}_H$ 2024	$\hat{\gamma}_W$ 2024
Surkhandarya	Southern	1,34	1,69	1,42	1,22	1,02	1,35	1,34
Fergana	Fergana V.	1,42	1,56	1,41	1,35	1,03	1,12	1,36
Karakalpakstan	L. Amudarya	1,10	1,53	1,42	1,47	1,36	1,53	1,19
Namangan	Fergana V.	1,30	1,51	1,31	1,15	0,97	1,00	1,38
Kashkadarya	Southern	1,10	1,44	1,28	1,09	1,05	1,15	1,35
Samarkand	Zarafshan	1,15	1,37	1,19	1,03	0,99	1,16	1,32
Khorezm	L. Amudarya	1,26	1,36	1,37	1,22	1,15	1,12	1,24
Andijan	Fergana V.	1,35	1,34	1,31	1,01	0,94	0,92	1,16
Jizzakh	Mirzachul	1,01	1,20	1,19	1,04	1,11	1,15	1,31
Syrdarya	Mirzachul	1,02	1,15	1,04	1,15	0,92	1,09	1,24
Bukhara	Zarafshan	0,97	1,01	0,96	1,04	0,96	1,07	1,23

Region	Zone	$\hat{\gamma}_E$ 2017	$\hat{\gamma}_E$ 2024	$\hat{\gamma}_E$ 2024, const. prices	$\hat{\gamma}_F$ 2024	$\hat{\gamma}_H$ 2017	$\hat{\gamma}_H$ 2024	$\hat{\gamma}_W$ 2024
Tashkent region	Tashkent	0,90	0,77	0,82	0,86	0,68	0,65	1,09
Tashkent City	Tashkent	0,48	0,44	0,45	0,93	1,16	1,09	0,61
Navoi	Zarafshan	0,54	0,31	0,53	0,49	0,74	0,45	0,77

Note: $\hat{\gamma} > 1$ - the region's share of the factor exceeds its output-weighted share (over-allocation); $\hat{\gamma} < 1$ - under-allocation; E - total employment; F - formal employees; H - employees with higher education; W - wage-gap index (Eq. 3). Regions are ordered by $\hat{\gamma}_E$ in 2024.

Three features qualify this reading. First, formal-employment indices are much closer to 1: in Andijan, Samarkand and Kashkadarya $\hat{\gamma}_F$ is 1,01-1,09 while $\hat{\gamma}_E$ is 1,34-1,44. Because total employment includes informal workers and migrants abroad, whose output is not in regional GRP, much of the "excess" labour lies outside the formal sector. Second, Navoi's position is largely a price effect: its share of current-price GRP rose from 5,8% in 2017 to 9,8% in 2024, while its share of constant-price GRP stayed at 5,7-5,9%. In constant prices its $\hat{\gamma}_E$ was 0,53 in both years. Third, the higher-education index orders regions differently: Tashkent City holds slightly *more* highly educated employees than its output share ($\hat{\gamma}_H$ = 1,09), Tashkent region (0,65) and Navoi (0,45) fewer, and Karakalpakstan the most (1,53). The wage-gap index compresses the range to 0,61 (Tashkent City) - 1,38 (Namangan): formal wages were 1,65 times the national average in Tashkent City and 1,29 in Navoi, but 0,72-0,74 in Namangan, Surkhandarya, Fergana and Kashkadarya.

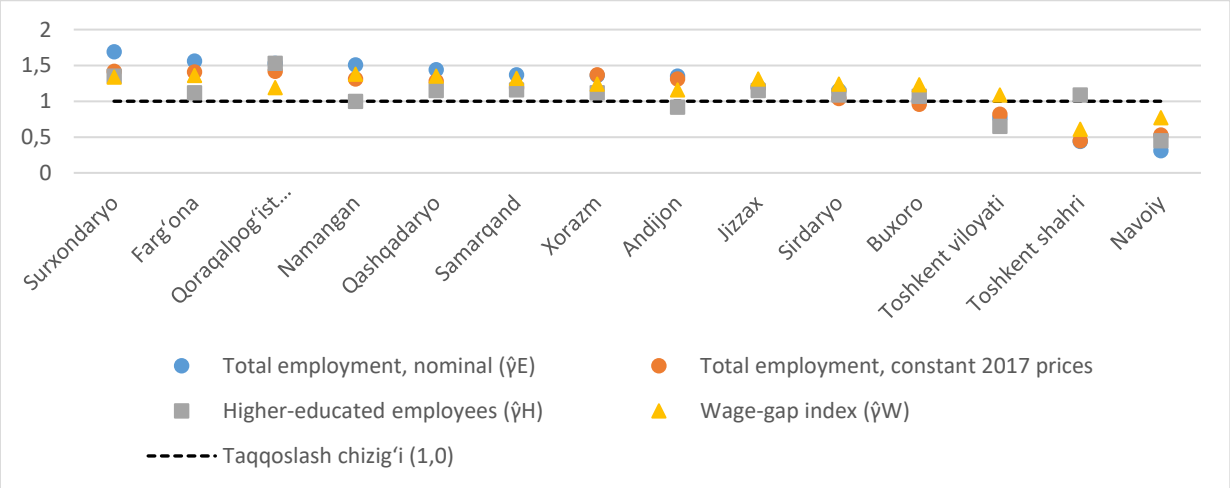

Figure 1. Relative allocation indices by region, 2024 [13]

Kashkadarya. Kashkadarya illustrates a region whose labour share has grown faster than its output. Its $\hat{\gamma}_E$ rose from 1,10 in 2017 to 1,44 in 2024 in current prices and from 1,10 to 1,28 in constant prices; only Karakalpakstan (+29%) and Jizzakh (+18%) recorded larger constant-price increases than Kashkadarya (+16%). Part of the rise in 2024 reflects a jump in recorded employment (from 1 220,1 to 1 296,3 thousand, +6,2% in one year), larger than in any earlier year of the period. The formal-employment index (1,09) and the higher-education index in constant prices (1,02) are close to 1, while the wage-gap index rose from 1,10 to 1,35, i.e., formal wages in the region fell from 0,91 to 0,74 of the national average. The region's misallocation is therefore concentrated in informal and migrant employment and in relative wages, not in the number of highly educated employees.

Dispersion and σ-convergence. Figure 2 and Table 3 show the evolution of dispersion. In current prices the SD of ln $\hat{\gamma}_E$ rose from 0,317 in 2017 to 0,485 in 2024, with a significant positive trend (slope 0,019 per year, p = 0,005); the same holds for formal and higher-educated employees. This would suggest growing misallocation - σ-divergence. In constant prices, however, the picture changes: dispersion of total employment rose only from 0,317 to 0,354 (slope 0,004, p = 0,014), and for formal (p = 0,63) and higher-

educated employees (p = 0,23) there is no significant trend. Most of the measured divergence is thus a relative-price effect rather than a change in the allocation of workers. The wage-gap index, which does not depend on output prices, shows a modest but significant increase in dispersion (0,170 to 0,228; p = 0,001), driven by rising relative wages in Tashkent City.

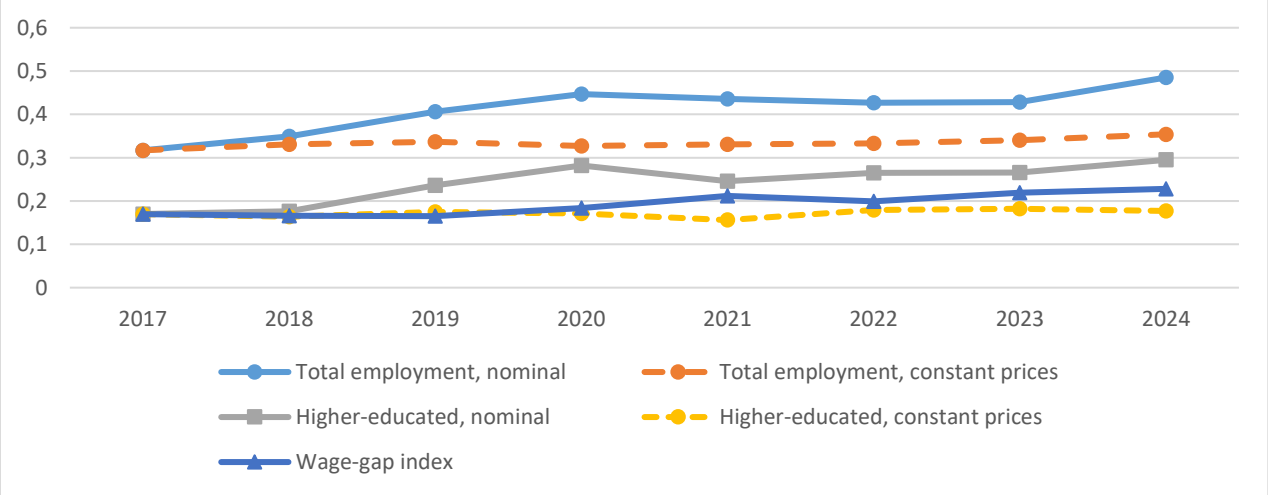

Figure 2. Dispersion of relative allocation indices, 2017-2024 [13]

Table 3. σ-convergence: SD of ln $\hat{\gamma}$ across regions and robustness [13]

Specification	2017	2019	2024	Trend per year	p-value
Total employment, current prices	0,317	0,406	0,485	0,019	0,005
Total employment, constant prices	0,317	0,337	0,354	0,004	0,014
Formal employees, constant prices	0,123	0,105	0,131	0,001	0,632
Higher-educated, current prices	0,169	0,236	0,295	0,016	0,006
Higher-educated, constant prices	0,169	0,175	0,177	0,002	0,232
Wage-gap index	0,170	0,165	0,228	0,010	0,001
Total employment, excl. Navoi and Tashkent City	0,143	0,192	0,209	0,009	0,014
Total employment, Tashkent merged (n = 13)	0,281	0,382	0,464	0,022	0,006

Note: trend - OLS slope of the SD on year, 2017-2024 (8 observations); p-values are indicative given the short series. Excluding the two outliers and merging Tashkent are computed in current prices.

Excluding Navoi and Tashkent City more than halves dispersion but leaves a positive current-price trend; merging Tashkent leaves results unchanged; for 2019-2024 alone no current-price trend is significant at 5%, because most of the increase occurred in 2018-2020.

Potential output gains. Table 4 reports the counterfactual gains from Eq. (4). Reallocating total employment towards output would raise aggregate output by 3,1-12,3% in 2017 and by 4,1-16,2% in 2024 in constant prices, depending on β. Reallocating formal employees would raise it by less than 1,2% in every year. In current prices the gains are larger (up to 28% for total employment in 2024) because Navoi's price-driven output share inflates the apparent productivity gap. Excluding Navoi and Tashkent City, the current-price gain for total employment in 2024 falls to 1,3-5,0%.

Table 4. Potential output gain from equalizing marginal products of labour, % [13]

Labour measure and price basis	β	2017	2020	2024
Total employment, constant prices	0,3	3,1	3,1	4,1
	0,5	7,7	7,8	10,3
	0,6	12,3	12,3	16,2
Formal employees, constant prices	0,3	0,3	0,2	0,3
	0,5	0,8	0,6	0,7
	0,6	1,2	0,8	1,0
Total employment, current prices	0,5	7,7	14,0	17,8
Formal employees, current prices	0,5	0,8	3,3	3,6

Note: static, partial-equilibrium upper bound under $Y_i = A_i L_i^{\beta}$ with capital and land fixed in place (Eq. 4).

Table 5. Dagum Gini decomposition of relative allocation indices by economic zone [17]

Index, year	G	G_w, %	G_{nb}, %	G_t, %	Permutation p
$\hat{\gamma}_E$ 2017	0,140	7,9	85,7	6,4	-
$\hat{\gamma}_E$ 2024	0,182	7,9	85,0	7,1	0,087
γE 2024, const. prices	0,148	6,9	88,8	4,4	-
$\hat{\gamma}_H$ 2017	0,088	9,2	65,0	25,9	-
$\hat{\gamma}_H$ 2024	0,123	11,5	70,8	17,7	0,602
$\hat{\gamma}_H$ 2024, const. prices	0,093	9,8	67,1	23,1	-

Note: G - overall Dagum Gini; G_w, G_{nb}, G_t - within-zone, net between-zone and transvariation contributions in % of G. Permutation p - share of 4 999 random assignments of regions to zones of equal size with a between-zone share (G_{nb} + G_t) at least as large as observed. Source: authors' calculations.

This seems to replicate Lu et al.'s (2024) finding that between-group differences dominate. However, with six zones of two or three regions, random grouping yields a between-zone share of about 89% on average; the observed share is only marginally higher for total employment (p = 0,087) and not higher for higher-educated employees (p = 0,60). Regional differences are driven by individual units - Tashkent City and Navoi versus Surkhandarya, Fergana and Karakalpakstan - not by zones. Within-zone inequality is highest in Zarafshan (Navoi versus Samarkand and Bukhara; within-zone Gini 0,26 in 2024).

β-convergence. Table 6 reports Eq. (5). In pooled OLS the coefficient on the lagged level is positive for total employment (b = 0,049; wild bootstrap p = 0,049, i.e., marginal divergence) and not significantly different from zero for the other indices according to the wild cluster bootstrap; the long-difference cross-section gives the same picture. There is thus no evidence of absolute β-convergence; if anything, regions with higher over-allocation in current prices drifted further from 1. In constant prices all pooled and long-difference coefficients are close to zero and insignificant. The two-way fixed-effects estimates for $\hat{\gamma}_E$ and $\hat{\gamma}_H$ are large and negative (b ≈ -0,41 to -0,56), but the Nickell bias alone is about -0,17 for b near zero, and the pooled and cross-section estimates show no convergence; they are therefore read as mean reversion around region-specific levels and noise, not as evidence that misallocation is disappearing.

Table 6. β-convergence of ln $\hat{\gamma}$, 2017-2024 [13]

Index	Pooled b (SE)	WCB p	Two-way FE b (SE)	Long-difference b (SE)	p
$\hat{\gamma}_E$, current prices	0,049 (0,012)	0,049	-0,433 (0,058)	0,064 (0,045)	0,157
$\hat{\gamma}_H$, current prices	0,046 (0,023)	0,253	-0,412 (0,045)	0,068 (0,065)	0,296
$\hat{\gamma}_W$	0,036 (0,024)	0,509	-0,227 (0,168)	0,036 (0,043)	0,405
$\hat{\gamma}_E$, constant prices	0,012 (0,005)	0,135	-0,550 (0,101)	0,011 (0,007)	0,086
$\hat{\gamma}_H$, constant prices	-0,015 (0,013)	0,271	-0,563 (0,185)	-0,000 (0,007)	0,946

Note: dependent variable $\Delta \ln \gamma_{it}$ (pooled and FE, 98 observations) or the average annual change 2017-2024 (long difference, n = 14). Pooled and FE standard errors are clustered by region; WCB p - wild cluster bootstrap p-value (Webb weights, 1 999 replications); long-difference standard errors are HC3.

Allocation and efficiency. In the authors' companion DEA analysis of the same regions, Kashkadarya, Navoi and Surkhandarya lie on the efficiency frontier and Tashkent City has the lowest score. The rank correlation between DEA efficiency (CCR) and the allocation indices is weak and insignificant: Spearman ρ = 0,21 (p = 0,46) for ln $\hat{\gamma}_E$, -0,03 (p = 0,91) for ln $\hat{\gamma}_H$ and 0,43 (p = 0,13) for |ln $\hat{\gamma}_H$|. Efficiency and allocation are thus distinct dimensions: Kashkadarya is DEA-efficient yet holds much more labour than its output share, while Navoi is efficient and under-allocated. With 14 units only large associations could have been detected.

Discussion. First, labour in Uzbekistan is far from proportional to output across regions, but most of the gap lies between the formal and the informal-plus-migrant segment of the labour force. Regions with higher $\hat{\gamma}_E$ tend to have larger informal economies: the rank correlation between $\hat{\gamma}_E$ and the informal share of GRP in 2024 is ρ = 0,56 (p = 0,04), against ρ = 0,45 (p = 0,11) for $\hat{\gamma}_F$; the informal share was 41-47% in Surkhandarya, Kashkadarya and Khorezm and 15-16% in Navoi and Tashkent City. Because employment includes migrants abroad, part of the measured over-allocation is not domestic misallocation at all: those workers produce elsewhere and contribute remittances, not GRP. SIAT does not publish regional migration series that would separate the two.

Second, the price basis is not a technicality. With current-price GRP, as is usual in applications of the relative distortion index, one would conclude that misallocation rose sharply after 2018; in constant prices most of that rise disappears. For resource-rich regions the productivity-gap index measures resource rents as much as labour distortions (Restuccia & Rogerson, 2017), so studies of commodity-exporting economies should report both price bases.

Third, unlike Lu et al. (2024) for China, there is no σ- or β-convergence, and the dominance of between-group differences is not robust to the small number of units per group. This does not contradict their findings, given different settings, but shows that these tools need small-sample diagnostics when applied to few regions. For human capital, $\hat{\gamma}_H$ partly reflects the geography of public services - teachers, doctors and civil servants located by population rather than output - and is better read as the departure of graduates' distribution from market production than as evidence that graduates should move.

The limitations are clear. Without regional capital stock, the common-elasticity index conflates labour distortions with capital intensity; without regional price levels, the wage-gap index overstates real wage differences; employment includes migrants; and trend tests rest on eight annual observations. All results are descriptive and do not identify the causes of misallocation - migration costs, housing, registration rules, credit or public employment policies.

Conclusion

Using only official SIAT statistics, this paper measured the allocation of labour and human capital across Uzbekistan's 14 regions relative to output in 2017-2024. Labour is over-allocated in the southern, Fergana Valley and Lower Amudarya regions and under-allocated in Tashkent City and Navoi, but most of the gap concerns informal and migrant employment; formal and highly educated employees are allocated much closer to output. The apparent divergence in current prices is largely a relative-price effect, there is no robust convergence or divergence in constant prices, and differences between economic zones are no larger than random grouping would produce. The main potential gain therefore lies less in moving formal or highly educated workers than in raising the productivity of informal employment and creating formal jobs in labour-abundant regions such

as Kashkadarya. Regional capital stock, regional labour migration and regional price indices are the three statistical additions that would make such measurement more reliable.

References:

1. Aoki, S. (2012). A simple accounting framework for the effect of resource misallocation on aggregate productivity. *Journal of the Japanese and International Economies*, 26(4), 473–494. https://doi.org/10.1016/j.jjie.2012.08.001
2. Brandt, L., Tombe, T., & Zhu, X. (2013). Factor market distortions across time, space and sectors in China. *Review of Economic Dynamics*, 16(1), 39–58. https://doi.org/10.1016/j.red.2012.10.002
3. Cameron, A. C., Gelbach, J. B., & Miller, D. L. (2008). Bootstrap-based improvements for inference with clustered errors. *Review of Economics and Statistics*, 90(3), 414–427. https://doi.org/10.1162/rest.90.3.414
4. Chen, Y., & Hu, W. (2011). Distortions, misallocation and losses: Theory and application. *China Economic Quarterly*, 10(4), 1401–1422. (In Chinese)
5. Combes, P.-P., Duranton, G., & Gobillon, L. (2008). Spatial wage disparities: Sorting matters! *Journal of Urban Economics*, 63(2), 723–742. https://doi.org/10.1016/j.jue.2007.04.004
6. Dagum, C. (1997). A new approach to the decomposition of the Gini income inequality ratio. *Empirical Economics*, 22(4), 515–531. https://doi.org/10.1007/BF01205777
7. Friedman, M. (1992). Do old fallacies ever die? *Journal of Economic Literature*, 30(4), 2129–2132.
8. Gollin, D., Lagakos, D., & Waugh, M. E. (2014). The agricultural productivity gap. *Quarterly Journal of Economics*, 129(2), 939–993. https://doi.org/10.1093/qje/qjt056
9. Hsieh, C.-T., & Klenow, P. J. (2009). Misallocation and manufacturing TFP in China and India. *Quarterly Journal of Economics*, 124(4), 1403–1448. https://doi.org/10.1162/qjec.2009.124.4.1403
10. Hsieh, C.-T., & Moretti, E. (2019). Housing constraints and spatial misallocation. *American Economic Journal: Macroeconomics*, 11(2), 1–39. https://doi.org/10.1257/mac.20170388
11. 12. Lu, W., Peng, L., & Fang, N. (2024). The impact of human capital misallocation on green economy efficiency: Empirical analysis of Chinese urban agglomerations. *Heliyon*, 10, e32695. https://doi.org/10.1016/j.heliyon.2024.e32695
12. (2026). *National Statistics Committee of the Republic of Uzbekistan. SIAT – Statistical information and analytical system [Database]*. https://siat.stat.uz (accessed October 2026).
13. Nickell, S. (1981). Biases in dynamic models with fixed effects. *Econometrica*, 49(6), 1417–1426. https://doi.org/10.2307/1911408
14. Quah, D. (1993). Galton's fallacy and tests of the convergence hypothesis. *Scandinavian Journal of Economics*, 95(4), 427–443. https://doi.org/10.2307/3440905
15. Restuccia, D., & Rogerson, R. (2008). Policy distortions and aggregate productivity with heterogeneous establishments. *Review of Economic Dynamics*, 11(4), 707–720. https://doi.org/10.1016/j.red.2008.05.002
16. Restuccia, D., & Rogerson, R. (2017). The causes and costs of misallocation. *Journal of Economic Perspectives*, 31(3), 151–174. https://doi.org/10.1257/jep.31.3.151
17. Roback, J. (1982). Wages, rents, and the quality of life. *Journal of Political Economy*, 90(6), 1257–1278. https://doi.org/10.1086/261120
18. Siddikov, A. J. (2022). Development of a critical level of indicative indicators for diagnosing the macroeconomic balance of Uzbekistan. *ISJ Theoretical & Applied Science*, 02 (106), 307-315. Soi: http://s-o-i.org/1.1/TAS-02-106-37 Doi: https://dx.doi.org/10.15863/TAS.2022.02.106.37
19. Vollrath, D. (2014). The efficiency of human capital allocations in developing countries. *Journal of Development Economics*, 108, 106–118. https://doi.org/10.1016/j.jdeveco.2014.01.008
20. Webb, M. D. (2023). Reworking wild bootstrap-based inference for clustered errors. *Canadian Journal of Economics*, 56(3), 839–858. https://doi.org/10.1111/caje.12661
21. Young, A. (2013). Inequality, the urban-rural gap, and migration. *Quarterly Journal of Economics*, 128(4),1727–1785. https://doi.org/10.1093/qje/qjt025

Impact Factor:					
	ISRA (India) = 6.317	SIS (USA) = 0.912	ICV (Poland) = 6.630
	ISI (Dubai, UAE) = 1.582	РИНЦ (Russia) = 0.191	PIF (India) = 1.940
	GIF (Australia) = 0.564	ESJI (KZ) = 8.100	IBI (India) = 4.260
	JIF = 1.500	SJIF (Morocco) = 6.004	OAJI (USA) = 0.350

SOI: 1.1/TAS DOI: 10.15863/TAS

International Scientific Journal

Theoretical & Applied Science

p-ISSN: 2308-4944 (print) **e-ISSN:** 2409-0085 (online)

Year: 2026 **Issue:** 10 **Volume:** 162

Received: 28.10.2026
Accepted/Published: 30.10.2026 https://T-Science.org

Issue Article

G. B. Suyunova
Karshi State Technical University
Doctoral Researcher, Uzbekistan
gulhayobotirovna40@gmail.com

N. N. Usmanov
University of Military Security and Defense of the Republic of Uzbekistan
Doctor of Agricultural Sciences (DSc), Professor,
Postgraduate Education Department, Military Aviation Institute,
usmon.nosir@inbox.ru

EFFECT OF DIFFERENT SOWING DATES AND PLANTING PATTERNS ON THE GROWTH AND DEVELOPMENT OF PEA (PISUM SATIVUM L.) VARIETIES

Abstract: *A field study was conducted under the conditions of long-cultivated, irrigated typical sierozem soils in Kashkadarya Region, Uzbekistan, to investigate the growth and development of forage pea (Pisum sativum L.) varieties sown at different dates and using different planting patterns. Sowing was carried out on 10, 20, and 30 October. The results showed that seed emergence was delayed by 3–5 days as the sowing date was postponed. Nevertheless, the average field emergence rate across all varieties was 99.8%. Increasing the area available to individual plants by changing the planting pattern from the control spacing of 60x20 cm to 60x25 cm and 60x30 cm positively affected the development of generative organs and prolonged the flowering and pod-setting phases by 2–5 days. The flowering and pod-setting periods of the Vostok-55 and K-295 varieties differed by several days from those of Osiyo-2001, influencing the overall duration of the growing season. In the treatments sown on 10 October, the growing season lasted an average of 217–230 days, providing favorable conditions for plant growth and development. These findings may be associated with more active development of vegetative and generative organs under wider plant-spacing arrangements.*

Key words: *forage pea, pea, variety, sowing date, planting pattern, plant nutritional area, field emergence, phenological phases, plant growth dynamics, growing season, generative organs, typical sierozem soils, agricultural technology.*

Language: *English*

Citation: Suyunova, G.B., & Usmanov, N.N. (2026). Effect of different sowing dates and planting patterns on the growth and development of pea (Pisum sativum L.) Varieties. *ISJ Theoretical & Applied Science, 10 (162),* 56-63.

Soi: https://s-o-i.org/1.1/TAS-10-162-9 ***Doi***: crossref https://dx.doi.org/10.15863/TAS.2026.10.162.9

Scopus ASCC: *1100.*

Introduction

UDC: 635.656:631.5

The continuous growth of the global population and the increasing demand for protein-rich plant products, environmentally sustainable food, and high-quality feed for livestock have made the cultivation of forage pea increasingly important. Owing to its high content of protein, starch, vitamins, and minerals, pea is an important raw material for the food industry and livestock production.

Previous studies have shown that forage pea varieties differ in their responses to sowing dates and that interactions between varietal biological characteristics and environmental conditions play an important role in yield formation. This highlights the

need to evaluate individual varieties not according to a single, universally applied sowing date, but with due consideration of their biological characteristics [1–3, 5, 11, 12, 14–24]. At the same time, improving pea cultivation technologies, scientifically determining the effects of sowing dates and planting patterns on productivity, and developing agronomic practices that ensure high and good-quality seed yields are important scientific and practical objectives.

Therefore, further research into the production of forage pea varieties for seed purposes, together with the development and recommendation of innovative agricultural technologies to increase productivity, establishes the relevance and practical necessity of this research.

Research objective

The objective of this study was to provide a scientific basis for improving the cultivation practices used to grow forage pea varieties for green manure and seed production under the conditions of long-cultivated, irrigated typical sierozem soils in Yakkabog District, Kashkadarya Region, Uzbekistan, using different sowing dates and planting patterns, with the aim of obtaining high-quality seed and grain yields.

Research objects

The research objects were long-cultivated, irrigated typical sierozem soils in Kashkadarya Region and three forage pea varieties: Osiyo-2001, Vostok-55 and K-295.

Research subject

The research focused on the growth and development of forage pea varieties cultivated for seed production under different sowing dates and planting patterns; grain yield; leaf area and the accumulation of biological dry matter; the effects of cultivation practices on the soil's agrophysical, agrochemical, hydrological, and microbiological properties; and the potential for obtaining grain and seed yields.

Research conditions, materials, and methods

Field experiments were conducted for the first time during 2023–2026 under the conditions of long-cultivated, irrigated typical sierozem soils at the Uyghur and Zafar farms in Yakkabog District, Kashkadarya Region, Uzbekistan. Groundwater was located at a depth of 8–12 m. The soil had a medium-loamy texture.

In the 0–30 cm plough layer, the humus content was reported as 1.0–1.8%. The soil bulk density ranged from 1.27 to 1.30 g/cm³, and particle density ranged from 2.58 to 2.65 g/cm³. Total nitrogen content was 0.094–0.095%, total phosphorus 0.144–0.163%, and potassium 2.6–2.9%. Nitrate nitrogen content ranged from 5.14 to 6.51 mg/kg, available phosphorus from 8 to 17 mg/kg, and exchangeable potassium from 156 to 193 mg/kg.

Soil analyses indicated a slightly acidic reaction, with pH values ranging from 5.9 to 6.7. The concentrations of these nutrients were found to be somewhat lower in the subsoil layer than in the plough layer.

During the 2023–2026 field experiments, the research was conducted on long-cultivated, irrigated typical sierozem soils in Yakkabog District, using the autumn-sown forage pea varieties Osiyo-2001 and Vostok-55, which are included in the State Register, together with the K-295 variety (Table 1).

Field experiments were established to address the research objectives and tasks. The experiments were conducted in three replications in accordance with B. A. Dospekhov's Methodology of Field Experiment.

The following experimental factors were studied:

Varieties (3): Osiyo-2001, Vostok-55, and K-295.

Sowing dates (3): 10 October, 20–21 October, and 30–31 October.

Planting patterns (3): 60 × 20 cm, 60 × 25 cm, and 60 × 30 cm.

The experiment comprised 27 treatment combinations (3 varieties × 3 sowing dates × 3 planting patterns).

Table 1. Experimental design

Sowing date	Planting pattern, cm	Variety
10 October	60 × 20 (control)	Osiyo-2001, Vostok-55, K-295
20–21 October	60 × 25	Osiyo-2001, Vostok-55, K-295
30–31 October	60 × 30	Osiyo-2001, Vostok-55, K-295

Experimental plot layout and dimensions

The area allocated to each experimental plot was 24 m², with a length of 20.0 m and a width of 1.2 m. Each plot consisted of two rows, with a row spacing of 60 cm and within-row plant spacing determined by the assigned planting pattern.

Each treatment was replicated three times, giving a total area of 72 m² per treatment (3 × 24 m²). The experiment included 81 plots in total (27 treatments × 3 replications).

The total net experimental area required for the 27 treatments was 1,944 m², equivalent to approximately 0.2 ha.

Forage pea varieties were sown in autumn on 10, 20–21, and 30–31 October at a depth of 5–6 cm.

Seed rates for different planting patterns

The calculated and practical seed rates per hectare were determined based on the 1,000-seed weight of each variety—200 g for Vostok-55, 165 g for Osiyo-2001, and 170 g for K-295—taking field emergence and a reserve allowance into account.

1. Planting pattern of 60 × 20 cm

Calculated stand density: approximately 83,300 plants/ha.

Vostok-55 (1,000-seed weight: 200 g): 175–180 kg/ha.

Osiyo-2001 (1,000-seed weight: 165 g): 145–150 kg/ha.

K-295 (1,000-seed weight: 170 g): 150–155 kg/ha.

2. Planting pattern of 60 × 25 cm

Calculated stand density: approximately 66,700 plants/ha.

Vostok-55: 140–145 kg/ha.

Osiyo-2001: 115–120 kg/ha.

K-295: 120–125 kg/ha.

3. Planting pattern of 60 × 30 cm

Calculated stand density: approximately 55,600 plants/ha.

Vostok-55: 115–120 kg/ha.

Osiyo-2001: 95–100 kg/ha.

K-295: 100–105 kg/ha.

Sowing was carried out using SZ-3.6 and SZA-3.6 seed drills [11]. The drills were adjusted to the required planting patterns before sowing the Vostok-55, Osiyo-2001, and K-295 varieties. Each variety was sown in two rows in each experimental plot [11, 13].

Before sowing, mineral fertilizers were applied at rates of $N_{30}P_{100}K_{75}$ kg/ha. The autumn-sown forage pea varieties received an additional nitrogen application of N_{30} in early spring. Following sowing, irrigation was applied at a rate of 450–500 m³/ha. The autumn-sown pea crop was irrigated three times, including two irrigations in spring. The experimental design is presented in Table 2.

Experiment 1. Evaluation of forage pea varieties sown in autumn using different sowing dates and planting patterns.

Table 2. Experimental treatment combinations

Variant	Sowing date	Sowing pattern (cm)	Variety
1	10 October	60 × 20 (control)	Osiyo-2001
2	10 October	60 × 25	Osiyo-2001
3	10 October	60 × 30	Osiyo-2001
4	20–21 October	60 × 20 (control)	Osiyo-2001
5	20–21 October	60 × 25	Osiyo-2001
6	20–21 October	60 × 30	Osiyo-2001
7	30–31 October	60 × 20 (control)	Osiyo-2001
8	30–31 October	60 × 25	Osiyo-2001
9	30–31 October	60 × 30	Osiyo-2001
10	10 October	60 × 20 (control)	Vostok-55
11	10 October	60 × 25	Vostok-55
12	10 October	60 × 30	Vostok-55
13	20–21 October	60 × 20 (control)	Vostok-55
14	20–21 October	60 × 25	Vostok-55
15	20–21 October	60 × 30	Vostok-55
16	30–31 October	60 × 20 (control)	Vostok-55
17	30–31 October	60 × 25	Vostok-55
18	30–31 October	60 × 30	Vostok-55
19	10 October	60 × 20 (control)	K-295
20	10 October	60 × 25	K-295
21	10 October	60 × 30	K-295
22	20–21 October	60 × 20 (control)	K-295
23	20–21 October	60 × 25	K-295
24	20–21 October	60 × 30	K-295
25	30–31 October	60 × 20 (control)	K-295
26	30–31 October	60 × 25	K-295
27	30–31 October	60 × 30	K-295

Research methods

Laboratory, field, and on-farm experiments were conducted, together with phenological observations and analyses of physiological and biometric indicators. The work was based on the following methodological publications:

Methods of Conducting Field Experiments; Scientific Research in Plant Production; Methods of State Variety Testing of Agricultural Crops; Photosynthetic Activity of Plants in Crops; Methods of Agrochemical, Agrophysical, and Microbiological Research in Irrigated Cotton-Growing Areas; Methods of Agrochemical Analysis of Soils and Plants in Central Asia; Basic Principles for Determining the Economic Efficiency of Using Research Results, New Technology, Inventions, and Rationalization Proposals in Agriculture. The experimental data were subjected to mathematical and statistical analysis using Microsoft Excel according to the method of B.A.Dospekhov [2, 4, 6–8, 10, 13].

Research results

Phenological development of forage pea varieties

According to the phenological observations, in the treatments sown on 10 October, 10% emergence was recorded on 13–15 October, while 75% emergence was observed on 16–18 October. Although emergence in the treatments sown on 20 and 30 October was delayed by 3–5 days, no substantial differences in the emergence process were observed among varieties or planting patterns.

The budding phase began during the first ten days of March, on 2–5 March, and lasted 19–22 days depending on the variety and treatment. The main differences in phenological development became apparent during flowering. The flowering phase lasted 24–27 days in Osiyo-2001, 26–30 days in Vostok-55, and 26–29 days in K-295.

The pod-setting and seed-formation phases became longer as the planting pattern widened. Under the 60 × 30 cm planting pattern, flowering and pod-setting lasted 2–5 days longer than in the control treatment with a spacing of 60 × 20 cm. This may be associated with the greater area available to each plant, which can promote the development of vegetative and generative organs.

Stem yellowing and full seed maturity within the pods occurred from the second half of May to early June, depending on the variety and sowing date. The total growing season averaged 217–230 days in treatments sown on 10 October, 208–223 days in treatments sown on 20 October, and 198–212 days in treatments sown on 30 October (Table 3).

Phenological observations and biometric measurements indicated that field emergence was high in all varieties, averaging 99.8%. This high value was attributed in the original study to harvesting the seeds at full physiological maturity, a relatively short storage period of 2–3 months, annual renewal of the seed material, and selection according to quality indicators before sowing. These factors were considered to help maintain seed viability and germination energy, resulting in uniform and rapid emergence under field conditions.

The observations also showed that, when Osiyo-2001 was sown on 10 October 2023 using the 60 × 30 cm planting pattern, the flowering phase lasted 27 days, pod setting and seed formation lasted 22 days, and the total growing season lasted 222 days. Compared with the control treatment, flowering was 3 days longer, pod setting was 1 day longer, and the total growing season was 5 days longer.

Table 3. Phenological observations of autumn-sown forage pea varieties under different sowing dates and planting patterns (mean values for 2023–2026)

№	Sowing date	Planting pattern (cm)	Plants/ha (thousand)	Sowing depth (cm)	Field emergence (%)	Emergence	True leaves	Stem formation	Budding	Flowering	Pod setting	Maturity	Growing season
	Variety Osiyo-2001												
1	10 Oct	60x20 (control)	83.3	5	99.8	6	6	16	21	24	19	21	217
2	10 Oct	60x25	66.7	5	99.8	6	6	15	22	26	19	22	220
3	10 Oct	60x30	55.5	5	99.8	6	6	15	22	27	21	22	222
	Variety Vostok-55												
1	10 Oct	60x20 (control)	83.3	6	99.8	7	7	16	19	26	24	23	225

2	10 Oct	60x25	66.6	6	99.8	7	7	15	22	28	26	22	227
3	10 Oct	60x30	55.5	6	99.8	7	7	15	22	30	29	22	230
	Variety K-295												
1	10 Oct	60x20 (control)	83.3	5	99.8	7	6	16	19	26	24	22	225
2	10 Oct	60x25	66.6	5	99.8	7	6	15	22	28	25	22	227
3	10 Oct	60x30	55.5	5	99.8	7	6	15	22	29	28	22	230
	Variety Osiyo-2001												
1	20 Oct	60x20 (control)	83.3	5	99.8	7	6	16	19	26	20	21	211
2	20 Oct	60x25	66.6	5	99.8	7	6	15	22	27	20	22	214
3	20 Oct	60x30	55.5	5	99.8	7	6	15	22	28	22	22	217
	Variety Vostok-55												
1	20 Oct	60x20 (control)	83.3	6	99.8	8	6	16	19	28	26	23	219
2	20 Oct	60x25	66.6	6	99.8	8	6	15	22	29	27	24	222
3	20 Oct	60x30	55.5	6	99.8	8	6	15	22	31	27	24	223
	Variety K-295												
1	20 Oct	60x20 (control)	83.3	5	99.8	8	6	16	19	28	26	22	218
2	20 Oct	60x25	66.6	5	99.8	8	6	15	22	29	27	23	221
3	20 Oct	60x30	55.5	5	99.8	8	6	15	22	31	27	23	222
	Variety Osiyo-2001												
1	30 Oct	60x20 (control)	83.3	5	99.8	7	7	15	19	26	18	24	201
2	30 Oct	60x25	66.6	5	99.8	7	7	14	22	27	18	25	204
3	30 Oct	60x30	55.5	5	99.8	7	7	14	22	28	20	25	206
	Variety Vostok-55												
1	30 Oct	60x20 (control)	83.3	6	99.8	8	7	15	19	28	23	26	208
2	30 Oct	60x25	66.6	6	99.8	8	7	14	22	29	24	28	211
3	30 Oct	60x30	55.5	6	99.8	8	7	14	22	31	24	27	212
	Variety K-295												
1	30 Oct	60x20 (control)	83.3	5	99.8	8	7	15	19	27	21	26	206
2	30 Oct	60x25	66.6	5	99.8	8	7	14	22	28	22	27	209
3	30 Oct	60x30	55.5	5	99.8	8	7	14	22	30	23	26	210

Overall, the phenological observations showed that sowing date and planting pattern substantially influenced the growth and development of pea varieties. In particular, widening the planting pattern to 60 × 25 cm or 60 × 30 cm created conditions that were more favorable for biological development and the formation of generative organs, and was associated with a longer growing season.

Thus, the results confirmed that sowing dates and planting patterns significantly affected the duration of growth and developmental stages of forage pea varieties under long-cultivated, irrigated typical sierozem soil conditions. Earlier sowing, particularly on 10–20 October, was associated with a longer growing season and favorable conditions for the completion of generative phases. Wider planting patterns of 60 × 25 cm and 60 × 30 cm prolonged flowering and pod-setting phases. In contrast, the phenological stages progressed more rapidly in the late-sown treatments of 30 October, where the growing season was shorter. These findings indicate that selecting appropriate sowing dates and planting patterns, while accounting for the biological characteristics of each variety, is an important agronomic factor in managing the phenological development of pea.

The results also demonstrated that sowing dates and planting patterns, particularly the area available to

each plant, significantly affected plant height and its changes across phenological stages (Table 4).

Table 4. Plant height of pea varieties at different phenological stages under different sowing dates and planting patterns (mean values for 2023–2026)

№	Planting pattern (cm)	Sowing date	Before wintering	Stem formation and branching	Budding	Flowering	Pod setting	Seed formation in pods	Before stem yellowing
	Variety Osiyo-2001								
1	60x20 (control)	10.10.	37,1	42,8	67,7	110,2	187,9	249,0	261,3
2	60x25		35,5	40,5	65,5	100,2	179,6	243,0	248,0
3	60x30		35,3	39,6	62,8	96,5	177,6	234,0	238,0
	Variety Vostok-55 navi								
1	60x20 (control)	10.10.	36,9	41,8	64,8	104,1	183,0	240,3	246,1
2	60x25		35,2	39,6	63,0	99,6	174,2	234,8	239,0
3	60x30		34,0	37,7	59,2	95,0	166,1	228,9	233,0
	Variety K-295 navi								
1	60x20 (control)	10.10.	36,8	41,6	64,3	105,1	182,5	239,6	247,4
2	60x25		35,3	39,1	62,6	99,4	173,7	233,7	238,2
3	60x30		33,6	37,4	59,0	94,8	165,7	228,4	232,0
	Variety Osiyo-2001 navi								
1	60x20 (control)	20.10.	31,6	40,2	62,5	108,5	186,7	237,7	244,4
2	60x25		29,4	37,1	59,7	100,0	178,2	230,7	234,7
3	60x30		27,7	35,2	56,4	96,0	172,2	226,4	230,0
	Variety Vostok-55 navi								
1	60x20 (control)	20.10.	31,5	39,0	62,2	102,2	181,4	233,0	237,7
2	60x25		30,5	36,6	59,2	95,5	172,2	220,4	223,1
3	60x30		28,5	34,1	57,3	91,1	164,6	218,0	220,7
	Variety K-295 navi								
1	60x20 (control)	20.10.	31,7	38,1	62,4	101,9	179,8	229,1	234,3
2	60x25		30,2	36,7	59,1	95,2	166,2	220,3	225,3
3	60x30		28,4	33,9	57,0	92,1	159,5	217,4	219,7
	Osiyo-2001 navi								
1	60x20 (control)	30.10.	28,5	35,0	59,6	100,5	178,5	227,2	234,7
2	60x25		26,8	32,6	57,7	97,0	174,2	218,9	222,6
3	60x30		24,6	28,9	55,3	92,8	169,9	216,4	218,8
	Variety Vostok-55 navi								
1	60x20 (control)	30.10.	28,7	34,1	62,2	101,3	177,2	226,3	231,8
2	60x25		27,1	32,1	58,6	99,0	171,6	218,7	221,6
3	60x30		25,4	29,4	56,6	96,8	167,0	216,6	218,2
	Variety K-295 navi								
1	60x20 (control)	30.10.	28,5	33,3	60,8	100,1	177,2	225,9	231,0
2	60x25		26,3	31,2	58,0	97,6	170,3	219,1	221,1
3	60x30		25,1	28,2	55,2	94,6	166,5	216,4	217,8

The multi-year study conducted during 2023–2026 on long-cultivated, irrigated typical sierozem soils in Yakkabog District, Kashkadarya Region, showed that the growth dynamics of forage pea varieties were closely associated with sowing date, plant nutritional area, and the biological characteristics of each variety.

The results indicated that plants in the treatments sown early, on 10 October, entered the winter

dormancy period in a relatively well-developed condition.

Before wintering, the average plant height was 35.3–37.1 cm for Osiyo-2001, 34.0–36.9 cm for Vostok-55, and 33.6–36.8 cm for K-295. When sowing was delayed until 20 or 30 October, the shorter autumn growing period was associated with reduced plant height before winter. The original text reports values of 31.6–24.6 cm, 25.4–31.5 cm, and 25.1–31.7 cm for the respective sowing-date comparisons; these ranges should be checked against the original observations before publication.During stem formation and branching in early spring, plant growth continued. In the treatments sown on 10 October, plant height across the varieties ranged from 37.4 to 42.8 cm. In the late-sown treatments of 30 October, this indicator ranged from 28.2 to 35.0 cm. The original study attributed the difference to the fact that plants sown at the more favorable dates had more time to develop their root systems and vegetative organs during autumn.

Conclusions

1. Under the conditions of long-cultivated, irrigated typical sierozem soils in Yakkabog District, Kashkadarya Region, the 2023–2026 study found that the average field emergence rate of the Osiyo-2001, Vostok-55, and K-295 forage pea varieties was 99.8%. Delaying sowing from 10 October to 20–21 October and 30–31 October affected the timing of seed emergence, with emergence occurring 3–5 days later in the later-sown treatments.

2. Changing the planting pattern from the control spacing of 60 × 20 cm to 60 × 25 cm and 60 × 30 cm influenced the phenological development of the plants. In particular, under the 60 × 30 cm pattern, flowering and pod-setting phases were prolonged by 2–5 days compared with the control. This was associated with the greater area available to individual plants and suggested more favorable conditions for the development of generative organs.

3. The interaction between sowing date and planting pattern was reflected in the duration of the growing season and the formation of plant height. The growing season lasted 217–230 days in the treatments sown on 10 October, 211–223 days in those sown on 20 October, and 201–212 days in those sown on 30 October. Plants in the earlier-sown treatments were also relatively taller before wintering. These findings indicate that, under the conditions of Kashkadarya Region, selecting sowing dates and plant nutritional areas according to the biological characteristics of each pea variety is an important agronomic factor.

References:

1. Atabaeva, H. N., & Xudayqulov, J. V. (2018). *Plant Production*. Tashkent. p. 407.
2. Azimov, B. J., & Azimov, B. B. (2002). *Methods of Conducting Experiments in Vegetable, Melon, and Potato Production.* Tashkent: National Encyclopedia of Uzbekistan, pp. 181–185.
3. Yushkevich, L. V., Yushchenko, D. N., Shchitov, A. G., et al. (2023). *Cultivation of Pea Varieties of Domestic and Foreign Breeding under the Soil and Climatic Conditions of Omsk Region.* Omsk: Omsk Agrarian Scientific Center. 30 p.
4. Dospekhov, B. A. (1985). *Methodology of Field Experiment.* Moscow: Kolos. 351 p.
5. Iminov, A., Karimov, Sh., & Usmonova, D. (2020). The effect of nitrogen-fixing nodule bacteria and mineral fertilizers on changes in soil microbiological processes in grain legume crops. *Agro Ilm, scientific supplement to the journal O‘zbekiston qishloq xo‘jaligi*, No. 2, pp. 33–34.
6. (1977). *Methods of Agrochemical Analysis of Soils and Plants*. 5th ed. Tashkent: Mekhnat, pp. 49–228.
7. (1974). *Methods of State Variety Testing of Agricultural Crops*. Moscow. 121 p.
8. (1963). *Methods of Agrochemical, Agrophysical, and Microbiological Research in Irrigated Cotton-Growing Areas.* Tashkent. 440 p.
9. (1973). *Methods of Agrochemical Analysis of Soils in Central Asia*. Tashkent. 187 p.
10. Metlina, G. V., Vasilchenko, S. A., Ashiev, A. R., & Kravchenko, N. S. (2024). Effect of sowing dates and seeding rates of winter pea varieties on protein content and nutrient yield. *Grain Economy of Russia*, 16(1), 97–103. https://doi.org/10.31367/2079-8725-2024-90-1-97-103
11. Oripov, R., & Khalilov, N. (2007). *Plant Production.* Tashkent: Publishing House of the National Society of Philosophers of Uzbekistan. 384 p.
12. Ostonaqulov, T. E., Zuev, V. I., & Qodirxo‘jaev, O. Q. (2018). *Vegetable Production*. Tashkent. 552 p.

13. Ostonaqulov, T. E., & Khalilov, N. X. (2020). *Biology and Cultivation Technology of Grain Legumes.* Tashkent: Mekhnat, pp. 39–42.
14. Ostonaqulov, T. E., & Usmanov, N. N. (2021). *Scientific Foundations of Using Green Manure Crops in Potato Production*. Tashkent. 210 p.
15. Strizhova, F. M., Tsareva, L. E., & Titov, Yu. N. (2008). *Plant Production: A Textbook*. Moscow and Barnaul: Publishing House of Altai State Agrarian University. 219 p.
16. Usmanov, N. N. (2023). *Scientific Foundations of Using Green Manure Crops in Potato Production.* Monograph. Tashkent: Voris Publishing House. 129 p.
17. Usmanov, N. N. (2026). *Green Manuring and the Scientific Foundations of Potato Production*. Monograph. Qarshi: USMON PRINT Publishing House. 214 p.
18. Shukis, S. K., Shukis, E. R., & Drobyshev, A. P. (2021). Biological characteristics of pea varieties and lines and their response to sowing dates under the conditions of Altai Krai. *Bulletin of Altai State Agrarian University*, No. 203, pp. 36–43. https://doi.org/10.53083/1996-4277-2021-203-36-43
19. Peoples, M. B., Brockwell, J., & Herridge, D. F. (2009). The contributions of nitrogen-fixing crop legumes to the productivity of agricultural systems. *Symbiosis*, 48, 1–17.
20. Jensen, E. S., Peoples, M. B., Boddey, R. M., et al. (2012). Legumes for mitigation of climate change and the provision of feedstock for biofuels and biorefineries: *A review. Agronomy for Sustainable Development*, 32, 329–364.
21. Lal, R. (2016). *Soil structure and soil aggregation. In Encyclopedia of Soil Science*. Boca Raton: CRC Press.
22. Bronick, C. J., & Lal, R. (2005). Soil structure and management: A review. *Geoderma*, 124, 3–22.
23. Food and Agriculture Organization of the United Nations (FAO). (2016). *Grain Legumes and Soil Fertility Improvement. FAO Plant Production and Protection Paper.* Rome.
24. Singh, R., et al. (2025). Effect of sowing dates and spacing on root rot and yield of pea. *International Journal of Farm Sciences*, 15(4), 75–80. https://doi.org/10.5958/2250-0499.2025.00060.0

Impact Factor:						
	ISRA (India)	= 6.317	SIS (USA)	= 0.912	ICV (Poland)	= 6.630
	ISI (Dubai, UAE)	= 1.582	РИНЦ (Russia)	= 0.191	PIF (India)	= 1.940
	GIF (Australia)	= 0.564	ESJI (KZ)	= 8.100	IBI (India)	= 4.260
	JIF	= 1.500	SJIF (Morocco)	= 6.004	OAJI (USA)	= 0.350

SOI: 1.1/TAS DOI: 10.15863/TAS

International Scientific Journal

Theoretical & Applied Science

p-ISSN: 2308-4944 (print) **e-ISSN:** 2409-0085 (online)

Year: 2026 **Issue:** 10 **Volume:** 162

Received: 29.10.2026
Accepted/Published: 30.10.2026

https://T-Science.org

Issue Article

Denis Chemezov
Vladimir Polytechnic College
MEng, Honorary Worker of the Education Field of the Russian Federation, Academician of International Academy of Theoretical and Applied Sciences, Lecturer, Russian Federation
https://orcid.org/0000-0002-2747-552X
vpk-science@yandex.ru

Elizaveta Kurzyakova
Vladimir Polytechnic College
Student, Russian Federation

Kirill Samokhvalov
Vladimir Polytechnic College
Student, Russian Federation

Kirill Lukashin
Vladimir Polytechnic College
Student, Russian Federation

Ekaterina Suslova
Vladimir Polytechnic College
Student, Russian Federation

Sergey Nizov
Vladimir Polytechnic College
Student, Russian Federation

Arseniy Timin
Vladimir Polytechnic College
Student, Russian Federation

Maksim Prokofyev
Vladimir Polytechnic College
Student, Russian Federation

Danil Isaev
Vladimir Polytechnic College
Student, Russian Federation

KINETICS AND SPATIAL ORGANIZATION OF A DETONATION WAVE IN THE ANFO SYSTEM: A THEORETICAL DESCRIPTION OF THE EVOLUTION OF DISTURBANCES IN A HETEROGENEOUS MEDIUM

Abstract: *This paper presents a comprehensive study of the physicochemical processes underlying the detonation of Ammonium Nitrate/Fuel Oil (ANFO). The sequence of physical and chemical processes is considered, including the stages of initiation, local heating, formation of a detonation wave and other processes. The presented results demonstrate the characteristic evolution of the pressure field over time: from the initial localization of high pressures in the initiation zone to the formation and expansion of the shock-detonation structure. The scientific novelty of the study lies in the comprehensive analysis of the relationship between hydrodynamic parameters and chemical kinetics under conditions of non-ideal detonation, characteristic of heterogeneous explosive systems. The practical value of the work lies in the possibility of using the obtained patterns to optimize the design of charges, increase the efficiency of industrial blasting operations, and develop safer methods for handling explosives.*

Key words: *ANFO, detonation, ammonium nitrate, shock wave, numerical modeling, initiation, pressure field.*

Language: *English*

Citation: Chemezov, D., et al. (2026). Kinetics and spatial organization of a detonation wave in the ANFO system: a theoretical description of the evolution of disturbances in a heterogeneous medium. *ISJ Theoretical & Applied Science, 10 (162),* 64-67.

Soi: https://s-o-i.org/1.1/TAS-10-162-10 ***Doi***: https://dx.doi.org/10.15863/TAS.2026.10.162.10

Scopus ASCC: *2211.*

1. Introduction

Ammonium Nitrate/Fuel Oil (ANFO) is widely used in industrial blasting operations. Its composition and properties are described in reference literature on explosives [1-2]. Despite the comparative simplicity of the composition, ANFO detonation is a complex physical and chemical process that depends on the properties of the components and loading conditions [2-3].

The classical Chapman-Jouguet theory describes an idealized detonation wave, whereas real explosive systems may exhibit non-ideal behavior [4-5]. For ANFO, the heterogeneity of the mixture, the structure of the nitrate granules, the porosity and distribution of the fuel are important. These characteristics influence the energy transfer and detonation stability [2-3, 6].

Experimental and theoretical studies of ANFO indicate that the porosity and internal structure of ammonium nitrate granules are linked to hot spot formation and reaction initiation [3, 6]. Therefore, when analyzing ANFO, it is necessary to consider not only thermodynamic parameters but also the material's microstructure and the heterogeneity of fuel distribution [2-3].

Numerical modeling of ANFO detonation requires the simultaneous consideration of hydrodynamics and chemical kinetics. Published models describe the influence of charge composition, density, and structure on the propagation of the detonation wave [3, 7]. In this regard, an analysis of the spatio-temporal evolution of ANFO detonation, taking into account the interplay between the shock wave and the chemical transformation, is of great importance.

2. Materials and methods

This study employs numerical modeling of ANFO detonation using ANSYS Autodyn. The model is based on an axisymmetric problem formulation, which allows for an adequate description of the radial propagation of the detonation front from the initiation point.

The Jones-Wilkins-Lee (JWL) model is used to describe the behavior of the explosive under detonation conditions; it is an equation of state that expresses the pressure of detonation products as a function of specific volume and internal energy.

The computational domain was a 100×100 m square. The initial charge density of ANFO was 850 kg/m³, which corresponds to typical values for industrial charges. Stoichiometric ratio of components: 94% ammonium nitrate, 6% diesel fuel. Initiation was effected using a point source located in the bottom-left corner of the computational domain.

To interpret the simulation results, a method of visualizing the pressure field at successive time points was used. The following parameters were analyzed: maximum pressure, front propagation radius, reaction zone thickness, and the nature of pressure field variation over time.

3. Results and discussion

3.1. Initiation and initial stage of detonation

Numerical modeling results show that, at the early stage, the pressure in the greater part of the computational domain remains close to zero. A localized high-pressure area near the bottom-left corner corresponds to the initiation point. The resulting shock wave compresses and heats the mixture, creating the conditions for the chemical reaction to begin.

ANFO has relatively low sensitivity to mechanical impact. As noted in [8], an oil film on the surface of ammonium nitrate granules hinders the transmission of the shock impulse. Therefore, initiation requires an impulse sufficient to locally heat the mixture and subsequently form a stable reaction front.

3.2. Formation and propagation of the detonation front

As the process develops, the high-pressure area assumes an arc-like shape and propagates from the point of initiation. This reflects the transition from a local disturbance to a shock-detonation front, in which

the material is compressed and a chemical transformation of the mixture components occurs behind the front.

The detonation of ANFO is driven by the redox interaction between ammonium nitrate and hydrocarbon fuel. According to [9], upon heating and shock compression, the nitrate decomposes to form gaseous products, while the fuel is oxidized by the oxygen from the oxidizer.

The actual course of the reaction also depends on the quality of component mixing, granule size, loading density, and porosity, which influences the formation of hot spots. In study [10], an optimal charge density of 820-880 kg/m³ is specified for ANFO.

3.3. Non-ideality of the detonation process

Numerical modeling reveals the non-ideal nature of detonation: the reaction zone has a finite thickness, and the parameters behind the front vary gradually. Consequently, the view of detonation as an instantaneous jump in parameters does not fully describe the behavior of a heterogeneous mixture.

This is consistent with the conclusions of study [11]: the non-ideal detonation of ANFO is associated with the heterogeneous distribution of reactants and the finite rate of chemical transformation. The front can be viewed as a quasi-stationary structure whose macroscopic stability is maintained by a collection of local reactions at hot spots.

3.4. Gas-dynamic expansion and destructive effect

After the front passes, the reaction products expand and act upon the surrounding medium. In the simulation, the high-pressure zone expands, and the field behind the front becomes more uniform. This reflects the redistribution of energy among the chemical reaction, the expansion of products, and the transmission of the shock load.

The destructive effect of ANFO is determined not only by peak pressure but also by the subsequent expansion of gases, which perform work to deform and fracture the surrounding material. The results of experimental studies [12] confirm that, during the explosive action of ANFO, the gas-dynamic phase of the process makes a significant contribution to rock fragmentation.

3.5. Influence of microstructure on detonation characteristics

The scientific novelty of this study lies in the detailed analysis of the influence of ANFO charge microstructure on the stability of the detonation regime. It has been established that the porosity of ammonium nitrate granules, the distribution of fuel over the particle surfaces, and the presence of microheterogeneities facilitate the formation of local hot spots where the reaction initiates earlier than in the average volume.

In this context, the ANFO detonation front can be characterized as a statistically heterogeneous zone in which macroscopic regularity is maintained by a multitude of microscopic events. This conclusion is of significant practical importance, as it enables the optimization of the composition and structure of ANFO charges to achieve maximum blasting efficiency.

4. Conclusion

The study established that the ANFO explosion mechanism consists of a sequence of interconnected physical and chemical processes, including shock-wave initiation, local heating, chemical decomposition of ammonium nitrate, fuel oxidation, formation of a detonation front, and expansion of gaseous products. Numerical modeling using the ANSYS made it possible to visualize the spatio-temporal evolution of the pressure field and identify key patterns of the detonation process.

The scientific novelty of the study lies in a comprehensive analysis of the relationship between hydrodynamic parameters and chemical kinetics under conditions of non-ideal detonation characteristic of heterogeneous explosive systems. It has been established that the detonation of ANFO is not an instantaneous event but a time-evolving process in which mechanical and chemical factors form a unified, self-sustaining mechanism.

The practical value of the work lies in the potential to use the established patterns to optimize charge design, enhance the efficiency of industrial blasting operations, and develop safer methods for handling explosives.

References:

1. Meyer, R., Köhler, J., & Homburg, A. (2007). Explosives (6th ed.). *Wiley-VCH*.
2. Cooper, P. W. (1996). Explosives engineering. *Wiley-VCH*.
3. Bement, L. J., & Schimmel, M. L. (1988). Characterization of ammonium nitrate/fuel oil (ANFO) explosive. *NASA Technical Memorandum 100390. National Aeronautics and Space Administration*.
4. Chapman, H. (1899). On the rate of explosion in gases. *Philosophical Magazine, 47(284)*, 90-104.

5. Jouguet, E. (1905). Sur la propagation des réactions chimiques dans les gaz. *Gauthier-Villars*.
6. Dobratz, B. M., & Crawford, P. C. (1985). LLNL explosives handbook: Properties of chemical explosives and explosives simulants (UCRL-52997, Rev. 2). *Lawrence Livermore National Laboratory*.
7. Baer, M. R., & Nunziato, J. W. (1986). A two-phase mixture theory for the deflagration-to-detonation transition (DDT) in reactive granular materials. *International Journal of Multiphase Flow, 12(6)*, 861-889.
8. Persson, P.-A., Holmberg, R., & Lee, J. (1994). Rock blasting and explosives engineering. *CRC Press*.
9. Oxley, J. C., Smith, J. L., & Rogers, E. (2002). Ammonium nitrate: Thermal stability and explosivity modifiers. *Thermochimica Acta, 384(1-2)*, 23-45.
10. Bohanek, V., Dobrilović, M., & Škrlec, V. (2013). Influence of the Initiation Energy on the Velocity of Detonation of ANFO Explosive. *Central European Journal of Energetic Materials, 10(4)*, 555-568.
11. Lee, J. H. S. (2008). The detonation phenomenon. *Cambridge University Press*.
12. Kutter, H. K., & Fairhurst, C. (1971). On the fracture process in blasting. *International Journal of Rock Mechanics and Mining Sciences & Geomechanics Abstracts, 8(3)*, 181-202.

SOI: 1.1/TAS DOI: 10.15863/TAS

International Scientific Journal

Theoretical & Applied Science

p-ISSN: 2308-4944 (print) **e-ISSN:** 2409-0085 (online)

Year: 2026 **Issue:** 10 **Volume:** 162

Received: 29.10.2026
Accepted/Published: 30.10.2026 https://T-Science.org

Issue Article

Denis Chemezov
Vladimir Polytechnic College
MEng, Honorary Worker of the Education Field of the Russian Federation, Academician of International Academy of Theoretical and Applied Sciences, Lecturer, Russian Federation
https://orcid.org/0000-0002-2747-552X
vpk-science@yandex.ru

Roman Gavrilov
Vladimir Polytechnic College
Student, Russian Federation

Andrey Kunaev
Vladimir Polytechnic College
Student, Russian Federation

Sergey Rakhuba
Vladimir Polytechnic College
Student, Russian Federation

Artyom Armyakov
Vladimir Polytechnic College
Student, Russian Federation

Arseniy Bezrukov
Vladimir Polytechnic College
Student, Russian Federation

Danil Kuznetsov
Vladimir Polytechnic College
Student, Russian Federation

Ilya Yantser
Vladimir Polytechnic College
Student, Russian Federation

SPATIOTEMPORAL DYNAMICS OF BTF EXPLOSION FRONT PROPAGATION

Abstract: *The article examines the spatiotemporal evolution of the computed pressure field during the propagation of an air shock wave initiated by a BTF explosion. Based on three-dimensional visualization, the propagation of the shock wave front from a source located at the origin and the variation in pressure with distance were analyzed. It was established that, by the end of the time interval considered, the shock wave front had reached a distance of approximately 80-100 m. Its propagation was accompanied by a decrease in velocity, while pressure diminished with increasing distance from the source. To quantify the radial dynamics of the shock wave front, the data were fitted with the power-law relation* $R(t) = 1.761428t^{0.85285}$, *where the radius is expressed in metres and time in milliseconds. The coefficient of determination in logarithmic space was* $R^2_{log} = 0.959086$. *An exponent below*

unity indicates sublinear growth in the radius over the time interval investigated. The resulting model can be used as a compact approximation for interpolating the position of the shock wave front under the conditions considered.

***Key words**: BTF explosion, shock wave, computed pressure field, shock front radius, power-law approximation, spatiotemporal dynamics.*

***Language**: English*

Citation: Chemezov, D., et al. (2026). Spatiotemporal dynamics of BTF explosion front propagation. *ISJ Theoretical & Applied Science, 10 (162),* 68-71.

Soi: https://s-o-i.org/1.1/TAS-10-162-11 ***Doi***: https://dx.doi.org/10.15863/TAS.2026.10.162.11

***Scopus ASCC**: 2211.*

1. Introduction

In this work, BTF refers to benzotrifuroxan, an energetic compound whose detonation produces explosion products and a pressure wave that propagates through the surrounding medium. Research on BTF encompasses the experimental determination of detonation and explosion product parameters [1], the distribution of electrical conductivity in the detonating material [2], and the investigation of the properties of BTF and its mixtures [3-10].

However, the studies considered primarily focus on the properties of the explosive itself and on detonation processes. A quantitative description of the radial propagation of the pressure front over time (particularly, an assessment of the power-law growth of its radius) remains insufficiently addressed. The aim of this study is to analyse the calculated spatiotemporal pressure field generated by a BTF explosion and to approximate the relationship between the pressure front radius and time using a power function.

2. Materials and methods

The study investigated the propagation of the pressure wave generated by the initiation of a BTF explosion in an air domain. The analysis was based on calculated pressure fields presented as three-dimensional spatiotemporal visualisations. The explosion source was located at the origin of the coordinate system, allowing the position of the shock wave front to be described relative to a common reference point.

In the visualisation, the spatial coordinates represented the field's position relative to the source, while the vertical axis represented time. Accordingly, it was interpreted as a temporal coordinate rather than as a spatial height. The colour field represented pressure magnitude on a logarithmic scale. This representation was used to clearly illustrate the spatial distribution of pressure and its evolution over time.

To quantitatively characterize the propagation of the shock wave, the radius R of its front was determined at successive time points t. The radius was defined as the distance from the source, located at the origin of the coordinate system, to the position of the shock wave front at the corresponding time. Time was expressed in milliseconds (ms), and the radius in meters (m). Thus, the dynamics of the shock wave front were described by the function of $R(t)$.

For each time point considered, the distance from the origin to the corresponding boundary of the shock wave front was recorded during data processing. The resulting radius values were correlated with the corresponding time points and used to describe the temporal evolution of the shock wave front's position.

3. Results and discussion

The three-dimensional plot (Figure 1) shows the evolution of the calculated pressure field following the initiation of the BTF explosion. The source is located at the origin, and the wavefront propagates through the air domain. When interpreting the plot, it is important to note that the vertical axis represents the time evolution of the explosion process. The surface represents the spatiotemporal distribution of the computed quantities, rather than an instantaneous profile of the shock wave in physical space.

As time progresses, the shock wave front propagates radially outward from the source, reaching a distance of approximately 80-100 m by the end of the interval considered. The nonuniform displacement of the front indicates a decrease in propagation velocity over time.

The color field represents pressure on a logarithmic scale. The highest values are concentrated near the source; pressure decreases with increasing distance, indicating that the shock wave weakens as it propagates.

A power-law regression was fitted to quantitatively describe the propagation of the front (Equation 1):

$$R(t) = at^b \quad (1)$$

where R is the radius of the front, measured in meters; t is time, measured in milliseconds; and $a = 1.761428$ and $b = 0.85285$. The coefficient of determination for the regression in logarithmic space was $R^2_{log} = 0.959086$.

The parameter b is the exponent that characterizes the dependence of the radius on time. For $b = 1$, the model would describe linear growth in the radius, corresponding to a constant velocity of the shock wave front. The obtained value $b < 1$ corresponds to sublinear growth: the radius increases, while its rate of change decreases over time within the framework of the power-law model.

The coefficient a determines the scale of the relationship and depends on the units of measurement chosen. When t is measured in milliseconds and R in meters, its units are m/ms^b. Therefore, the value of a cannot be interpreted as the propagation velocity of the shock wave front. The coefficient R^2_{log} quantifies the model's goodness of fit to the data after logarithmic transformation. It is not an estimate of the error relative to the physical experiment.

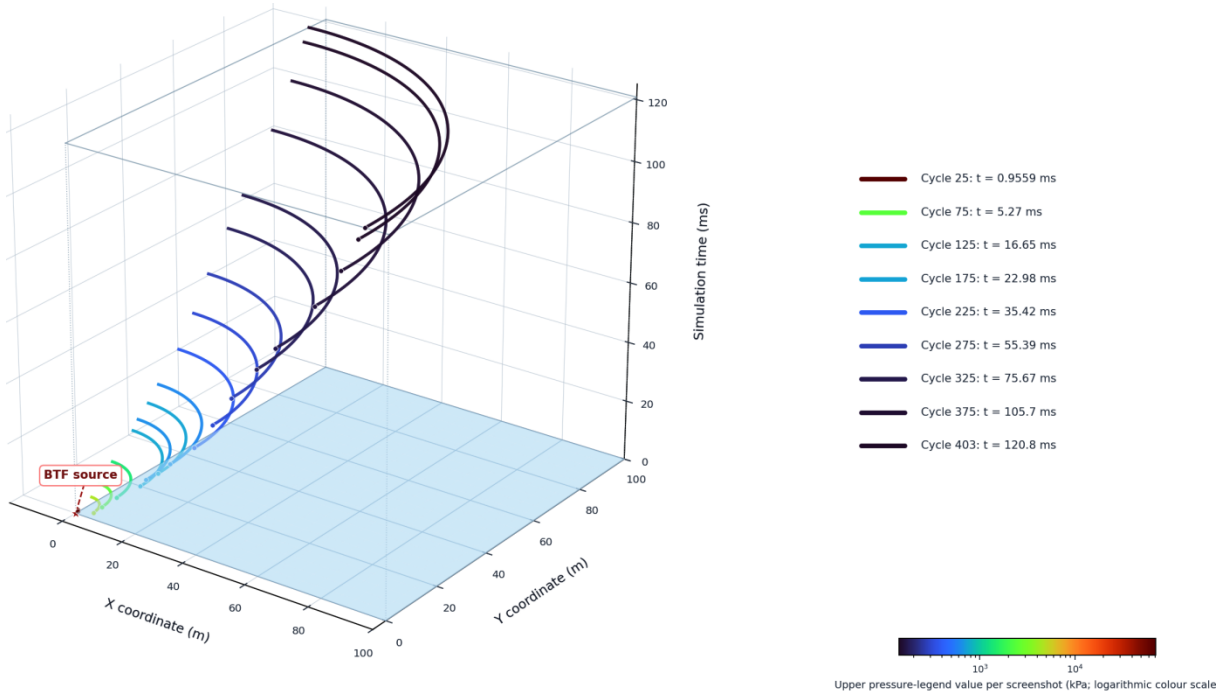

Figure 1. Spatiotemporal evolution of the calculated pressure field following the initiation of the BTF explosion in the air domain.

The analysis presented combines spatiotemporal visualization of the computed field with a preliminary quantitative approximation of the shock wave front radius using a power-law function. This makes it possible to move beyond a qualitative observation of shock wave expansion toward a parametric description of its radial dynamics, while formulating a testable hypothesis that the radius grows sublinearly over the time interval investigated.

The practical significance of this result lies in the potential use of the power-law relationship as a compact approximation for interpolating the shock front radius within the investigated time range and under the conditions of the BTF explosion process.

4. Conclusion

The analysis of the calculated pressure field demonstrates the radial propagation of the BTF explosion front and the attenuation of pressure with increasing distance from the source. The power-law model $R(t) = 1.761428t^{0.85285}$, with a coefficient of determination $R^2_{log} = 0.959086$, characterizes the sublinear evolution of the front radius over the investigated time interval. The resulting relationship can be used to interpolate the shock wave radius under the conditions considered. Its extrapolation requires further validation.

References:

1. Dolgoborodov, A., et al. (2014). Detonation performance of high-dense BTF charges. *Journal of Physics: Conference Series*, 500(5), 052010.
2. Satonkina, N., et al. (2018). Electrical conductivity distribution in detonating benzotrifuroxane. *Scientific Reports*, 8, 9635.

3. Turek, O. (1931). Le 2,4,6-trinitro-1,3,5-triazido-benzene, nouvel explosif d'amorcage. In: *Chimie et industrie*, Band 26, 781-794.
4. Ji, W., Xu, Y., Liu, L., Guo, C., Wei, X., & Wang, D. (2023). The influence of three binders on the properties of BTF-based composite explosive. *Central European Journal of Energetic Materials*, 20(3), 369-385.
5. Suponitsky, K. Y., et al. (2021). Energetic co-crystal of a primary metal-free explosive with BTF: Ideal pair for co-crystallization. *Molecules*, 26(24), Article 7452.
6. Kashkarov, A. O. (2026). Detonation products of mixed explosive compositions based on benzotrifuroxan. Combus*tion, Explosion, and Shock Waves*, 62(2), 53-61.
7. Virchenko, V. A., Aniskevich, V. V., Akhmetzyanov, A. I., Egorov, A. P., & Kulikov, V. G. (2014). Explosive characteristics of the benzotrifuroxane-anthracene molecular complex. *Combustion, Explosion, and Shock Waves*, 50(2), 223-226.
8. Du, S., et al. (2024). A Novel Insensitive Cocrystal Explosive Composed of BTF and the Non-Energetic 2-Nitroaniline. *Crystals*, 14(8), 722.
9. Huang, X., et al. (2020). Comparison study of carbon clusters formation during thermal decomposition of 1,3,5-triamino-2,4,6-trinitrobenzene and benzotrifuroxan: A ReaxFF based sequential molecular dynamics simulation. *Physical Chemistry Chemical Physics*, 22(9), 5154-5162.
10. Zhang, Z., & Zhu, S. (2026). Molecular Dynamics Simulation of Thermal Decomposition of BTF/TNB. *Fire*, 9(8), 318.

Contents

		p.
1.	**Ibrahimova, M.J., et al.** Some physical and thermal properties of ionic liquids.	1-9
2.	**Ochilova, M.I.** Influence of foliar fertilizers on the formation of fruiting branches in cotton.	10-14
3.	**Saparniyazov, A.T.** The social structure and social differentiation of Karakalpak society in the eighteenth century.	15-19
4.	**Chikovani, M., Gegetchkori, L., Samkharadze, M., Didbaridze, I., & Chkhartishvili, N.** Quantitative Determination of Biologically Active Ions in the Spring Waters of the Lagvilava Neighborhood, Inchkhuri Village, Martvili Municipality, Samegrelo-Zemo Svaneti (Georgia).	20-25
5.	**Tojiboev, J.** Refugees in Turkestan during the first world war: territorial distribution and administrative approaches.	26-30
6.	**Quziev, D.N.** Effect of bentonite application method, timing and rate on field emergence, growth, nodulation and yield structure of soybean.	31-37
7.	**Zhanatauov, S. U.** Mathematical splitting of the mathematical formula for the Y-reaction.	38-46
8.	**Siddikov, A.J., & Ne'matova, G.** Regional misallocation of labour and human capital in uzbekistan.	47-55
9.	**Suyunova, G.B., & Usmanov, N.N.** Effect of different sowing dates and planting patterns on the growth and development of pea (Pisum sativum L.) Varieties.	56-63
10.	**Chemezov, D., et al.** Kinetics and spatial organization of a detonation wave in the ANFO system: a theoretical description of the evolution of disturbances in a heterogeneous medium.	64-67
11.	**Chemezov, D., et al.** Spatiotemporal dynamics of BTF explosion front propagation.	68-71

Impact Factor:						
	ISRA (India)	= **6.317**	**SIS** (USA)	= **0.912**	**ICV** (Poland)	= **6.630**
	ISI (Dubai, UAE)	= **1.582**	**РИНЦ** (Russia)	= **3.939**	**PIF** (India)	= **1.940**
	GIF (Australia)	= **0.564**	**ESJI** (KZ)	= **8.771**	**IBI** (India)	= **4.260**
	JIF	= **1.500**	**SJIF** (Morocco)	= **7.184**	**OAJI** (USA)	= **0.350**

Impact Factor:						
	ISRA (India)	= **6.317**	**SIS** (USA)	= **0.912**	**ICV** (Poland)	= **6.630**
	ISI (Dubai, UAE)	= **1.582**	**РИНЦ** (Russia)	= **3.939**	**PIF** (India)	= **1.940**
	GIF (Australia)	= **0.564**	**ESJI** (KZ)	= **8.771**	**IBI** (India)	= **4.260**
	JIF	= **1.500**	**SJIF** (Morocco)	= **7.184**	**OAJI** (USA)	= **0.350**



Scientific publication

Impact Factor

Impact Factor	2013	2014	2015	2016	2017	2018	2019	2020	2021	2022	2023	2024	2025
JIF		1.500											
ISRA (India)		1.344				3.117	4.971		6.317				
ISI (Dubai, UAE)	0.307	0.829							1.582				
GIF (Australia)	0.356	0.453	0.564										
SIS (USA)	0.438	0.912											
РИНЦ (Russia)		0.179	0.224	0.207	0.156	0.126		3.939	0.671	0.177	0.191		
ESJI (KZ)		1.042	1.950	3.860	4.102	6.015	8.716	8.997	9.035	8.771	8.502	8.100	
SJIF (Morocco)		2.031				5.667			7.184	6.296			
ICV (Poland)		6.630											
PIF (India)		1.619	1.940										
IBI (India)			4.260										
OAJI (USA)						0.350							

Deadlines

	Steps of publication	Deadlines	
		min	max
1	Article delivered	-	
2	Plagiarism check	1 hour	2 hour
3	Review	1 day	30 days
4	Payment complete	-	
5	Publication of the article preprint	1 day	5 days
	publication of the journal	30th of each month	
6	doi registration	before publication	
7	Publication of the journal	1 day	2 days
8	Shipping journals to authors	3 days	7 days
9	Database registration	5 days	6 months

Impact Factor:						
	ISRA (India)	= **6.317**	**SIS** (USA)	= **0.912**	**ICV** (Poland)	= **6.630**
	ISI (Dubai, UAE)	= **1.582**	**РИНЦ** (Russia)	= **3.939**	**PIF** (India)	= **1.940**
	GIF (Australia)	= **0.564**	**ESJI** (KZ)	= **8.771**	**IBI** (India)	= **4.260**
	JIF	= **1.500**	**SJIF** (Morocco)	= **7.184**	**OAJI** (USA)	= **0.350**

INDEXING METADATA OF ARTICLES IN SCIENTOMETRIC BASES:

International Scientific Indexing ISI (Dubai, UAE)	http://isindexing.com/isi/journaldetails.php?id=327
Cl.An. // THOMSON REUTERS, EndNote (USA)	https://www.myendnoteweb.com/EndNoteWeb.html
Research Bible (Japan)	http://journalseeker.researchbib.com/?action=viewJournalDetails&issn=23084944&uid=rd1775
Scientific Object Identifier (SOI)	http://s-o-i.org/
РИНЦ (Russia)	http://elibrary.ru/contents.asp?issueid=1246197
Google Scholar (USA)	http://scholar.google.ru/scholar?q=Theoretical+t-science.org&btnG=&hl=ru&as_sdt=0%2C5
Turk Egitim Indeksi (Turkey)	http://turkegitimindeksi.com/Journals.aspx?ID=149
DOI (USA)	http://www.doi.org
CrossRef (USA)	http://doi.crossref.org
Open Academic Journals Index (Russia)	http://oaji.net/journal-detail.html?number=679
Collective IP (USA)	https://www.collectiveip.com/
Japan Link Center (Japan)	https://japanlinkcenter.org
PFTS Europe/Rebus:list (United Kingdom)	http://www.rebuslist.com
Kudos Innovations, Ltd. (USA)	https://www.growkudos.com
Korean Federation of Science and Technology Societies (Korea)	http://www.kofst.or.kr
AcademicKeys (Connecticut, USA)	http://sciences.academickeys.com/jour_main.php
Cl.An. // THOMSON REUTERS, ResearcherID (USA)	http://www.researcherid.com/rid/N-7988-2013
RedLink (Canada)	https://www.redlink.com/
Cl.An. // THOMSON REUTERS, ORCID (USA)	http://orcid.org/0000-0002-7689-4157
TDNet Library & Information Center Solutions (USA)	http://www.tdnet.io/
Yewno (USA & UK)	http://yewno.com/
RefME (USA & UK)	https://www.refme.com
Stratified Medical Ltd. (London, United Kingdom)	http://www.stratifiedmedical.com/

THE SCIENTIFIC JOURNAL IS INDEXED IN SCIENTOMETRIC BASES:

Advanced Sciences Index (Germany)	http://journal-index.org/
SCIENTIFIC INDEXING SERVICE (USA)	http://sindexs.org/JournalList.aspx?ID=202
CiteFactor (USA) Directory Indexing of International Research Journals	http://www.citefactor.org/journal/index/11362/theoretical-applied-science
International Institute of Organized Research (India)	http://www.i2or.com/indexed-journals.html
JIFACTOR	http://www.jifactor.org/journal_view.php?journal_id=2073
Eurasian Scientific Journal Index (Kazakhstan)	http://esjindex.org/search.php?id=1
Open Access Journals	http://www.oajournals.info/
SJIF Impact Factor (Morocco)	http://sjifactor.inno-space.net/passport.php?id=18062
Indian citation index (India)	http://www.indiancitationindex.com/
InfoBase Index (India)	http://infobaseindex.com
Index Copernicus International (Warsaw, Poland)	http://journals.indexcopernicus.com/masterlist.php?q=2308-4944
Электронно-библиотечная система «Издательства «Лань» (Russia)	http://e.lanbook.com/journal/

Signed in print: 30.10.2026. Size 60x84 1/8

«Theoretical & Applied Science» (USA, Sweden, KZ)
Scientific publication. The circulation is 90 copies.
https://T-Science.org E-mail: **T-Science@mail.ru**

Printed «Theoretical & Applied Science»

Philadelphia, USA